DISS. ETH NO. 25448

The role of Ral GTPases in Schwann cell development and myelination

A thesis submitted to attain the degree of

DOCTOR OF SCIENCES of ETH ZURICH

(Dr. sc. ETH Zurich)

presented by

ANDREA OMMER

M.Sc. University of Bonn

born on 05.11.1988

citizen of Germany

accepted on the recommendation of

Prof. Dr. Ueli Suter, examiner

Prof. Dr. Martin E. Schwab, co-examiner

PD Dr. Hauke B. Werner, co-examiner

2018

Table of contents

1. Summary

Myelination enables the fast conduction of action potentials along axons that is called saltatory conduction. In the peripheral nervous system (PNS) Schwann cells (SCs) form myelin by wrapping their membrane spirally around a segment of a single axon. To enable this process SC precursors have to increase in numbers by proliferation and select an axon suitable for myelination in a process called radial sorting. The 1:1 relationship between SC and axon that is established during radial sorting is necessary for myelination. These processes require the integration of cellular signals deriving from multiple sources such as the axon and the extracellular matrix (ECM) surrounding the SC. In search of novel proteins that regulate the development of SCs, we found screening approaches from other groups that identify the Ral family of small GTPases as potential candidates. The Ras-like GTPases RalA and RalB have been implicated in a variety of cellular functions that are known to be crucial for SCs such as proliferation, cell-cycle progression, formation of cellular protrusions, vesicle targeting, and polarity. Most of this knowledge is derived from studying tumor cells since Rals are an important effector of the proto oncogene Ras.

In this study, we aimed to investigate the function of the Ral GTPases RalA and RalB in the development of SCs. We used mice lacking expression of either RalA in SCs, or RalB in all cell types, or a combination of both as a model to investigate the impact that absence of Rals had on developmental myelination in the sciatic nerve. Our results show that Ral GTPases are required for the radial sorting of axons by SCs and also potentially for the long-term maintenance of axons and myelin. We show that during SC development Ral GTPases are either functionally redundant or can compensate for the loss of the other Ral since only mice deficient for both GTPases developed radial sorting defects. In contrast, we identify a function in the homeostasis of mature myelin that is unique to RalB. We show that the observed radial sorting defect was not due to decreased proliferation of SCs but rather caused by a deficiency in the extension of cellular protrusions. By culturing primary SCs of Ral deficient mice, we

were able to identify the exocyst complex as the Ral effector that mediates the effect of Ral signaling on the cytoskeleton to promote process extension in SCs. Integrating our work with the published work of others, we propose a model in which Ral GTPases and the exocyst complex act downstream of Ras to regulate the actin cytoskeleton by recruiting actin nucleating factors to the sites of process formation.

2. Zusammenfassung

Die Myelinisierung von Axonen ermöglicht die schnelle Weiterleitung von Aktionspotenzialen, was als saltatorische Reizweiterleitung bezeichnet wird. Im peripheren Nervensystem (PNS) bilden Schwann-Zellen (SZ) die Myelinscheide, indem sie ihre Membran spiralförmig um ein Segment eines einzelnen Axons wickeln. Um diesen Prozess zu ermöglichen müssen SZ-Vorläuferzellen zunächst ihre Anzahl durch Proliferation erhöhen. Anschließend findet das „radial sorting“ statt, ein Verfahren bei dem die SZ ein für die Myelinisierung geeignetes Axon auswählt. Das so entstandene 1:1 Verhältnis von SZ zu Axon ist für den Beginn der Myelinisierung notwendig. Diese Prozesse erfordern die Integration extrazellulärer Signale unterschiedlichen Ursprungs, wie beispielsweise vom Axon und der extrazellulären Matrix um die SZ. Um neue Proteine zu finden, die eine wichtige Rolle in der Entwicklung von SZ spielen, nutzten wir die durch Screening-Experimente gewonnenen Daten anderer Gruppen und identifizierten so die Familie der Ral GTPasen (abgeleitet vom englischen „Ras-like“) als potenzielle Kandidaten. Die GTPasen RalA und RalB wurden bereits mit verschiedenen zellulären Funktionen in Verbindung gebracht von denen bekannt ist, dass sie für die Entwicklung von SZ wichtig sind wie zum Beispiel die Proliferation, die Regulation des Zellzyklus‘, die Bildung von Zellfortsätzen, der gezielte Transport von Vesikeln und die Polarität der Zelle. Ein Großteil der Erkenntnisse über Ral GTPasen stammt aus Experimenten mit Tumorzellen, da Ral GTPasen ein wichtiger Effektor des Protoonkogens Ras sind.

Ziel dieser Arbeit war es die Funktion der Ral GTPasen in der SZ-Entwicklung zu Untersuchen. Dafür verwendeten wir transgene Mäuse, die entweder kein RalA in SZ exprimierten oder in denen alle Zelltypen defizient für RalB waren, sowie eine Kombination beider Modelle. Anschließend analysierten wir, welchen Einfluss das Fehlen der Ral GTPasen auf die Myelinisierung im *Nervus ischiadicus* hatte. Unsere Ergebnisse zeigen, dass Ral GTPasen für das „radial sorting“ von Axonen durch SZ und möglicherweise auch für die

langfristige Erhaltung von Axonen und Myelin erforderlich sind. Wir zeigen außerdem, dass RalA und RalB wärhend der SZ-Entwicklung entweder funktionell redundant sind oder den Verlust der anderen GTPase kompensieren können, denn nur der Verlust beider GTPasen führte zu einer Beeinträchtigung des „radial sortings“ in Mäusen. Im Gegensatz dazu hat RalB Funktionen in der Homöostase von Myelin, die nicht von RalA übernommen werden konnten. Wir zeigen, dass die beobachtete Beeinträchtigung im „radial sorting“ nicht durch eine verminderte Proliferation von SZ bedingt ist, sondern auf eine verminderte Bildung und Aufrechterhaltung von Zellfortsätzen zurückzuführen ist. *In vitro* Experimente mit primären SZs von Ral-defizienten Mäusen identifizierten den sogenannten Exocyst-Komplex als den Effektor der Ral GTPasen, der in SZs auf das Zytoskelett einwirken kann um die Bildung von Zellfortsätzen zu fördern. Im Zusammenhang mit publizierten Arbeiten anderer Gruppen schlagen wir daher ein Modell vor, in welchem aktives Ras die Ral GTPasen aktiviert und diese zusammen mit dem Exocyst-Komplex direkte Effektoren des Aktin-Zytoskeletts dorthin rekrutieren, wo diese zur Bildung von Zellfortsätzen benötigt werden.

3. Introduction

3.1. Cells of the nervous system

The cells of the central nervous system (CNS) and peripheral nervous system (PNS) can be broadly divided in two categories: neurons and glia cells. Neurons are the cells that are responsible for the unique functions of the brain. They generate electrical pulses (action potentials) in response to changes in their membrane potential, propagate these to other neurons, or to muscles and secretory cells to control the body's reactions (Bear et al., 2007). Although there are on the order of 10^{11} neurons in the human brain they are far outnumbered by the glia cells, which provide support to the neurons (Alberts et al., 2015). There are different types of glia cells: astrocytes, microglia, and oligodendrocytes in the CNS, as well as Schwann cells (SCs) and satellite glia in the PNS. Astrocytes are the most numerous glia cells in the CNS, their main task is to regulate the chemical content of the extracellular space to generate a healthy environment for neurons (Bear et al., 2007). Microglia are phagocytic cells that become active in response to infection, disease, and injury of the brain, thus managing the brain's immune response (Kandel et al., 2012). Satellite glia help regulate the external chemical environment and surround neurons in ganglia (Hanani, 2005). Oligodendrocytes in the CNS and SCs in the PNS are the myelinating glia, providing insulation to axons to increase the speed of action potential propagation (Bear et al., 2007).

From an evolutionary perspective, rapid nerve conduction provides many advantages, as it enables faster reaction times and a higher precision of signal transduction (Castelfranco and Hartline, 2016). One way by which the speed of action potential propagation along an axon can be increased is by an increase in the axonal diameter. A common example is the giant axon of the squid, which can be 1 mm in diameter (Bear et al., 2007). However, very large axons naturally have very high energy demands and in addition take up a lot of space in the body. Myelination provides a different mechanism to increase conduction speed without these repercussions for the axon (Castelfranco and Hartline, 2016). Myelinating glia cells wrap their

membranes multiple times around segments of the axon, the internodes. The space between internodes is called the node of Ranvier. By providing insulation in this manner, the myelinating glia cells cause the action potential to jump from node to node, a process called saltatory conduction (Bear et al., 2007).

3.2. Schwann cell development

The development of SCs is a complex process that is closely linked to the architecture and appearance of developing peripheral nerves. There are 4 developmental stages of SCs that will be introduced in the following section: Neural crest cells, SC precursors (SCPs), immature SCs, and pro-myelinating SCs. For reference, an overview of SC development is shown in Figure 1.

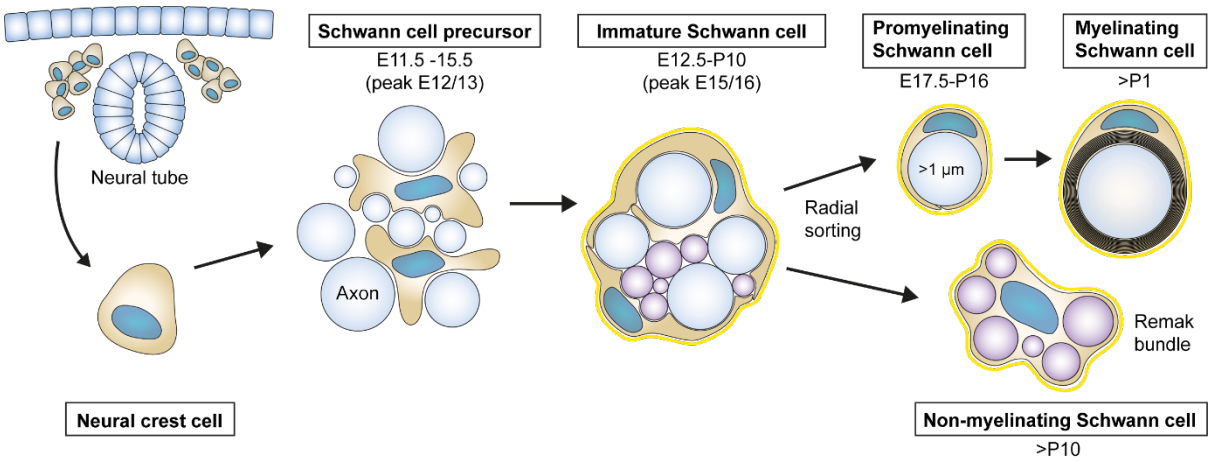

Figure 1: Development of Schwann cells. Neural crest cells are highly migratory and give rise to SCPs. The transition to immature SCs is accompanied by a change in nerve architecture as families of immature SCs, identifiable by a common basal lamina depicted here in yellow, surround bundles of unsorted axons. During radial sorting, immature SCs segregate individual large axons from the bundle and enter the pro-myelinating stage, characterized by a 1:1 relationship between axon and SC. Only pro-myelinating SCs start myelination. SCs that stay in contact with a number of small axons differentiate into a non-myelinating SC, separating axons with cytoplasmic processes to form a Remak bundle (see also Figure 2). Illustration by Dr. D.Gerber.

3.2.1. Neural crest cells

During embryonic development the nervous system arises from the ectoderm. A critical step in the formation of the nervous system is neurulation, the process during which the neural plate folds to form the neural groove and subsequently the neural tube (Bear et al., 2007). As

the neural tube closes, the neural crest arises on both sides at the tip of the fold. Neural crest cells are a population of progenitor cells that give rise to a remarkable variety of different cell types including melanocytes and cardiac cells, as well as neurons and glia cells of the PNS (Monk et al., 2015). All neural crest cells, independent of their fate, are highly migratory and different migratory pathways will give rise to distinct populations of precursor cells (Duband, 2006). Schwann cells derive mostly from a population of trunk neural crest cells that migrate along a ventral pathway and give rise to SCPs (Monk et al., 2015). An exception are the Schwann cells that populate ventral and dorsal spinal roots, since these arise from a specialized neural-crest derived progenitor pool, the boundary cap cells (Maro et al., 2004).

The generation of SCPs from neural crest cells requires a variety of molecular changes. It was shown that expression of the transcription factor FoxD3 prevents the development of neurons and melanocytes but is compatible with glial differentiation (Nitzan et al., 2013). Similarly, Sox10 is expressed in neural crest cells and expression is maintained in Schwann cells and melanocytes, while it is downregulated in neurons and other crest-derived cell types (Britsch et al., 2001; Kuhlbrodt et al., 1998). In addition, Neuregulin 1 (NRG1) was reported to suppress neuronal and promote glial differentiation (Shah et al., 1994). Furthermore, the histone deacetylases 1 and 2 (HDAC1/2) regulate expression of the early SC lineage marker myelin protein zero (P0) directly, and of fatty acid binding protein 7 through regulation of the transcription factor Pax3, thus playing a critical role in the generation of SCPs from neural crest cells (Jacob et al., 2014). Interestingly, SCPs seem to retain the potential to give rise to other neural crest-derived cell types, and in recent years it has become evident that they not only give rise to immature SCs but also have other functions, such as the guidance of blood vessels (Furlan and Adameyko, 2018).

3.2.2. Schwann cell precursors

SCPs populate embryonic nerves that contain tightly packed axons without much extracellular space or matrix (Jessen et al., 2015). Similar to neural crest cells, they are highly proliferative and migrate along the developing nerves to spread through the embryonic body. SCPs depend

on axonal signals for their survival, specifically on NRG1 (Dong et al., 1995). NRG1, in conjunction with its heterodimeric ErbB2/ErbB3 receptor, is an essential regulator of many steps of SC development and in SCPs it not only promotes survival but also directs migration (Newbern and Birchmeier, 2010).

SCPs give rise to immature SCs. An important regulator of the transition from SCP to immature SC is Notch. Notch ligands are expressed on embryonic axons, and enhanced Notch signaling was shown to accelerate the generation of immature Schwann cells, potentially through an increase of the NRG1 receptor ErbB3 (Woodhoo et al., 2009). Furthermore it was shown that both endothelin and the transcription factor AP2α negatively regulate the formation of immature SCs (Brennan et al., 2000; Stewart et al., 2001).

3.2.3. Immature Schwann cells

In contrast to SCPs, immature SCs no longer depend on axonal signals for their survival but instead support their own survival through the secretion of autocrine survival factors (Jessen and Mirsky, 2005). This autocrine survival signaling enables immature SCs, as well as fully differentiated SCs, to survive nerve injuries even after axons have degenerated, which is crucial for nerve regeneration (Jessen et al., 2015).

The transition from SCPs to immature SCs is accompanied by a reorganization of the embryonic nerves. Immature SCs surround large families of axons, forming irregular axon-Schwann cell bundles (Figure 2). Each bundle is surrounded by extracellular matrix (ECM) and a basal lamina that is produced by the immature Schwann cells (Webster et al., 1973). Furthermore, connective tissue spaces appear containing endoneurial fibroblasts and blood vessels, similar to the architecture seen in adult nerves (Jessen and Mirsky, 2005). These changes are actively influenced by the immature SCs, which secrete vascular endothelial growth factor (VEGF) to promote arterial differentiation as well as Desert hedgehog (Dhh) to enhance perineurial differentiation (Mukouyama et al., 2005; Parmantier et al., 1999). In turn,

endoneurial fibroblasts were shown to promote the deposition of the basal lamina by SCs *in vitro* (Obremski et al., 1993).

Immature SCs give rise to myelinating and non-myelinating (Remak) SCs during a process called radial sorting (see Figure 1).

3.2.3.1. Radial sorting

In contrast to oligodendrocytes in the CNS, SCs can only myelinate a single axonal segment. Thus, for myelination to occur in the PNS, SCs need to enter a 1:1 relationship with an axon which happens during radial sorting. In brief, Schwann cell numbers are matched to the number of axons through proliferation and apoptosis. Immature Schwann cells that are in contact with a bundle of unsorted axons, i.e. a bundle of axons in which axons are packed tightly and no Schwann cell cytoplasm separates them (Figure 2), extend a process into the bundle to contact a single large caliber axon. This axon is subsequently removed from the bundle and engulfed by the Schwann cell, now a promyelinating SC that will become a myelinating SC. Electron microscopy images have led to the idea that the Schwann cell first moves the targeted axon to the edge of the bundle while still within the common basal lamina which a family of Schwann cells produces around bundles of unsorted axons. Only then will the Schwann cell divide, after which the daughter Schwann cell will separate the axon from the bundle, produce its own basal lamina, and finally start myelination (Monk et al., 2015; Webster et al., 1973). Through this process the number of large axons in a bundle is gradually reduced until only small caliber axons are left. The Schwann cells in contact with these axons will then differentiate into Remak Schwann cells that can ensheath several axons but do not form myelin (Monk et al., 2015). While these processes happen in a set order for each individual Schwann cell, they happen simultaneously in the developing nerve starting around embryonic day (E) 11 with the arrival of SCPs in the embryonic mouse nerve, and lasting until around postnatal day (P) 15, when the majority of Remak bundles have differentiated.

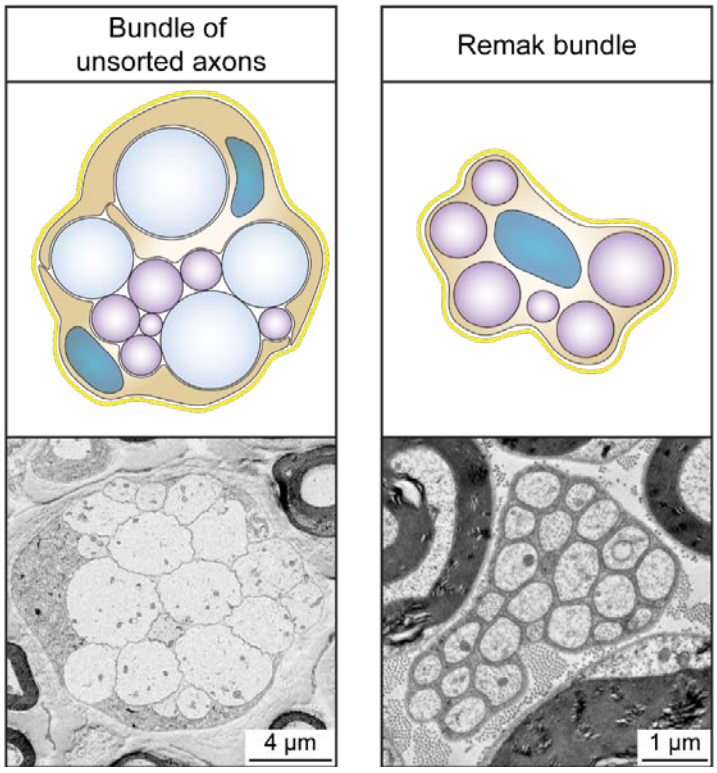

Figure 2: Differences in axonal bundles. Schematic drawings and electron micrographs of two different types of axonal bundles that can be found in mouse sciatic nerves. The left panel shows a bundle of unsorted axons, containing small (purple) and large (blue) axons tightly packed and without SC processes to separate the axons. Note that while the EM image is taken from a pathological adult nerve, such bundles naturally occur during development (see also Figure 1). The right panel shows a fully differentiated Remak bundle containing only small axons (purple) engulfed by cytoplasmic SC processes. Both types of bundles are surrounded by a basal lamina (depicted in yellow). Illustration by Dr. D.Gerber.

3.2.3.1.1. Control of SC proliferation, survival, and cell cycle progression

Proliferation of immature SCs is a tightly regulated process that is critical for successful radial sorting and myelination. It is regulated by a mix of axonal, soluble, and basal lamina-derived signals. As mentioned previously, axons express NRG1, which binds to the heterodimeric ErbB2/ErbB3 receptors on Schwann cells and plays an important role in many aspects of Schwann cell biology (Birchmeier and Bennett, 2016). *In vitro*, NRG1 is a potent mitogen for Schwann cells and in zebrafish blockage of ErbB2/3 receptor signaling leads to reduced Schwann cell proliferation (Levi et al., 1995; Lyons et al., 2005; Raphael et al., 2011). Similarly, sciatic nerves of mice lacking ErbB3 and ErbB4 expression showed a severe lack of Schwann cells (Brinkmann et al., 2008). Surprisingly, a mouse model with a relatively late deletion of

ErbB2 in SCs (around E16) showed an increase in proliferating cells in the sciatic nerve, while earlier recombination in spinal roots around E11 led to a severe reduction in the number of SCs (Garratt et al., 2000). Thus, the effect of the NRG1-ErbB2/ErbB3 signaling axis on the proliferation of immature SCs is not yet fully understood.

Laminin is the major component of the SC basal lamina and binds to surface receptors expressed by SCs such as integrin β1 and dystroglycan. As such, laminin is a major regulator of radial sorting. It was reported that ablation of laminin γ1 depletes all other laminin chains in SCs, and that mice carrying this mutation display decreased SC proliferation and an increase in apoptosis (Yu et al., 2005). Additionally, the small GTPase Cdc42 which is activated downstream of integrin β1, was also found to be crucial for SC proliferation during radial sorting (Benninger et al., 2007). Similarly, focal adhesion kinase (FAK), which is linked to signaling of α6β1 integrin and ErbB2, is required for SC proliferation (Grove et al., 2007). Reports on whether or not deletion of integrin β1 influences proliferation are controversial, and it was suggested that the effect might depend on the genetic background of the mutant animals (Berti et al., 2011; Feltri et al., 2002). It was described recently that the laminin-integrin and NRG1-ErbB2/3 signaling axes cooperate to regulate SC development, and although proliferation was not investigated in this report, since the utilized *Lama2* knockout mice proliferate normally it is possible that signaling downstream of laminin γ1 converges with NRG1 signaling to control SC proliferation (Ghidinelli et al., 2017).

Another axonal signal that controls proliferation of SCs is activation of the Notch receptor. Mice lacking Notch activity in SCs or the downstream transcriptional activator recombining binding protein suppressor of hairless (RBP-J) showed decreased proliferation of immature SCs (Woodhoo et al., 2009). Supporting these observations, activation of Notch signaling in cultured SCs increased proliferation (Woodhoo et al., 2009). In these mice the reduced number of Schwann cells was closely reflected in a similarly reduced number of sorted axons (myelinated and non-myelinated), showing that the number of immature SCs directly influences radial sorting (Woodhoo et al., 2009). Furthermore it was shown that mice lacking

beta-secretase 1 (BACE1) have increased numbers of SCs and proliferation (Hu et al., 2017). The authors showed that BACE1 regulates the cleavage of the Notch ligands Jagged-1 and Delta-1 and that BACE1 deficiency leads to elevated Notch receptor signaling (Hu et al., 2017).

Among the soluble signaling molecules, transforming growth factor β (TGFβ) has a prominent role in regulating SC proliferation and survival. It was shown that TGFβ can act as a potent mitogen on cultured Schwann cells, but can also induce apoptosis depending on culture conditions (Einheber et al., 1995; Parkinson et al., 2001; Ridley et al., 1989). Mice lacking the type II TGFβ receptor displayed decreased proliferation and apoptosis, resulting in similar numbers of SCs compared to control animals and normal myelination (D'Antonio et al., 2006). TGFβ also induces Schwann cell death after nerve injury, however this has only been reported for neonatal but not adult nerves (D'Antonio et al., 2006; Parkinson et al., 2001).

In recent years, progress has been made in identifying nuclear signals that regulate the cell cycle of SCs. Proliferation, apoptosis, and differentiation are very closely linked in Schwann cells, since differentiation only happens after cell cycle exit (Morgan et al., 1991). HDAC1 was found to be crucial for SC survival during radial sorting by limiting the levels of active β-catenin (Jacob et al., 2011). Mice deficient of β-catenin function in SCs show decreased proliferation while over-activation of the β-catenin pathway showed the opposite effect (Grigoryan et al., 2013). The cyclin-dependent kinase inhibitor 1b (p27) was shown to be an important regulator of Schwann cell differentiation *in vitro* (Li et al., 2011). Similar results were obtained *in vivo*, where it was shown that the nuclear Jun activation domain-binding protein 1 (Jab1) acts downstream of laminin signaling to regulate p27 and thus cell cycle progression of SCs (Porrello et al., 2014). Loss of Jab1 led to aberrant cell cycle progression and differentiation, resulting in a radial sorting defect (Porrello et al., 2014). Furthermore, the transcription factor Miz1 (myc-interacting zinc finger protein) was shown to repress the expression of the histone $H3K36^{me2}$ demethylase Kdm8, and loss of Miz1 led to re-entry of adult SCs into the cell cycle due to demethylation of critical cell cycle genes by Kdm8 (Fuhrmann et al., 2018). While the

loss of functional Miz1 in SCs led to a late-onset neuropathy and no obvious radial sorting defect (Fuhrmann et al., 2018), it is possible that this mechanism also plays a role in regulating the cell cycle exit of SCs during development.

Recently, the Hippo pathway has attracted a lot of attention in Schwann cells. Poitelon and colleagues showed that the transcriptional coactivators Yes-associated protein 1 (Yap) and Tafazzin (Taz) downstream of the Hippo pathway regulate proliferation of SCs as well the transcription of basal lamina receptor genes (Poitelon et al., 2016). It was further shown that Taz represses transcription of Gnas, encoding the Gαs-protein, and that Gαs opposes Yap/Taz activity to repress proliferation, thus providing evidence for a signaling loop that allows precise regulation of proliferation and differentiation (Deng et al., 2017). In conjunction with the TEA domain transcription factor Tead1, Yap and Taz also regulate the expression of the transcription factor early growth response 2 (Egr2/Krox20), often referred to as the master transcriptional regulator of myelination, as well as expression of the peripheral myelin protein 22 (Pmp22) (Grove et al., 2017; Lopez-Anido et al., 2016). Interestingly, hyperactivity of the Hippo-Yap/Taz axis, leading to increased proliferation, was found in SC-derived malignant peripheral nerve sheath tumors (MPNST) (Wu et al., 2018).

3.2.3.1.2. Process extension for radial sorting

It is critical for radial sorting that immature Schwann cells are able to contact axons that are located inside the bundles as well as those that are positioned at the edge. To this end immature Schwann cells need to establish apico-basal polarity, apical facing towards the axon and basal towards the basal lamina surrounding the bundle (Ozcelik et al., 2010). They further need to rearrange the cytoskeleton to form protrusions reaching into the bundle, and lastly need to contact and recognize a large axon to sort (Feltri et al., 2015). These cellular processes happen simultaneously and are heavily intertwined at the molecular level.

The common basal lamina that is formed by a family of immature Schwann cells around each bundle of axons is essential for radial sorting (Feltri and Wrabetz, 2005). Mice lacking the laminin receptor integrin β1 show defects in the early stages of radial sorting since the

Schwann cells fail to send their processes into the bundles (Feltri et al., 2002). Interestingly it was later shown that the integrins α6 and α7 are required for PNS development, and lack of both these α subunits led to a much milder radial sorting defect than that observed in integrin β1 knockout mice, indicating that there may be an additional α-subunit involved in radial sorting (Pellegatta et al., 2013). Deficiency for dystroglycan, another laminin receptor, led to a similar phenotype (Berti et al., 2011). Notably, mice lacking both β1 integrin and dystroglycan showed an even more pronounced defect in radial sorting. This resulted in virtually complete failure of sorting, prompting the idea that these are the only two laminin receptors that are required for radial sorting (Berti et al., 2011). Contrasting this theory is data from zebrafish that establishes the g-protein coupled receptor 126 (GPR126) as a third laminin receptor that is required for radial sorting in both zebrafish and mice (Mogha et al., 2013; Monk et al., 2011; Petersen et al., 2015). A second GPR known to bind to collagen, GPR56, was also reported to be critical for radial sorting in mice and zebrafish (Ackerman et al., 2018).

On the intracellular side, a lot of work has been done to identify the signaling cascades that act downstream of integrins. As mentioned above, FAK responds to integrin signaling to regulate proliferation and process extension of SCs (Grove and Brophy, 2014; Grove et al., 2007). Another kinase downstream of integrins is integrin-linked kinase (ILK). It was shown that deletion of ILK in SCs impairs radial sorting due to defective process extension of Schwann cells (Pereira et al., 2009). This effect was largely mediated through a negative regulation of Rho and Rho-associated protein kinase (ROCK), leading to shorter processes of the SCs in culture (Pereira et al., 2009). Downstream of Rho/ROCK, the actin-binding protein Profilin 1 regulates the formation of lamellipodia in Schwann cells (Montani et al., 2014). Another protein that is known to control actin dynamics and regulate the cytoskeleton is neural Wiskott-Aldrich syndrome protein (N-WASP). N-WASP integrates pathways from different membrane receptors and acts through activation of the actin-related protein 2/3 (Arp2/3) complex. In Schwann cells, lack of N-WASP leads to a mild impairment of radial sorting *in vivo* and defective lamellipodia formation *in vitro* (Jin et al., 2011; Novak et al., 2011).

In SCs, ILK also influences the activity of the small GTPases Rac1 and Cdc42 (Pereira et al., 2009). Both of these are important for radial sorting but for different reasons. As mentioned above, Cdc42 was found to regulate proliferation of immature SCs to enable radial sorting (Benninger et al., 2007). Meanwhile Rac1 was found to be important for the formation of processes and radial lamellipodia, and expression of active Rac1 in nerves of β1 integrin-deficient mice improved sorting (Benninger et al., 2007; Nodari et al., 2007). As reported by another group, Rac1 seems to play an additional role in the onset of myelination (Guo et al., 2012). In addition to ILK, protein kinase A (PKA) was suggested to regulate Rac1 activity in SCs. Increased PKA activity in SCs led to a defect in radial sorting that was attributed in parts to a role in SC proliferation and process extension (Guo et al., 2013).

Since Schwann cells need to establish polarity during radial sorting the identification of proteins that specifically regulate polarity is of great interest. Two such proteins have been identified in recent years, liver kinase B1 (LKB1/Par-4) and protein associated with Lin-7 (Pals1) (Shen et al., 2014; Zollinger et al., 2015). LKB1/Par-4 localizes to the SC-axon interface after phosphorylation by PKA, and this asymmetric localization is important for the progression of radial sorting (Shen et al., 2014). Meanwhile Pals1 was found at the initial contact site between axon and SC, where it co-localized and interacted with proteinase-activated receptor 3 (Par3) (Zollinger et al., 2015). Notably Pals1 deficiency led to a delay in radial sorting that was eventually overcome (Zollinger et al., 2015). Other polarity proteins have been studied in the context of Schwann cells and are implicated in the onset of myelination (Masaki, 2012).

3.2.3.1.3. Other cellular processes can influence radial sorting

Other cell biological processes were shown to influence radial sorting, such as microRNA signaling. Loss of the microRNA processing protein Dicer leads to a mild radial sorting defect and a more severe block of myelination, although it is not clear which microRNAs are important for this function (Pereira et al., 2010; Yun et al., 2010).

Endosomal trafficking was disturbed in SCs by targeting the phosphatidylinositol 3-kinase Vps34, and resulted in delayed radial sorting (Logan et al., 2017). The authors attributed this to altered trafficking of the ErbB2/3 receptor.

Furthermore there is evidence indicating that lipids play a role in radial sorting as well. Plasmalogens were shown to be crucial for normal progression of radial sorting, possibly due to a regulation of the glycogen synthase kinase-3 beta (GSK3β)-Akt signaling axis (da Silva et al., 2014).

3.2.4. Promyelinating Schwann cells and myelination

Once the Schwann cell has achieved a 1:1 relationship with an axon (promyelinating Schwann cell; Figure 1), myelination itself can start. The process is heavily regulated by axonal signals to assure that only axons with a diameter of and above 1 µm are myelinated and that the correct amount of myelin is produced, since the ratio of axonal diameter to diameter of the myelinated fiber (g-ratio) is more or less constant (Birchmeier and Bennett, 2016). Myelination is metabolically very demanding for SCs since it requires a remarkable expansion of the cell's surface area. Thus, a large amount of both lipids and proteins needs to be synthesized in a very short timeframe, and a disruption of the metabolic activity of Schwann cells often leads to defects in myelination (Figlia et al., 2018). Myelin has a very high lipid content, predominantly cholesterol and phospholipids (Norton and Poduslo, 1973) while also containing specialized myelin proteins such as myelin protein zero (MPZ/P0), myelin basic protein (MBP), Cyclic nucleotide phosphodiesterase (CNP), Pmp22, and Myelin-associated glycoprotein (MAG) (Nave and Werner, 2014; Patzig et al., 2011).

One of the most important axonal signals that regulate Schwann cell biology is NRG1, and it is probably the best studied as well. A threshold of axonal NRG1 expression determines if an axon will be myelinated or not (Taveggia et al., 2005). In addition, the thickness of the myelin sheath is proportional to the amount of axonal NRG1 (Michailov et al., 2004). NRG1 binds to the ErbB2/3 receptor expressed on Schwann cells and activates three major downstream

effectors: phosphatidylinositol 3-kinase (PI3K), phospholipase C (PLCγ), and mitogen-activated protein kinase kinase (MEK). Each of these effectors acts on intracellular signaling cascades that have been shown to regulate myelination (Monk et al., 2015; Pereira et al., 2012).

The mammalian target of rapamycin (mTOR) complex has been established as a crucial signaling hub to regulate myelination, integrating signals from growth factor receptors such as ErbB2/ErbB3 (Figlia et al., 2018). Loss of mTOR complex 1 (mTOC1) activity through ablation of Raptor or mTOR itself led to hypomyelination of peripheral axons, while loss of mTORC2 activity by itself did not lead to a defect (Norrmen et al., 2014; Sherman et al., 2012). This effect was mainly attributed to a role of mTOR in the regulation of lipid biosynthesis in Schwann cells, consistent with its function in other cell types (Norrmen et al., 2014). mTORC1 was also shown to control expression of the transcription factor Egr2, often referred to as the master transcription factor for myelination, thus playing a crucial role in the initiation of myelination in promyelinating SCs (Beirowski et al., 2017; Figlia et al., 2017). In addition, Oct6, which is highly expressed in promyelinating SCs, as well as the negative regulators of myelination cJun and Notch were downregulated by mTORC1 signaling, further highlighting the role of mTOR in the control of myelination (Figlia et al., 2017).

3.2.5. Myelinating Schwann cells and the maintenance of myelin and axons

Once developmental myelination is completed, myelin is by no means static. Increasing evidence suggests that in both CNS and PNS there is a continuous turn-over of myelin proteins and lipids (Figlia et al., 2018). Furthermore, Schwann cells show a remarkable plasticity upon nerve damage in order to support the regrowth of peripheral nerves (Jessen et al., 2015). Many studies have highlighted the importance of different proteins in the process of myelin maintenance in adult peripheral nerves.

Notch is a Schwann cell-expressed receptor that plays a critical role in myelination. Notch signaling during development promotes the generation of Schwann cells from precursors and

inhibits myelination (Woodhoo et al., 2009). Congruently, hyperactivity of Notch in adult nerves counteracted established myelination and resulted in demyelination (Woodhoo et al., 2009).

Another example of proteins that are required for developmental myelination as well as maintenance of adult myelin are HDAC1/2 (Brugger et al., 2015; Jacob et al., 2011). In this case, ablation of HDAC1/2 expression in adult SCs led to partial de- and remyelination and defects in the ultrastructure of nodes of Ranvier (Brugger et al., 2015). Both abnormalities seemed to be caused by decreased expression of the myelin protein P0.

Not all proteins that are critical for developmental myelination are required for the maintenance of adult myelin. A prominent example is NRG1-ErbB2/3 signaling, as SC-specific deletion of ErbB2 receptor in adult nerves had no apparent effect (Atanasoski et al., 2006). Similarly, ablation of ILK expression in adult SCs did not hamper myelin maintenance (Pereira et al., 2009).

Other reports have focused on the support of axons by Schwann cells. It has been observed that disruption of mitochondrial metabolism in Schwann cells leads to axonal loss and demyelination (Viader et al., 2013). The authors show that the disruption of mitochondria function results in a shift in lipid metabolism leading to a depletion of important myelin lipids (Viader et al., 2013). The authors further show that in this scenario SCs release acylcarnitines, which are intermediates of fatty acid oxidation and induce axonal degeneration (Viader et al., 2013). Two other reports have highlighted the importance of LKB1 for the maintenance of axons and myelin (Beirowski et al., 2014; Pooya et al., 2014). Furthermore it was shown that MAG plays a crucial role in axonal survival and early postnatal motorneuron apoptosis (Nguyen et al., 2009; Palandri et al., 2015).

3.3. The Ras superfamily of small GTPases

As highlighted throughout this chapter, the last decades have established a great amount of knowledge about the development of Schwann cells and myelination. Yet while some processes and signaling cascades are very well defined, others are less well understood or

established, and research is needed to address these points. In order to understand how Schwann cells integrate all the different extracellular signals from the ECM and the axons in order to perfectly time proliferation, radial sorting, differentiation, and myelination, and to use this knowledge to successfully treat common diseases of the PNS, the SC signaling network needs to be unraveled further. In an attempt to identify new proteins that are involved in SC biology, we turned towards small GTPases. GTPases are ideal hubs to integrate multiple signaling pathways since they can be regulated by a wide variety of cellular mechanisms: transcription, translation, post-translational modifications, as well as modulation of their activity. Some small GTPases such as Rac1 and Cdc42 have already been shown to be crucial for SC biology, while others have as of yet gone mostly unnoticed.

The Ras superfamily of small GTPases contains more than 150 proteins (Wennerberg et al., 2005). All of these small GTPases act as binary molecular switches, cycling between an inactive GDP-bound and an active GTP-bound state (Vetter and Wittinghofer, 2001). The small GTPases of the Ras superfamily influence and regulate a diverse range of cellular processes despite their overall similarities in structure and biochemical properties. This is due to differences in post-translational modifications that regulate cellular localization, the proteins that regulate their activity, the proteins that act as their effectors, and small but impactful differences in sequence and structure (Wennerberg et al., 2005).

In their 2005 review of the Ras superfamily, Wennerberg and colleagues took a systematic approach to classify the small GTPases into 5 families based on similarities in sequence and function (Wennerberg et al., 2005). The Ras family is centered on the Ras proto oncogenes, which serve as signaling hubs downstream of various extracellular stimuli (Wennerberg et al., 2005). Due to the importance of Ras in many tumors, mechanisms of Ras signaling are well-established. Similar to Ras, GTPases of the Ras homologous (Rho) family are regulators of signaling pathways originating from extracellular stimuli. They are mostly known for their influence on the actin cytoskeleton, although they have been shown to also play pivotal roles in cell polarity, microtubule dynamics, membrane transport, and control of transcription factor

activity (Etienne-Manneville and Hall, 2002). The best-studied members of the Rho family are RhoA, Cdc42, and Rac1. The Rab family, first described as Ras-like proteins in brain (Rab), is the largest branch of the Ras superfamily, containing 61 GTPases that generally regulate intracellular vesicle transport and the trafficking of proteins (Wennerberg et al., 2005). A family all by itself is the Ras-like nuclear (Ran) GTPase (Wennerberg et al., 2005). Although it is similar to Rab proteins in sequence, its function in nucleocytoplasmic transport of RNA and proteins as well as its biochemical properties distinguish it from the Rab family (Weis, 2003). Finally, the ADP-ribosylation factor (Arf) family is the last branch of the Ras superfamily. Similar to Rabs, Arf GTPases are known for their role in vesicle transport (Wennerberg et al., 2005).

3.4. Ral GTPases

In 1986 Chardin and Tavitian used an oligonucleotide probe to screen a cDNA library from immortalized simian B-lymphocytes for *RAS*-related genes, thus identifying the Ras-like gene *RALA* (Chardin and Tavitian, 1986). Three years later the same authors identified the sequences of the human *RALA* and a closely related second gene, named *RALB*, by using the simian *RALA* cDNA to probe a human pheochromocytoma cDNA library (Chardin and Tavitian, 1989). Comparing the sequences, the authors reported that RalA and B share 85% of their amino acid sequence, and both Rals have approximately 50% sequence overlap with Ras (Chardin and Tavitian, 1989). Interestingly, invertebrates such as *Drosophila melanogaster* and *Caenorhabditis elegans* possess only a single Ral gene, while no yeast orthologues of Ral have been identified so far (Shirakawa and Horiuchi, 2015).

Rals belong to the Ras branch of the Ras superfamily of small GTPases and share general structural and biochemical features with the other GTPases of the Ras family (Wennerberg et al., 2005). They contain a G domain, which is essential for guanine nucleotide binding and guanosine 5'-triphosphate (GTP) hydrolysis, a C-terminal membrane targeting sequence, containing most of the sequence variability between the two isoforms, and at the N-terminus an 11 amino acid extension that is not found in Ras (Gentry et al., 2014). Like all members of

the Ras superfamily, Rals act as a binary molecular switch, cycling between an inactive, GDP-bound and an active, GTP-bound state. During the transition two switch regions, SI and SII, change conformation thereby altering the binding capabilities of both effectors and regulators of the GTPases (Nicely et al., 2004). The intrinsic activities of Rals for both GDP-GTP exchange and GTP hydrolysis are very low, which is common for small GTPases. Thus, other proteins fulfill the task of regulating and fine-tuning Ral activity. These proteins are grouped into two categories: Ral-selective guanine nucleotide exchange factors (RalGEFs) and GTPase activating proteins (RalGAPs). RalGEFs stimulate nucleotide exchange, and with intracellular levels of GTP being much higher than those of GDP, generally stimulation of RalGEFs leads to an increase in the active GTP-bound form of Ral. RalGAPs on the other hand catalyze the hydrolysis of the bound GTP, thus returning the GTPase to its inactive state. The regulation of Ral GTPases by GEFs and GAPs and their most important effectors are summarized in Figure 3.

Expression of Ral GTPases in Schwann cells has been reported in two distinct studies. Patzig and colleagues used a systematic approach to identify novel myelin and Schwann cell proteins in the sciatic nerve of mice (Patzig et al., 2011). RalA was detected among the cytoplasmic proteins. The authors further performed microarray analyses to assess expression of the genes encoding the novel proteins throughout development. RalA mRNA expression was found to be highest at P15 and subsequently downregulated (Patzig et al., 2011). Another study aiming to specifically identify proteins involved in axo-glial interactions used isolated SC pseudopods, small and temporary cytoplasmic projections that cells form in response to a stimulus, induced by stimulation with neuronal membranes or growth factors (Poitelon et al., 2015). While RalA was detected in the SC cytoplasm and pseudopods, RalB was only

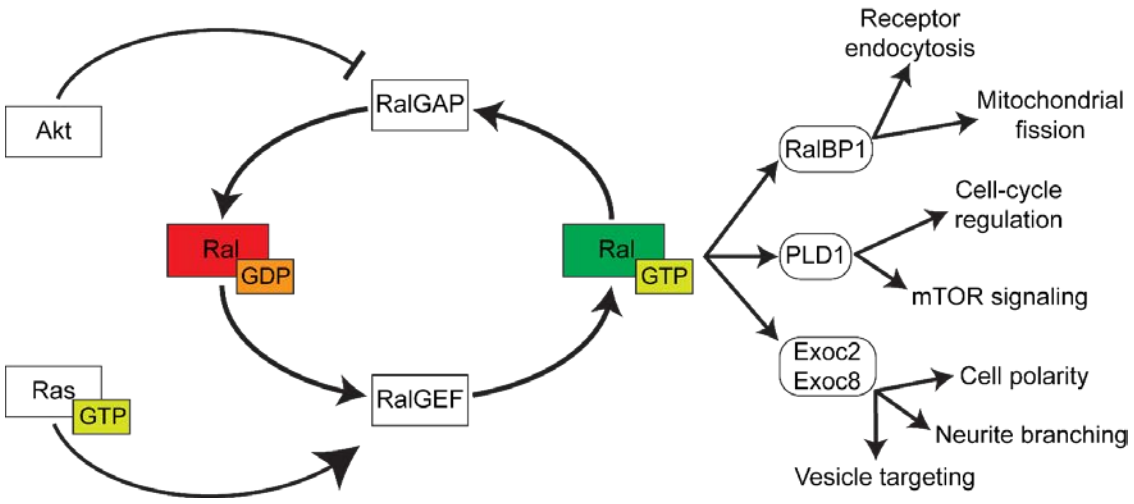

Figure 3: The Ral GTPase cycle. Schematic representation of the regulation of Ral signaling. RalGEFs and RalGAPs are essential to control the amount of active GTP-loaded Ral. GTP-loading of Ral is required for most of the interactions with downstream effectors, which can influence a variety of different cellular processes.

detected in pseudopods (Poitelon et al., 2015). Both studies indicated that Ral GTPases could play a role in SC biology.

3.4.1. Regulation of Ral GTPases

3.4.1.1. RalGEFs

Ral guanine nucleotide dissociation stimulator (RalGDS) was identified as the first RalGEF in a study attempting to identify novel mammalian GDS proteins (Albright et al., 1993). Shortly after, several groups not only reported a number of new RalGEFs, namely Rgl (RalGDS-like), Rgl2, and Rgl3, but also established them as Ras effectors (Hofer et al., 1994; Kikuchi et al., 1994; Peterson et al., 1996; Shao and Andres, 2000; Spaargaren and Bischoff, 1994), thus increasing interest in Rals and their role in Ras-mediated transformation. These aforementioned RalGEFs are structurally very similar. At the N-terminus they contain a Ras exchanger motif (REM) domain followed by a Cdc25 homology domain and a C-terminal Ras-association (RA) domain. In RasGEFs the REM domain has been shown to be important for membrane association and localization (Czikora et al., 2017). The REM domain of RalGDS has also been reported to have an important role in the regulation of RalGDS activity by blocking the catalytic Cdc25 domain (Rusanescu et al., 2001; Tian et al., 2002). Interestingly,

other small GTPases of the Ras family are also able to interact with the RA domain of RalGEFs, indicating that Rals could be activated also by other small GTPases (Peterson et al., 1996; Shao and Andres, 2000).

Another RalGEF was identified as a RalGDS-related (Rgr) oncogene in rabbit squamous cell carcinoma (D'Adamo et al., 1997). It was later termed Rgl4, highlighting the similarities to the RalGDS-like proteins. While Rgl4 contains a Cdc25 homology domain, it lacks both the REM and RA domains present in other Rgl family members. Interestingly, while the other RalGEFs are highly selective activators of Rals, Rgl4 was shown to act as GEF for both Ras and Ral (Osei-Sarfo et al., 2011).

In 2000, two proteins were identified as RalGEFs by sequence homology of the Cdc25 domain (de Bruyn et al., 2000; Rebhun et al., 2000). Besides the Cdc25 homology domain however, they did not resemble the structure of the RalGDS proteins, as they possessed neither a REM nor a RA domain. Instead, the Cdc25 homology domain is located at the N-terminus, followed by a central proline-rich sequence with PxxP motifs and a C-terminal pleckstrin homology (PH) domain (Rebhun et al., 2000). These RalGEFs were thus classified as a new family of RalGEFs and were named RalGPS1 and RalGPS2 (RalGEF with PH domain and SH3-binding motif). Similar to the REM domain in RalGDS, the central PxxP motifs of RalGPS have been shown to have auto-inhibitory function, although the precise mechanism is not clear (Ceriani et al., 2007). Most notably though, the absence of the RA domain uncouples these RalGEFs from direct association with Ras family small GTPases. Instead, the PH domain functions as a membrane anchor and is also necessary for activity of the protein (de Bruyn et al., 2000); the precise regulation of these proteins is however not yet understood. Interestingly, RalGPS2 was shown to control cell cycle progression and survival in non-small cell lung carcinoma cell lines, and this function was not mediated by Ral GTPases (Santos et al., 2016), indicating that also other RalGEFs may have additional signaling targets that have not yet been described.

RalGEFs have attracted a lot of research due to being a direct target of oncogenic Ras signaling, and targeting of Rals, RalGEFs or Ral effectors has emerged as a promising

strategy for treatment of Ras-dependent cancers (Yan and Theodorescu, 2018). Interestingly it was shown that RalB conveys survival downstream of Ras in acute myeloid leukemia (Eckfeldt et al., 2016) but could also be activated independently of Ras if Ras signaling was genetically or pharmacologically inhibited, leading to spontaneous relapse (Pomeroy et al., 2017). The mechanism of this Ras-independent activation is not yet clear, but the authors showed an involvemend of Cyclin-dependent kinase 5 (Pomeroy et al., 2017).

In Schwann cells, hyperactive Ras is a prominent cause for malignant transformation, especially in the context of neurofibromatosis type 1 (Durbin et al., 2016). Neurofibromatosis type 1 is a genetic tumor predisposition syndrome linked to mutations in the neurofibromin (*NF1*) gene, which encodes a RasGAP. One clinical feature is the development of numerous tumor types, including SC-derived MPNSTs. It was shown that Rals are hyperactive in MPNST cell lines, and that reduction of Ral activity led to diminished proliferation, invasiveness, *in vivo* tumorigenicity, and expression of epithelial to mesenchymal transition markers (Bodempudi et al., 2009). Thus, tight control of Ral activity is important for Schwann cells to prevent malignant transformation.

3.4.1.2. RalGAPs

Counteracting the activity of RalGEFs, RalGAPs catalyze the hydrolysis of bound GTP to GDP. Thus, an increase in RalGAP activity leads to a decrease in the levels of active Ral. Already in 1991 the existence of a Ral-specific GAP was demonstrated; however, the identity of the protein remained unknown (Emkey et al., 1991). It was only in 2009 that RalGAP proteins were successfully identified as large heterodimeric complexes containing a catalytic α subunit and a regulatory β subunit (Shirakawa et al., 2009). Mammals express two highly similar catalytic subunits, α1 and α2, but only one regulatory subunit that can associate with both α subunits, thus creating two distinct complexes RalGAP1 and RalGAP2 (Chen et al., 2011; Shirakawa et al., 2009). Both α subunits had previously been identified as proteins with the same sequence as the GAP catalytic domain of the tuberous sclerosis complex 2 (TSC2).

RalGAPα1 was referred to as GARNL1/TULIP1 (Schwarzbraun et al., 2004) and RalGAPα2 as Akt substrate of 250 kDa, short AS250 (Gridley et al., 2006).

Notably, the RalGAP complexes are structurally similar to the TSC complex, which is a heterodimer of TSC1 and TSC2 and acts as a GAP for Rheb, another small GTPase of the Ras family (Wennerberg et al., 2005). Despite structural and functional similarities, RalGAPs show no GAP activity for Rheb (Shirakawa and Horiuchi, 2015). Still, a crosstalk of the Ral and mTOR signaling pathways has been described. In *C.elegans*, RalGAPα/β seem to perform a similar function in regulating mTOR activity as TSC1/2 do in mammalian cells, since TSC1/2 is not expressed in the worm (Martin et al., 2014). In mouse embryonic fibroblasts (MEFs), the authors reported that RalGAP and RalB control mTORC1 activity, and a rat model with germline deletion of TSC2 showed increased activity of RalB (Martin et al., 2014). This evidence places Rals in a position to regulate one of the very prominent regulators of myelination and SC development (see section 3.2.4). Further studies implicating mTOR as an effector of Ral GTPases will be discussed in section 3.4.2.3.

Modulation of RalGAP function is crucial for the regulation of Ral activity. Interestingly, aside from the C-terminal GAP domain of the α-subunits, RalGAPs do not have any known functional domains. It is therefore not fully understood how RalGAPs are regulated by other signaling pathways. Studies addressing the regulation of glucose transport in response to insulin in skeletal muscle cells and adipocytes established posttranslational modifications as one way in which RalGAPs can be regulated. Upon muscle contraction or stimulation with insulin, PKB/Akt can phosphorylate Thr^{735} of RalGAPα1 and Thr^{715} of RalGAPα2 (Chen et al., 2014; Leto et al., 2013). Both phosphorylations enable an inhibitory interaction between RalGAP and 14-3-3, thus increasing RalA activity which in turn leads to an increased translocation of glucose transporter 4 to the plasma membrane (Chen et al., 2011). Another regulator of RalGAP function is κB-Ras, a small GTPase of the Ras family that enhances Ral activity by inhibiting RalGAP function (Oeckinghaus et al., 2014). It is currently unclear how κB-Ras exerts its effect on RalGAPs. However it has been shown in HeLa cells that RalGAPβ localizes

to the Golgi and nucleus during interphase, but relocates to the mitotic spindle and intercellular bridge during mitosis (Personnic et al., 2014).

3.4.1.3. Post-translational modifications

Besides RalGEFs and RalGAPs, posttranslational modifications play a critical role in regulating the activity of Rals, mostly through modifications of their intracellular localization. A well-established concept of GTPase regulation involves lipid modification of the C-terminal CAAX motif (C: cysteine, A: aliphatic amino acid, X: terminal amino acid), an amino acid motif that is found in the majority of Ras family small GTPases (Wennerberg et al., 2005). In Ral GTPases, a C20 geranylgeranyl isoprenoid is covalently bound to the cysteine of the CAAX motif by geranylgeranyltransferase type I (Falsetti et al., 2007; Kinsella et al., 1991). Subsequently, the terminal AAX tripeptide is removed by Ras converting enzyme 1 (RceI) and the now terminal prenylcystein is carboxymethylated by isoprenylcystein carboxyl methyltransferase (ICMT) (Wang and Casey, 2016). The prenylation of RalA and RalB is necessary to localize both GTPases to cell membranes (Falsetti et al., 2007), which was further shown to be necessary for RalGDS but not RalGAP function, and to enhance the binding of Rals to their effectors (Hinoi et al., 1996). It was established more recently that Rce1-mediated cleavage of the AAX tripeptide is necessary for the association of Rals with the plasma membrane but not with endomembranes, and that this modification of the GTPases is necessary to control their activity levels (Gentry et al., 2015). Meanwhile diverging effects of carboxymethylation of the terminal cysteine by ICMT were shown for RalA and RalB. For RalA, the modification is necessary to enable association with endomembranes, while for RalB it conveys plasma membrane association (Gentry et al., 2015).

The CAAX motif of Rals contains a second cysteine residue (CCAX) and thus belongs to a subset of these motives that can undergo an alternative modification. It was first shown for the Rho GTPase Cdc42 that after the initial prenylation instead of the established modifications by Rce1 and ICMT, a Golgi-associated protein acetyltransferase (PAT) can covalently bind a palmitate fatty acid to the adjacent cysteine residue (Nishimura and Linder, 2013). Rals can

undergo the same modification (Gentry et al., 2015; Nishimura and Linder, 2013), although the functional significance is not yet fully established. In the case of Cdc42, palmitoylation prevents interaction with Rho guanine nucleotide-dissociation inhibitor (RhoGDI), a protein that binds to and disrupts membrane association of Cdc42 (Nishimura and Linder, 2013). Interestingly, ERp57 has been suggested as a RalGDI (Brymora et al., 2012) and disruption of palmitoylation led to decreased plasma membrane association and increased cytosolic accumulation of RalB, although not of RalA (Gentry et al., 2015).

Ral GTPases can also be regulated by reversible phosphorylation. Since the C-terminal domains of RalA and RalB harbor most of their sequence discrepancy it is not surprising that C-terminal phosphorylation events are not identical between the two proteins. RalA can be phosphorylated by PKA and Aurora-A kinase on Ser^{194} (Wang et al., 2010; Wu et al., 2005) and protein phosphatase 2A was shown to dephosphorylate Ser^{194} and Ser^{183} (Sablina et al., 2007). Phosphorylation of Ser^{194} by Aurora-A kinase was critical in promoting anchorage-independent growth of tumor cells (Lim et al., 2010). The phosphorylation event increased the association of RalA with endomembranes instead of the plasma membrane, and promoted the interaction with the effector Ral binding protein 1 (RalBP1) (Lim et al., 2010). In human embryonic kidney (HEK) cells, Kashatus and colleagues were able to show that phosphorylation of RalA by Aurora-A kinase translocated the GTPase to mitochondria, where it recruited RalBP1 and DRP1 to enable mitochondrial fission (Kashatus et al., 2011). Meanwhile, protein kinase Cα (PKCα) has been reported to regulate RalB in a similar manner through phosphorylation of Ser^{198} (Martin et al., 2012; Wang et al., 2010). The phosphorylation increased RalB activity, caused a shift in intracellular localization from the plasma membrane to endocytic vesicles, and changed the association with downstream effectors (Martin et al., 2012). Functionally, Ser^{198} phosphorylation by PKCα was shown to influence anchorage-independent growth, cell migration, and cytoskeletal organization of human bladder cancer cells (Wang et al., 2010), as well as trafficking of exocytic vesicles in SW480 cells (Martin et al., 2012).

A second type of reversible posttranslational modification of Ral GTPases is ubiquitination. Generally, polyubiquitination marks proteins for degradation by the proteasome, but addition of single ubiquitin molecules or special polyubiquitin chains can function as components of cellular signaling (Alberts et al., 2015). Both RalA and RalB can undergo non-degradative ubiquitination (Neyraud et al., 2012). Ubiquitination of RalB at Lys^{47} was shown to promote association of RalB with its effector Exoc2 to activate the innate immune response, while non-ubiquitinated RalB associated preferentially with Exoc8 to enhance autophagy (Simicek et al., 2013). Ubiquitination of RalA on the other hand led to enrichment at the plasma membrane and increased lipid raft exposure (Neyraud et al., 2012).

3.4.2. Effectors of Ral GTPases

In general, small GTPases bind to and signal through their effectors in their GTP-bound, active form. A single GTPase can interact with multiple effectors and thus influence a variety of signaling pathways. As RalA and RalB have very high sequence identity they have been shown to interact with the same effectors *in vitro*, although binding affinities may differ (Shipitsin and Feig, 2004).

3.4.2.1. The exocyst complex

Probably the most studied effector of Ral GTPases is the octameric exocyst complex that is mainly known for its function in tethering secretory vesicles to sites of exocytosis on the plasma membrane, but is also involved in cell polarity, signaling and cell-cell communication (Chen and Saltiel, 2011; Martin-Urdiroz et al., 2016). The complex was first identified in yeast, and while the mammalian complex contains homologues of every subunit of the complex, yeast nomenclature is still very predominant (Table 1). In the following, the mammalian nomenclature will be used. The exocyst complex consists of eight subunits, most of which can interact with multiple other subunits as well as other interaction partners (Wu and Guo, 2015).

In 2002, Brymora and colleagues identified the exocyst complex components as Ral effectors in a screen for proteins that interacted with RalA in a GTP-dependent manner (Brymora et al.,

2001). Subsequently it was shown that RalA and RalB can both interact with two subunits of the exocyst complex, Exoc2 and Exoc8 (Moskalenko et al., 2002; Moskalenko et al., 2003; Sugihara et al., 2002). Crystal structure analysis showed though that the interaction sites for Exoc2 and Exoc8 on Rals are overlapping, indicating that Ral GTPases interact with distinct subcomplexes of the exocyst, containing either Exoc2 or Exoc8 (Fukai et al., 2003; Jin et al., 2005; Moskalenko et al., 2003).

Table 1: Nomenclature of the exocyst complex components.

Mammalian	Yeast
Exoc1	Sec3
Exoc2	Sec5
Exoc3	Sec6
Exoc4	Sec8
Exoc5	Sec10
Exoc6	Sec15
Exoc7	Exo70
Exoc8	Exo84

Functionally, the importance of the interaction between RalA and the exocyst complex in targeted delivery of exocytic vesicles to specialized membrane compartments is well established. In adipose and muscle tissues, RalA was demonstrated to be activated by insulin in a PI3K-dependent manner to regulate the trafficking of the glucose transporter Glut4 to the plasma membrane (Chen et al., 2007). This function depended on the association of active RalA with the exocyst, as well as a constitutive interaction of RalA with a motor complex containing Myo1c (Chen et al., 2007). As mentioned above, it was later determined that the activation of RalA in this context involved the inhibition of RalGAP by 14-3-3 (Chen et al., 2011), as well as a Rab10-dependent recruitment of the RalGEF Rlf to the Glut4 containing vesicles (Karunanithi et al., 2014).

Other types of vesicles also depend on the interaction between RalA and the exocyst to reach their destination. Lipid rafts are endocytosed when cells are detached from their substrate, and rapidly exocytosed upon replating. In MEFs, RalA but not RalB was shown to mediate exocytosis of membrane rafts downstream of integrin receptors through interaction with the exocyst complex (Balasubramanian et al., 2010). Further investigations demonstrated the involvement of Arf6 in this process and that crosstalk between Arf6 and Rals regulates anchorage independent growth signaling (Pawar et al., 2016). In *Drosophila melanogaster*, Ral also regulates trafficking of membrane vesicles to specialized sites; specifically, it was reported that Ral and the exocyst mediate activity-dependent enlargement of the postsynaptic neuromuscular junction (Teodoro et al., 2013).

A number of different studies have highlighted the importance of Ral signaling through the exocyst for tightly regulated exocytosis of specific vesicles. In Cos-1 cells, RalA and the exocyst mediate trafficking of recycling endosomes during mitosis, a step that is crucial for successful completion of cytokinesis (Chen et al., 2006). It was shown that Rals regulate Ca^{2+}-triggered secretion of dense granules through interaction with Exoc2 in PC12 cells (Li et al., 2007; Wang et al., 2004) as well as platelets (Kawato et al., 2008), and also mediate cAMP-induced release of von Willebrand factor from endothelial cells (de Leeuw et al., 2001; Rondaij et al., 2004). Furthermore, Ral and the exocyst can regulate pools of readily releasable vesicles, as was shown in synaptosomes from transgenic mice expressing a dominant negative form of RalA, as well as in pancreatic β cells (Lopez et al., 2008; Polzin et al., 2002).

In Schwann cells, myelin proteins such as P0 need to travel from the endoplasmic reticulum to the place of ongoing myelination. It was shown that disruption of P0 trafficking can lead to demyelination (Fratta et al., 2011). While so far no study has reported a role for Ral GTPases in the trafficking of myelin proteins, the exocyst complex subunit Exoc4 was reported to be involved in the homeostasis of membrane addition during myelin formation in conjunction with myotubularin-related protein 2 (Mtmr2) and discs large homolog 1 (Dlg1) (Bolis et al., 2009). Loss of Mtmr2 function leads to demyelinating Charcot-Marie-Tooth disease characterized by

myelin outfoldings (Berger et al., 2002; Bolino et al., 2004; Bolino et al., 2000). Mtmr2 was shown to negatively regulate membrane formation to limit myelination, while Exoc4 promotes membrane formation and myelination (Bolino et al., 2004; Bolis et al., 2009). Both of these proteins were reported to interact with Dlg1, which is thought to recruit them to sites of active membrane addition (Bolis et al., 2009). It is possible that Rals and the exocyst cooperate to regulate membrane addition in myelination.

Interaction of RalA with the exocyst is involved in establishing and maintaining cell polarity. In MDCK cells, RalA regulates delivery of basolateral proteins, such as E-cadherin and epidermal growth factor (EGF) receptor, through interaction with Exoc2, while RalB seems to be dispensable for this process (Moskalenko et al., 2002; Shipitsin and Feig, 2004). Furthermore, RalA regulates the association of the exocyst complex with Par3 and Par6 to establish neuronal polarity (Das et al., 2014; Lalli, 2009). In Schwann cell development, polarity is established by axonal signals and signals derived from the ECM during radial sorting (see section 3.2.3.1.2). Canonical polarity proteins such as Par3 have been reported to be localized asymmetrically in SCs and to be crucial for myelination (Chan et al., 2006). Little is known about how polarized expression of membrane receptors or trafficking of vesicles to sites of membrane expansion for process extension or myelination is regulated in Schwann cells. It was however shown that the polarity protein Pals1 plays an important role in establishing polarity in SCs (Ozcelik et al., 2010).

The exocyst complex physically interacts with many regulators of the actin cytoskeleton, such as the Wave regulatory complex (WRC) and the Rho GTPases Rac, Rho, and Cdc42 (Zago et al., 2017). It may therefore be an ideal signaling hub to control the formation of cellular protrusions, such as during cell migration, when rearrangements of the cytoskeleton and the targeted trafficking of vesicles for membrane addition are required. A few studies indicate that Rals can control the formation of cytoskeletal protrusions through the exocyst complex. In Swiss 3T3 cells the interaction between RalA and Exoc2 is necessary for filopodia formation induced by the inflammatory cytokines tumor necrosis factor-α (TNF-α) and interleukin-1 (IL-

1) (Sugihara et al., 2002). Furthermore, laminin-induced neurite branching was regulated by RalA in an exocyst-dependent manner, and by RalB through phospholipase D1 (PLD1), another Ral effector (Lalli and Hall, 2005). Defective process extension is a common cause of radial sorting defects in Schwann cells (Jin et al., 2011; Montani et al., 2014; Nodari et al., 2007; Pereira et al., 2009). Specifically, the small GTPases Rac1 and Rho downstream of laminin signaling have been implicated in this process (Nodari et al., 2007; Pereira et al., 2009). It is thus possible that Rals could modulate localization and/or activity of Rac1 or Rho in Schwann cells through the exocyst to control the actin cytoskeleton and process extension during radial sorting.

Besides the described function in exocytosis, Rals and the exocyst are also crucial players in autophagy. It was first reported in 2011 that RalB is activated upon nutrient starvation, and that interaction with Exoc8 is required to induce autophagy (Bodemann et al., 2011). Meanwhile the opposite reaction, repression of autophagy in response to nutrient stimulation, requires association of RalB with Exoc2 and modulates mTOR activity (Bodemann et al., 2011; Martin et al., 2014). Further evidence for an involvement of Rals in autophagy comes from a study in *Drosophila melanogaster*, where Ral was shown to act in conjunction with the exocyst to promote autophagy in dying cells via Notch signaling, but did not impact autophagy in cells of starved animals (Tracy et al., 2016). Schwann cells have been shown to remove excess cytoplasmic organelles during myelination by macroautophagy, while mTOR represses autophagy in SCs (Jang et al., 2015). However the precise regulation of the process is not yet well understood.

3.4.2.2. RalBP1/RLIP76

RalBP1, also known as Ral-interacting protein of 76kDa (RLIP76), was identified as the very first Ral effector through screens for proteins that interacted preferentially with GTP-bound Ral (Cantor et al., 1995; Jullien-Flores et al., 1995; Park and Weinberg, 1995). It immediately evoked interest in the field of small GTPase signaling since RalBP1 contains a RhoGAP domain, and indeed RalBP1 was shown to have GAP activity towards Rac1 and Cdc42, but

not RhoA (Cantor et al., 1995; Jullien-Flores et al., 1995; Park and Weinberg, 1995). Since Cdc42 and Rac1 both regulate the actin cytoskeleton, with Cdc42 inducing filopodia formation and Rac1 stimulating lamellipodia formation, RalBP1 could enable Rals, and Ras as their upstream regulator, to influence the actin cytoskeleton. While direct evidence for such a control of the actin cytoskeleton through Rals is still missing, it was shown that RalBP1 directly binds to Arno, a GEF for Arf6, to modulate the activity of Rac1 as well as PI3K and regulate cell spreading and motility of 3T3 fibroblasts (Lee et al., 2014). Similar to the exocyst complex, this link between RalBP1 and the actin cytoskeleton places Ral GTPases in a prime position to influence process extension during SC development.

In addition to the RhoGAP domain, RalBP1 also contains two ATP binding motifs and was shown to be involved in ATP-dependent transport of glutathione-conjugated electrophiles (Awasthi et al., 2000; Awasthi et al., 2001). This transport function has gained a lot of interest in the context of tumor resistance to chemotherapeutics, since those can be exported by RalBP1 and increasing efforts are made to target RalBP1 in different forms of cancer in order to overcome drug resistance (Singhal et al., 2017; Singhal et al., 2015; Vatsyayan et al., 2010). Although conclusive proof showing that the transport function of RalBP1 is regulated by Ral GTPases is missing, there is some evidence pointing in this direction. In pancreatic cancer cell lines, RalB was found to be crucial for K-Ras-mediated invadopodia formation and this process unexpectedly depended on the ATPase activity of RalBP1, and not its GAP activity (Neel et al., 2012).

Other aspects of cancer progression have also been shown to be mediated by Rals and RalBP1. In various human cancer cell lines, RalA signals through RalBP1 to enable metastasis, although RalA seemed to have additional functions that are not conveyed through RalBP1 (Wu et al., 2010). Similarly, RalBP1 has been reported to be targeted by at least 3 different microRNAs, indicating that Ral GTPases may not be the only regulators of RalBP1 function (Yang et al., 2015; Zhang et al., 2016; Zhang et al., 2017). Along these lines, multiple studies have reported the involvement of RalBP1 in invasion, cell cycle regulation, and

apoptosis in various types of cancer cells, but the involvement of Ral GTPases in these functions has not been addressed (Wang et al., 2013a; Wang et al., 2013b; Wang et al., 2016; Yang et al., 2015; Yao et al., 2014; Zhang et al., 2015).

Rals and RalBP1 have been implicated in receptor-mediated endocytosis. In this context, RalBP1 acts as a scaffold that enables Rals to recruit a number of distinct proteins that regulate endocytosis. One such protein is the μ2 subunit of the clathrin adaptor protein complex AP2 which is essential for clathrin-mediated endocytosis (Jullien-Flores et al., 2000). Furthermore, RalBP1 can interact with the epsin homology proteins Reps1 (Yamaguchi et al., 1997) and Reps2 (Ikeda et al., 1998) which have been implicated in receptor-mediated endocytosis through interaction of Reps1 with Rab11-FIP2 (Rab11 family interacting protein2) (Cullis et al., 2002) and of Reps2 with Epsin, or Eps15 (Morinaka et al., 1999). Specifically it has been shown that Ral, RalBP1, and Reps2 in conjunction regulate ligand-dependent endocytosis of insulin and EGF receptors (Nakashima et al., 1999). The critical role of clathrin-mediated endocytosis for Schwann cell myelination is demonstrated through mutations in Dynamin 2 (DNM2) that lead to dominant intermediate Charcot-Marie-Tooth neuropathy type B. *In vitro* experiments have shown that these mutations impair myelination (Sidiropoulos et al., 2012).

Furthermore, RalA and RalBP1 are crucial to switch off endocytosis during mitosis. RalBP1 can bind cyclin B1, which complexes with cyclin-dependent kinase 1 (Cdk1), and RalBP1-associated Cdk1 phosphorylates Epsin to render it incompetent for endocytosis (Rosse et al., 2003). RalA can further recruit RalBP1 and the associating cyclinB-Cdk1-complex to mitochondrial membranes, where phosphorylation of dynamin-related protein 1 by Cdk1 is essential to enable mitochondrial fission during mitosis (Kashatus et al., 2011). As described above, this relocalization of RalA to mitochondrial membranes is dependent on its phosphorylation by Aurora A. The importance of mitochondria function for SC biology has been reported previously (Niemann et al., 2005). As for any dividing cell type, the regulation of mitosis is critical for Schwann cell development. For example, in animals lacking Cdc42,

proliferation is impaired and subsequently radial sorting does not complete (Benninger et al., 2007). It is possible, that Rals are involved in regulating the proliferation of SCPs or immature SCs, potentially even through RalBP1 and Cdc42.

3.4.2.3. PLD1

Ral GTPases were shown to mediate v-Src-induced PLD1 activation downstream of Ras (Jiang et al., 1995). In contrast to most other Ral effectors, PLD1 does not interact with the switch regions of Rals but rather with the unique N-terminal sequence and is thus not directly dependent on Ral activity (Jiang et al., 1995). It has been shown that association of PLD1 with RalA is necessary but not sufficient for PLD1 activation, and requires further binding of ADP-ribosylation factor proteins Arf1 or Arf6 by PLD1 (Kim et al., 1998; Luo et al., 1998; Xu et al., 2003). As a type D phospholipase, PLD1 catalyzes the conversion of phosphatidylcholine to phosphatidic acid (PA) and choline (Exton, 1990). PA is further hydrolyzed by PA phosphatases to diacylglycerol (DAG), a potent second messenger that can activate protein kinase C (Alberts et al., 2015).

Signal transduction from Ral GTPases through PLD1 is involved in a variety of cellular processes. It was shown that RalA regulates mTORC1 activity in response to nutrients, such as glucose and amino acids, through activation of PLD1 (Xu et al., 2011). While other proteins are involved in this regulation, it was shown that PA generated by PLD1 facilitates the association between mTOR and Raptor, thus exerting direct control over mTORC1 activity. In conjunction with a study indicating cross-talk between the mTOR and Ral signaling pathways via RalGAP (Martin et al., 2014), this places Rals in an interesting position to regulate one of the key modulators of metabolism in Schwann cells.

Furthermore, interaction of Rals with PLD1 was shown to be critical for cytokinesis of HeLa cells, although other Ral effectors were involved in the same process (Cascone et al., 2008). In addition, Ral GTPases regulate the intracellular localization of the cyclin-dependent kinase inhibitor p27 through both RalBP1 and PLD1, thus influencing signaling of TGF-β (Tazat et al., 2013). In Schwann cells, p27 is an important regulator of the cell cycle and was reported

to be influenced by Jab1 (Porrello et al., 2014). Finally, while RalA can regulate neurite branching mostly through the exocyst complex, RalB was shown to exert a similar function through interaction with PLD1 (Lalli and Hall, 2005). These findings raise the prospect that Rals may regulate the extension of processes in Schwann cells which is crucial during radial sorting.

Interestingly, there is evidence suggesting that Rals can also influence the activity of PLD2. It was first shown in 2004 that Rals, RalGDS, and PLD2 are required for the constitutive internalization of metabotropic glutamate receptors, and that this function does not depend on RalBP1, PLD1, Arf1, or Arf6 (Bhattacharya et al., 2004). Later on it was proposed that RalA-mediated activation of PLD2 but not PLD1 is important for caveolae-mediated endocytosis in endothelial cells (Jiang et al., 2016). In addition, both Rals can regulate Fcγ-receptor-mediated phagocytosis in macrophages, and RalA performs this function via PLD1 as well as PLD2 (Corrotte et al., 2010).

3.4.2.4. Other effectors

A variety of additional effectors for the small GTPases RalA and RalB have been described, but their function downstream of Rals is less thoroughly studied. One example is the actin filament crosslinking protein Filamin, which is bound by RalA in a GTP-dependent manner, and is crucial for RalA-induced filopodia formation in Swiss 3T3 cells (Ohta et al., 1999). Regulation of the actin cytoskeleton is crucial for Schwann cells to be able to sort axons (Feltri et al., 2015). It has been reported that the actin-modulating proteins N-WASP and Profilin are crucial for radial sorting (Jin et al., 2011; Montani et al., 2014; Novak et al., 2011). However, the precise machinery regulating the extension of processes for radial sorting as well as longitudinal extension of a SC along the axon are not fully understood. Their multiple connections to the cytoskeleton through different effectors suggest that Rals could play an important role in process extension in SCs.

In a screen for novel Ral effector proteins, Frankel and colleagues identified the ZO-1-associated nucleic acid-binding protein (ZONAB) as a protein that interacts with RalA in a

GTP-dependent manner (Frankel et al., 2005). The interaction also depended on the density of the investigated epithelial MDCK cell line. At low cell density, ZONAB localizes to the nucleus where it represses transcription of its target genes. As cell density increases, ZONAB relocalizes to the cytoplasm where it is engaged by RalA, thus relieving its transcriptional inhibition (Frankel et al., 2005).

Additional studies have implicated Rals in c-Jun N-terminal kinase (JNK) signaling. For example, low levels of oxidative stress stimulate Ral GTPases, which can in turn activate the transcription factor forkhead box protein O4 (FOXO4) through JNK-mediated phosphorylation (Essers et al., 2004). It was further shown that this activation is mediated by JNK-interacting protein 1 (JIP1) acting as a scaffold, since JIP1 interacts with both Rlf and RalA, thus enabling activation of RalA. On the other hand, JIP1 can also bind to JNK and other components of the JNK signaling cascade, which are recruited by activated RalA (van den Berg et al., 2013).

3.4.3. Distinct and redundant functions of Ral GTPases

Since the effector binding domains of RalA and RalB are identical, it is no surprise that they were shown to interact with many of the same effectors *in vitro*, albeit with different binding affinities due to sequence differences just distal to the effector binding domain (Shipitsin and Feig, 2004). Surprisingly though, a number of studies have reported distinct functions for RalA and RalB in various cell types. RalA, but not RalB, enhanced polarized delivery of membrane proteins to the basolateral surface of epithelial MDCK cells (Shipitsin and Feig, 2004). In contrast, RalB but not RalA was critical for migration of bladder and prostate carcinoma cell lines while both Rals were able to promote proliferation (Oxford et al., 2005). In various pancreatic cancer cell lines RalA was shown to be important for tumor initiation, while RalB was implicated in metastasis (Lim et al., 2006). It was further shown in pancreatic cancer cell lines that RalA promotes anchorage-independent growth while RalB promotes survival (Falsetti et al., 2007).

In contrast, the generation of RalA and RalB knockout mice revealed mostly redundant functions for the two small GTPases (Peschard et al., 2012). While the authors reported that RalA plays a critical role in neural tube closure that is not mimicked by loss of RalB, they further demonstrated that presence of either RalA or RalB is sufficient for viability of adipocytes as well as proliferation of MEFs (Peschard et al., 2012). However, the biggest discrepancy between the mouse model and studies on human cancer cell lines stems from investigations of Ras-driven tumorigenesis. By crossing the RalA and RalB knockout mice to a mouse model of inducible Ras-driven non-small cell lung carcinoma, it was shown that either Ral GTPase is sufficient to promote tumorigenesis (Peschard et al., 2012). Meanwhile a number of studies have demonstrated that in human cancer cell lines RalA but not RalB mediates Ras-driven transformation (Chien and White, 2003; Lim et al., 2005; Lim et al., 2006; Sablina et al., 2007), while RalB has been reported to be crucial for other tumorigenic events such as tumor cell survival, invasion, and metastasis (Chien et al., 2006; Chien and White, 2003; Falsetti et al., 2007; Lim et al., 2006; Oxford et al., 2005).

The cause of this discrepancy between human and murine Ral GTPases is so far not known. It has become increasingly clear that intracellular localization of Ral GTPases plays a major role in their regulation and function (see section 3.4.1.3). It was shown that the C-terminal domain of Ral GTPases, which harbors most of the sequence divergence between the two proteins, is largely responsible for their intracellular localization (Shipitsin and Feig, 2004). Interestingly, a chimeric protein of RalB containing the C-terminal sequence of RalA not only showed the intracellular localization of RalA instead of RalB but was also able to enhance secretion in MDCK cells, a function that is normally exclusive to RalA (Shipitsin and Feig, 2004). The same observation was made for the opposite chimeric RalA protein containing C-terminal domain of RalB, thus suggesting that the distinct functions of Ral GTPases are merely a consequence of differential intracellular targeting.

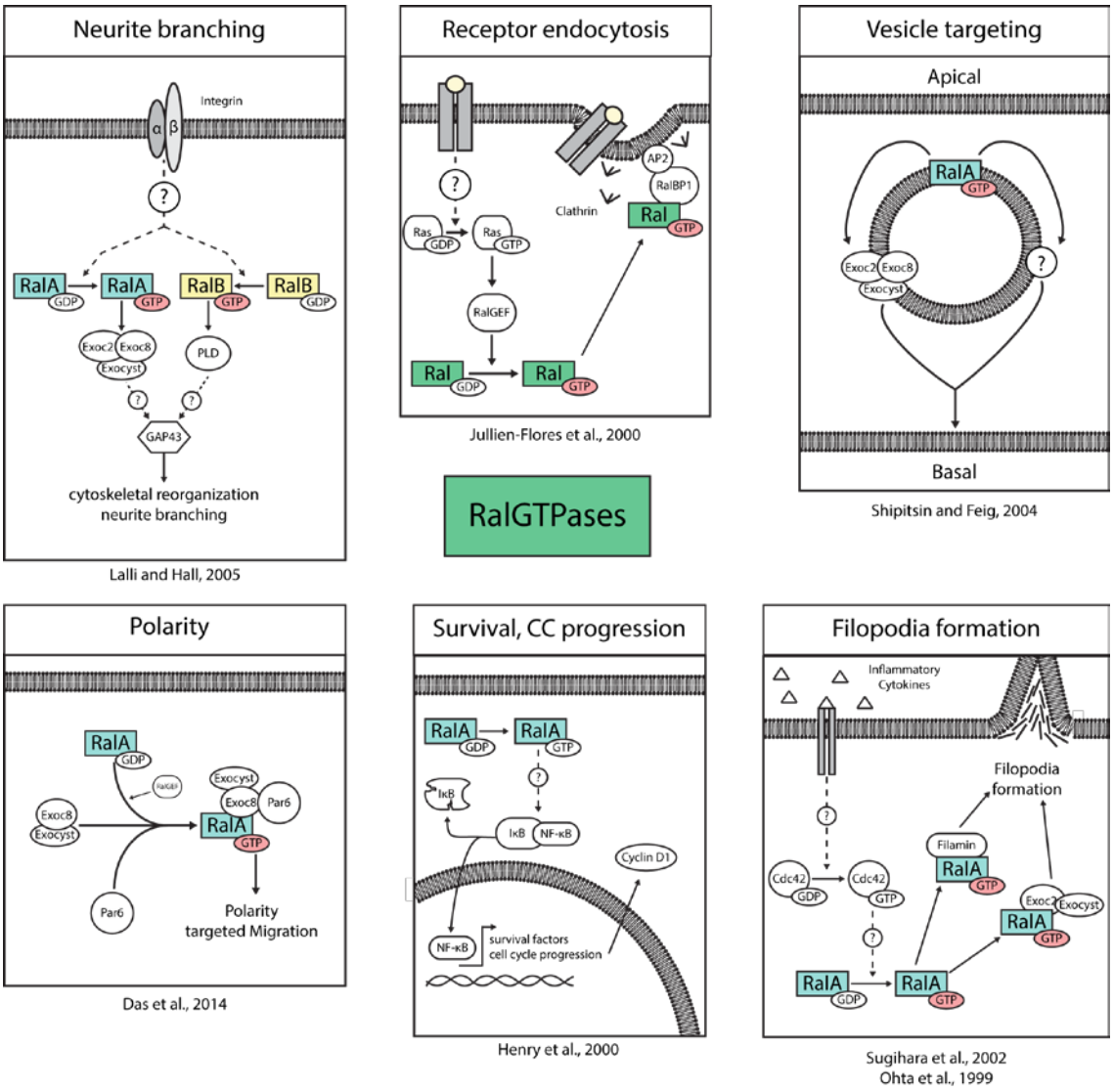

Figure 4: Potential functions of Ral GTPases in SCs. Abundant literature on the function of Ral GTPases in other cell types shows their involvement in cellular processes that are crucial for SC development. Examples shown here are the control of the cytoskeleton as seen in neurite branching (top left) and filopodia formation (bottom right), receptor endocytosis (top middle), targeted vesicle delivery (top right), cell polarity (bottom left), cell survival and cell cycle progression (CC; bottom middle).

4. Aim of the study and experimental outline

Understanding Schwann cell biology is a critical step on the way to treat diseases of the peripheral nervous system such as Charcot-Marie-Tooth disease or malignant peripheral nerve sheath tumors. While knowledge on the proteins that are critical for development and maintenance of myelin is constantly growing, there remain gaps, especially in the intracellular integration of multiple extracellular signals that converge on Schwann cells and regulate their development. In search of novel proteins that could be important in this process, the small GTPases RalA and RalB evoked our interest as 2 independent screenings showed that Rals could potentially play a role in SC development (Patzig et al., 2011; Poitelon et al., 2015). In addition, literature attributed a variety of functions to these GTPases that are known to be crucial for SC development (Figure 4). In particular, their activity can be modulated by Ras and Akt signaling, two signaling hubs of major importance in Schwann cells. Downstream, they can modulate process extension through the actin cytoskeleton, the mTOR signaling pathway and thus possibly protein and lipid production, proliferation and cell cycle progression, as well as polarity and targeted exocytosis. Therefore, the aim of this work is to study the role of Ral GTPases in the regulation of Schwann cell development and PNS myelination.

5. Results

5.1. Schwann cell specific deletion of RalA on the background of constitutive RalB deletion leads to motor impairment in transgenic mice

As described in chapter 3, the two Ral GTPases RalA and RalB are key regulators of many cellular processes and signaling pathways. Since many of these cellular events are important for SC development (Figure 4), we hypothesized that Ral GTPases could play a role in the development of SCs and peripheral nerves. To start investigating this hypothesis, mice deficient for one or both Ral GTPases were generated. Mice containing loxP sites flanking exons 2 and 3 of the *Rala* gene (Peschard et al., 2012) were crossed with mice expressing the Cre transgene under control of the Schwann cell-specific *Mpz* promoter (Feltri et al., 1999), thus generating *Mpz*$^{Cre/+}$ *Rala*$^{fl/fl}$ mice (Figure 5A, left), hereafter AKO, resulting in a deletion of RalA specifically in SCs. *Rala*$^{fl/fl}$ *Ralb*$^{-/-}$ mice (hereafter BKO) were generated by crossing previously generated mice in which exon 2 of the Ralb locus was excised by a Cre under control of the *Pgk* promoter (Figure 5A, right) (Lallemand et al., 1998) to mice containing the *Rala* allele described above, resulting in a constitutive deletion of RalB in all cell types. Double knockout mice were generated by crossing *Mpz*$^{Cre/+}$ *Rala*$^{fl/fl}$ mice with *Rala*$^{fl/fl}$ *Ralb*$^{-/-}$ mice to obtain *Mpz*$^{Cre/+}$ *Rala*$^{fl/fl}$ *Ralb*$^{-/-}$ mice, hereafter ABKO, resulting in a conditional deletion of RalA in SCs on the background of a constitutive deletion of RalB in all cell types. *Rala*$^{fl/fl}$ mice served as controls (hereafter CTR).

In order to investigate the efficiency of Ral GTPase depletion, we first analyzed lysates of P5 sciatic nerves by qPCR. We saw a marked reduction of RalA mRNA in AKO and ABKO mice (Figure 5B). Similarly, RalB mRNA was reduced in BKO and ABKO mice but was mildly increased in AKO mice (Figure 5C). We were able to confirm these observations on the protein level as assessed by immunoblot analysis of P5 sciatic nerve lysates (Figure 5D-F). While we detected a significant reduction in RalA protein levels in AKO and ABKO nerves (Figure 5E), the reduction was less pronounced than what we observed on mRNA level (Figure 5B). With

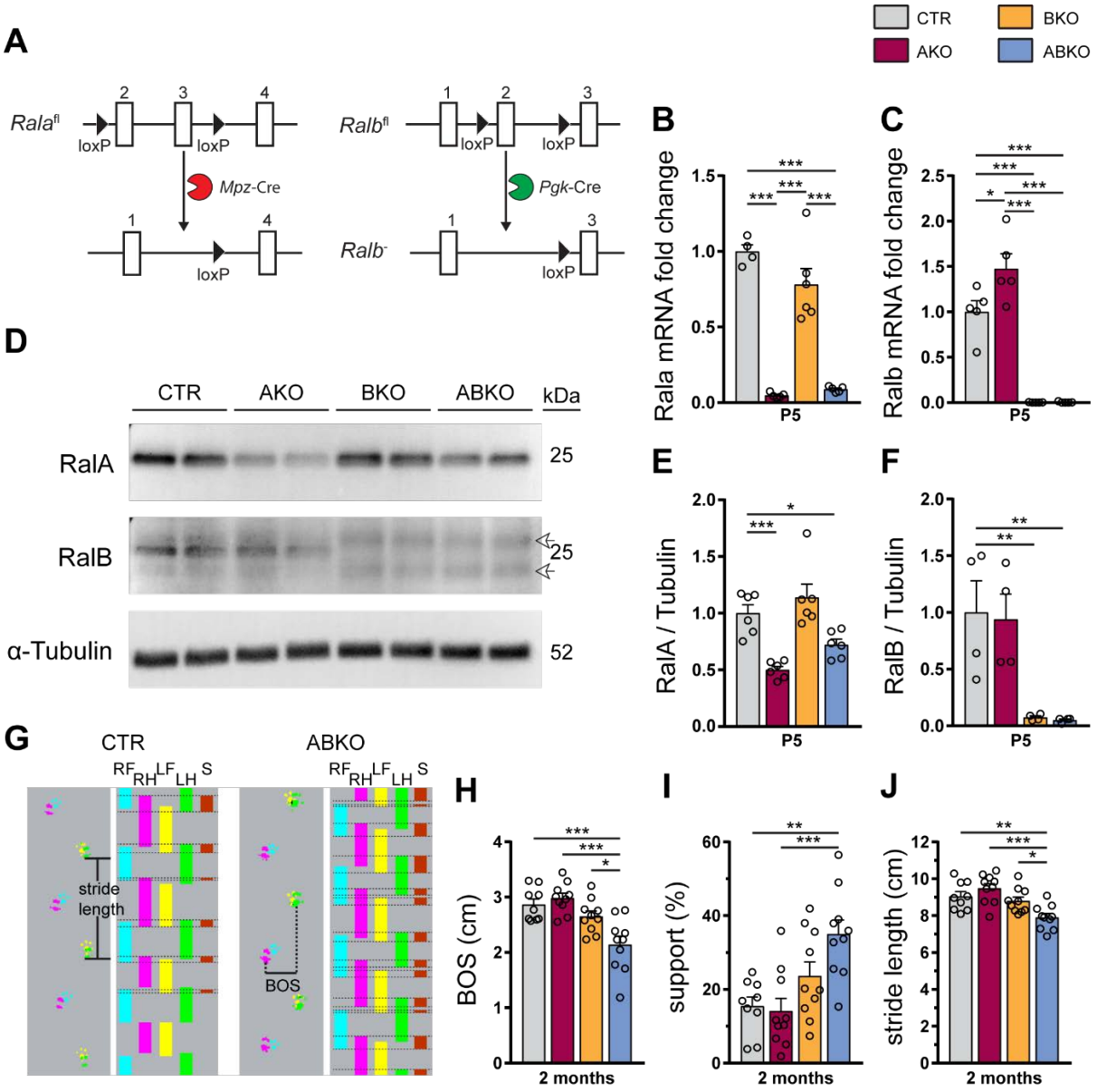

Figure 5: Loss of RalA in Schwann cells on a RalB null background leads to impaired motor function. (**A**) Schematic depicting floxed alleles for RalA and RalB as well as knockout alleles derived by Cre-mediated recombination. (**B**) mRNA expression in P5 sciatic nerves of RalA (B) and RalB (C), analyzed by qPCR and shown as fold change relative to controls after normalization to β-actin. n = 4 (RalA expression in B) or 5 (RalB expression in C) mice per genotype. One-way Anova with Tukey's multiple comparisons test. (**D-F**) Immunoblot of RalA and RalB protein expression in P5 sciatic nerve lysates. On representative immunoblots, arrows indicate unspecific binding of the RalB antibody (D). Quantification of protein expression of RalA (E) and RalB (F) relative to tubulin. n = 6 (RalA expression in E) or 4 (RalB expression in F) mice per genotype. One-way Anova with Dunnett's multiple comparisons test. (**G**) Exemplary traces of footprints and footfall patterns of two-month-old CTR and ABKO mice obtained by Catwalk analysis. RF = right front, RH = right hind, LF = left front, LH = left hind, S = support. (**H-J**) Quantification of catwalk analysis of two-month-old mice. Shown are base of support (BOS; distance between hind paws; H), support (percentage of the step cycle spend on more than two paws, I; also shown as "S" in G), and stride length (J). n = 9 (CTR) or 10 (AKO, BKO, ABKO) mice per genotype. One-way Anova with Tukey's multiple comparisons test. All data are shown as mean ± SEM. *: $p < 0.05$; **: $p < 0.01$; ***: $p < 0.001$.

regards to RalB, we found that the protein was not detectable in BKO and ABKO nerves. Instead, the antibody unspecifically recognized two other bands very close in position (Figure 5D), which resulted in residual detection by desitometric quantification (Figure 5F). In contrast to our observations on mRNA expression of RalB, we did not see an increase of RalB protein expression in AKO nerves (Figure 5F). It is of note that detection of RalB was generally weak and therefore highly variable.

Mice of all three knockout genotypes were healthy and fertile, and indistinguishable from control mice up to two months of age. Despite that, catwalk analysis at the same age showed that ABKO mice had mildly impaired motor function (Figure 5G) which was apparent by a shorter distance between hind paws (base of support, BOS, Figure 5H), an increase in the percentage of a step cycle that was spent on more than two paws (support, Figure 5I), and a shorter stride length (Figure 5J). AKO and BKO mice did not show any significant differences compared to control mice.

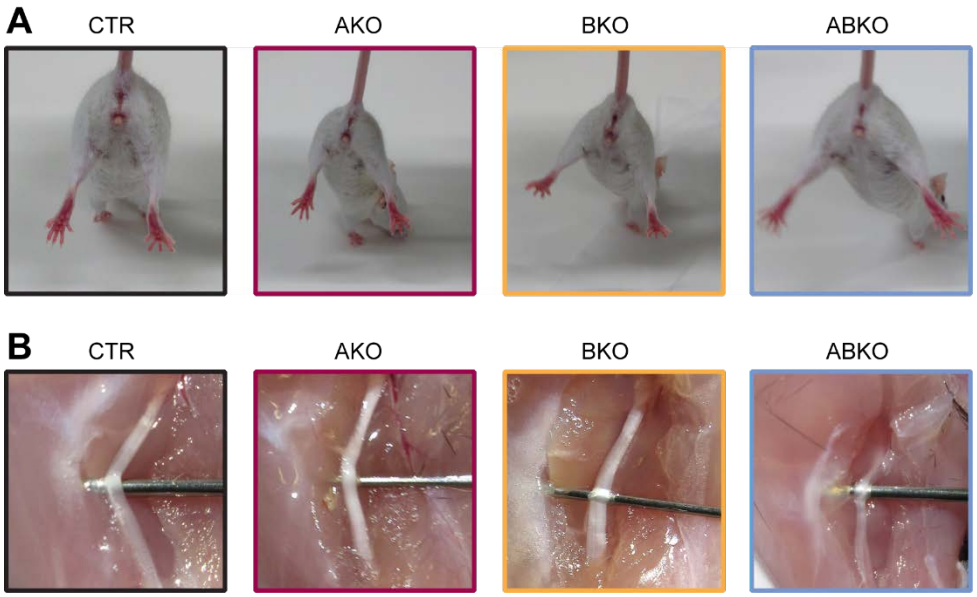

Figure 6: ABKO mice do not show hind limb clasping, but sciatic nerves are thin and translucent. (**A**) Two-month-old Control, AKO, BKO, and ABKO mice were lifted by the tail to check for hind limb clasping. n = at least 20 mice per genotype. (**B**) Sciatic nerves of Control, AKO, BKO, and ABKO mice at two months of age were exposed to check general appearance. n = at least 30 mice per genotype.

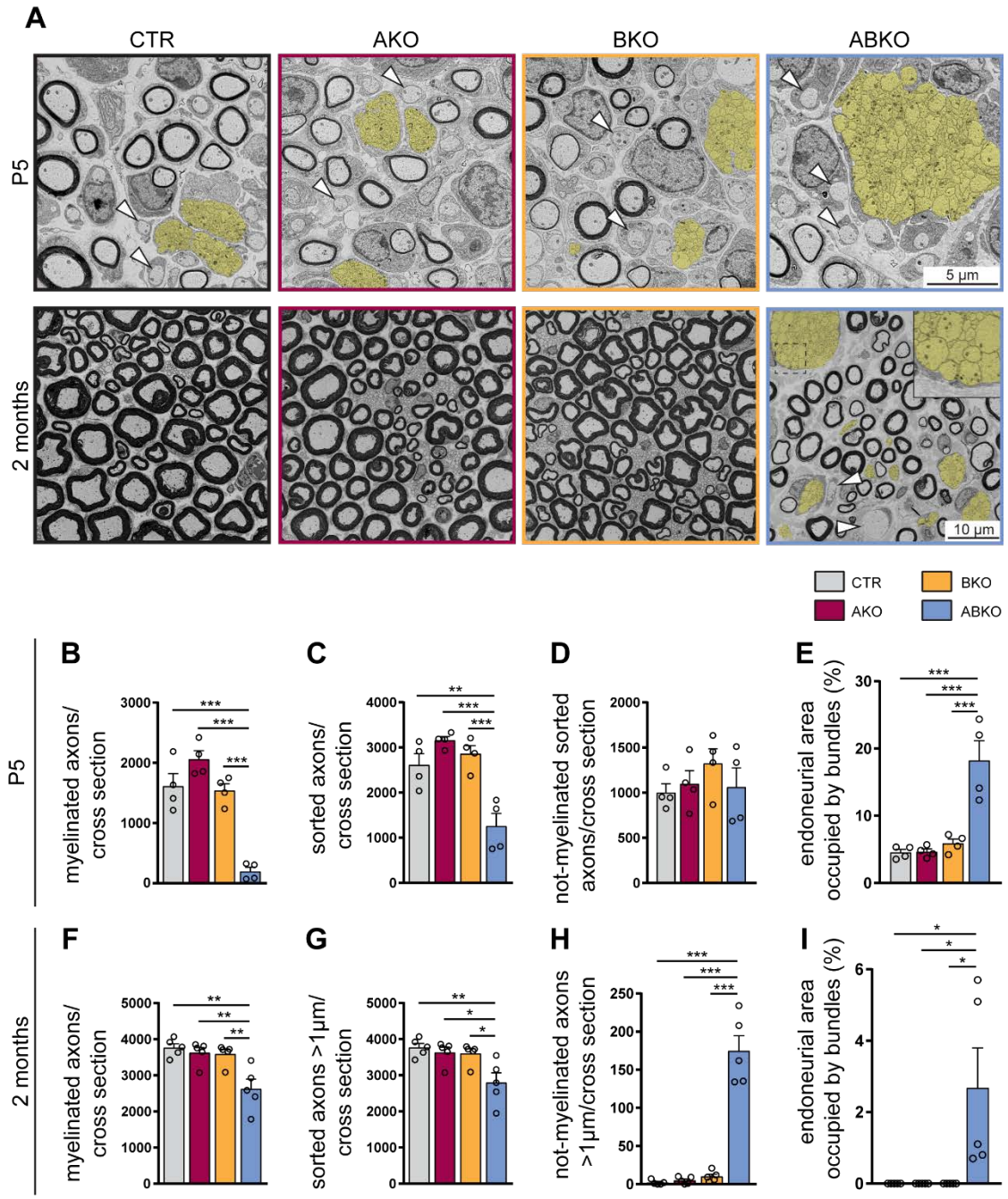

Figure 7: Absence of RalA in Schwann cells and RalB in all cells impairs radial sorting. (**A**) Electron micrographs of sciatic nerves of P5 (upper panel) and two-months-old (lower panel) CTR, AKO, BKO, and ABKO mice. Bundles of unsorted axons are highlighted in yellow. Arrowheads indicate sorted but not-myelinated fibers. (**B – E**) Quantifications of morphological features on P5 sciatic nerve images. The number of myelinated axons (B), all sorted axons (C), and not-myelinated but sorted axons (D) was determined per cross section. The area of endoneurium that is occupied by bundles of unsorted axons was quantified relative to the total endoneurial area (E). n = 4 mice per genotype. One-way Anova with Tukey's multiple comparisons test. (**F – I**) Quantifications of morphological features on two-month sciatic nerve images. The number of myelinated axons (F, shown again in Figure 14B), all sorted axons (G, shown again in Figure 14C), and not-myelinated but sorted axons (H) was determined per cross section. For G and H only axons with a diameter > 1 µm were considered. The area of endoneurium that is occupied by bundles of unsorted axons was quantified relative to the total endoneurial area (I) n = 5 animals per genotype. One-way Anova with Tukey's multiple comparisons test. All data are shown as mean ± SEM. *: $p < 0.05$; **: $p < 0.01$; ***: $p < 0.001$.

When lifted by the tail, none of the two-month-old mice showed clasping of hind limbs (Figure 6A). Dissection of sciatic nerves revealed that nerves of two-month-old ABKO mice were thinner and more translucent than those of CTR mice, while nerves of AKO and BKO mice appeared normal (Figure 6B). Abnormalities in the opacity of the sciatic nerve are often due to reduced myelin content, which could also account for the observed thinning of the sciatic nerve.

5.2. Loss of RalA and RalB impairs radial sorting, while loss of one Ral is dispensable for early PNS development

To investigate if Rals play a role in SCs we asked if peripheral nerves of knockout mice show impaired development or myelination. To address this question, we analyzed cross sections of sciatic nerves at two different time points by scanning electron microscopy (Figure 7A). At P5, ABKO mice showed fewer myelinated (Figure 7B) and total sorted axons (Figure 7C), while the number of sorted but not-myelinated axons was not significantly changed (Figure 7D). A larger part of the endoneurium was occupied by bundles of unsorted axons in ABKO nerves compared to CTR (Figure 7E). These findings indicate that ABKO SCs are able to perform radial sorting of axons, but do so at slower pace than CTR SCs. Once axons are sorted, myelination progresses at a similar rate as in CTR animals.

Similar observations were made when analyzing sciatic nerves of two-month-old ABKO mice, as we found fewer myelinated (Figure 7F) and sorted axons (Figure 7G) along with bundles of unsorted axons that still occupied a significant fraction of the endoneurial area at this age (Figure 7I). In addition, we observed a significant increase in the number of not-myelinated axons with a diameter > 1 µm (Figure 7G). At this age, CTR nerves are fully myelinated, but radial sorting is still not finished in ABKO mice. The presence of not-myelinated axons indicates that radial sorting is potentially still progressing. At both analyzed time points we did not detect changes in the nerves of AKO and BKO mice, suggesting that the presence of one Ral GTPase is enough to ensure normal PNS development. Taken together these findings indicate that deletion of both RalA and RalB in Schwann cells leads to a defect in radial sorting.

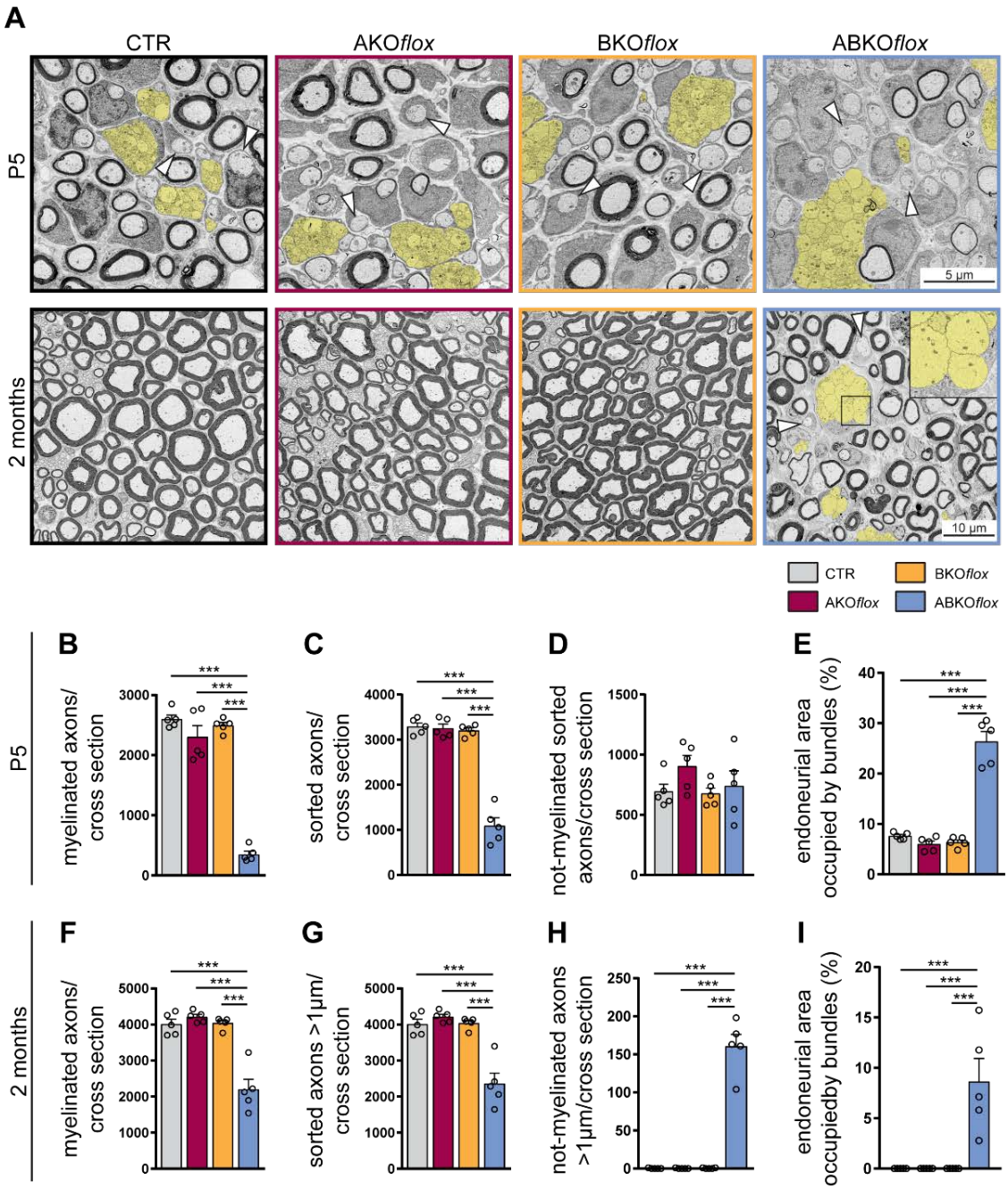

Figure 8: Loss of RalB in cells other than Schwann cells does not contribute to the observed radial sorting defect. (**A**) Electron micrographs of sciatic nerves of P5 (upper panel) and two-month-old (lower panel) Control, AKO*flox*, BKO*flox*, and ABKO*flox* mice. Bundles of unsorted axons are highlighted in yellow. Arrowheads indicate sorted but not-myelinated fibers. (**B – E**) Quantifications of morphological features on P5 sciatic nerve images. The number of myelinated axons (B), all sorted axons (C), and not-myelinated but sorted axons (D) was determined per cross section. The area of endoneurium that is occupied by bundles of unsorted axons was quantified relative to the total endoneurial area (E). n = 5 mice per genotype. One-way Anova with Tukey's multiple comparisons test. (**F – I**) Quantifications of morphological features on two months sciatic nerve images. The number of myelinated axons (F), all sorted axons (G), and not-myelinated but sorted axons (H) was determined per cross section. For G and H only axons with a diameter > 1 µm were considered. The area of endoneurium that is occupied by bundles of unsorted axons was quantified relative to the total endoneurial area (I). n = 5 mice per genotype. One-way Anova with Tukey's multiple comparisons test. All data is shown as mean ± SEM. *: $p < 0.05$; **: $p < 0.01$; ***: $p < 0.001$.

Since Ral GTPases are ubiquitously expressed and were shown to have important functions in various cell types (Gentry et al., 2014), we wanted to verify that the phenotype of ABKO mice resulted from the absence of both Rals specifically in Schwann cells. To this end we obtained mice harboring the floxed *Ralb* allele. We crossed these mice with mice expressing Cre under the control of the *Mpz* promotor (Feltri et al., 1999) to obtain *Mpz*$^{Cre/+}$ Ralb$^{fl/fl}$ (BKO*flox*) mice as well as *Mpz*$^{Cre/+}$ *Rala*$^{fl/fl}$ *Ralb*$^{fl/fl}$ (ABKO*flox*) and *Mpz*$^{Cre/+}$ *Rala*$^{fl/fl}$ mice (AKO*flox*). EM analysis of sciatic nerves at P5 and two months confirmed that radial sorting was impaired in ABKO*flox* mice (Figure 8A). As with the previously analyzed ABKO mice, in comparison to the single knockouts and controls the ABKO*flox* mice had fewer myelinated axons (Figure 8B, F), fewer sorted axons (Figure 8C, G), and a larger fraction of the endoneurium occupied by bundles of unsorted axons (Figure 8E, I). In addition, the number of not-myelinated axons was unchanged at P5 (Figure 8D), indicating that myelination progresses at a normal rate after sorting, but significantly increased at two months (Figure 8H) when control nerves are fully myelinated. We did not detect any morphological changes in AKO*flox* or BKO*flox* mice compared to controls. Taken together these observations indicate that the loss of RalA and RalB specifically in Schwann cells impairs radial sorting. The loss of RalB in other cells does not importantly contribute to the phenotype observed in ABKO mice. They furthermore validate that loss of a single Ral GTPase in Schwann cells does not impair early PNS development.

5.3. Transcriptomic changes in ABKO and ABKO*flox* mice show an upregulation of negative effectors of myelination, downregulation of myelin protein genes, and an upregulation of cyclins

Ral GTPases have been implicated in a wide variety of cellular processes and signaling pathways (see also Figure 4), such as branching of neurites (Lalli and Hall, 2005), formation of filopodia (Ohta et al., 1999; Sugihara et al., 2002), receptor endocytosis (Jullien-Flores et al., 2000), cell polarity (Das et al., 2014), and cell cycle progression (Henry et al., 2000). As radial sorting is a complex event that requires the coordination of many cellular processes

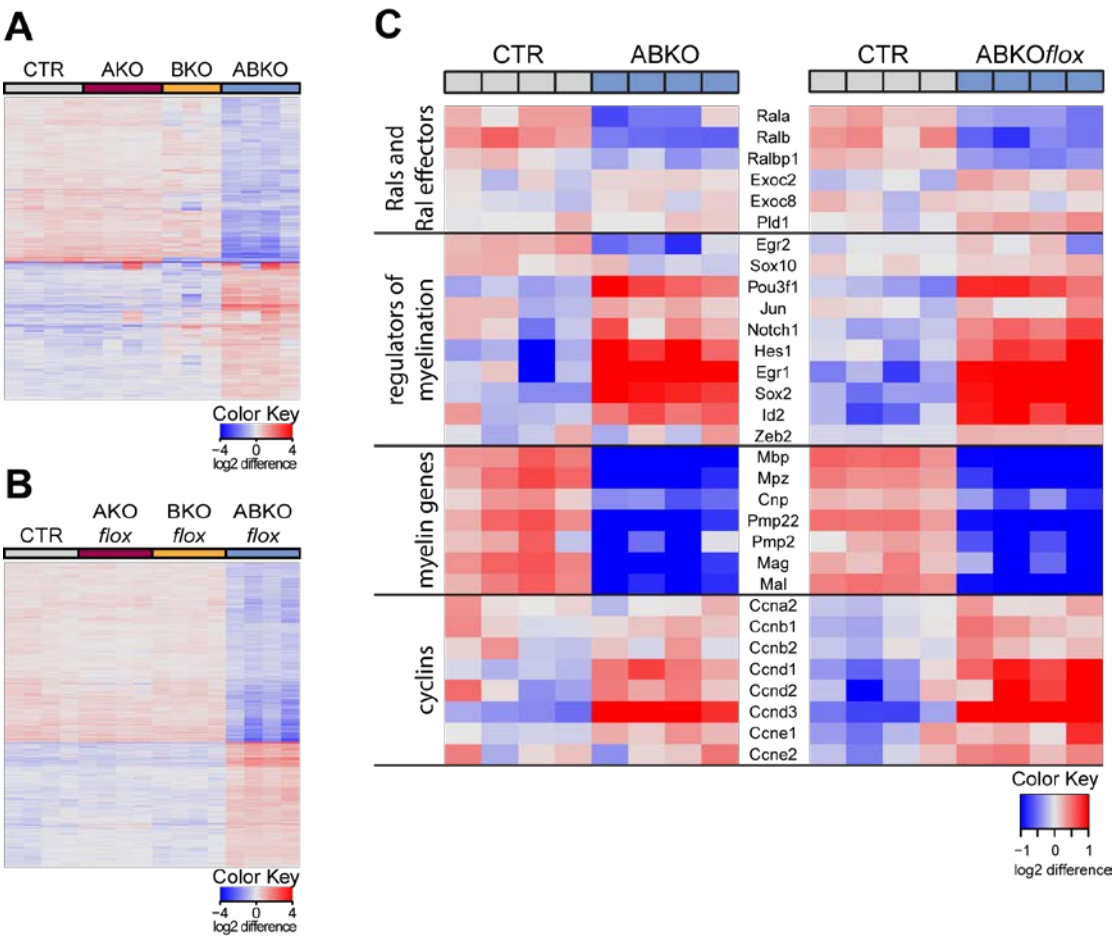

Figure 9: ABKO sciatic nerves show increased expression of negative regulators of myelination and cell cycle genes. (**A**) Heatmap of all differentially expressed genes in sciatic nerves of P5 Control, AKO, BKO, and ABKO mice. n = 4 (CTR, AKO, ABKO) or 3 (BKO) mice per genotype. (**B**) Heatmap of all differentially expressed genes in sciatic nerves of P5 Control, AKO*flox*, BKO*flox*, and ABKO*flox* mice. n = 4 mice per genotype. (**C**) Heatmap showing expression of selected differentially expressed genes in P5 sciatic nerves of Control and ABKO, as well as Control and ABKO*flox* mice. n = 4 mice per genotype. Cut-off for differential expression: FDR < 0.05.

(Feltri et al., 2015), there are numerous different signaling pathways that could be affected by the absence of Rals and could cause the radial sorting defect observed in ABKO mice. We hypothesized that the loss of Rals would lead to changes in the transcriptome of SCs that could help us to identify the overarching deregulated processes. Therefore, we performed sequencing of total mRNA extracted from sciatic nerves of CTR, AKO, BKO, and ABKO mice at P5. Considering all differentially expressed mRNAs (false discovery rate < 0.05), we saw that ABKO mice showed a very different transcriptomic profile compared to the other three genotypes, while profiles of AKO and BKO mice were similar to those of controls (Figure 9A). We repeated the experiment with mRNA from CTR, AKO*flox*, BKO*flox*, and ABKO*flox* mice,

and obtained similar results (Figure 9B). We proceeded to look at the regulation of Rals and their effectors, regulators of myelination, myelin genes, and cyclins in ABKO and ABKO*flox* mice compared to their respective controls (Figure 9C). Both Ral GTPases were downregulated as expected, while among the established effectors (*Ralbp1*, *Pld1*, *Exoc2*, and *Exoc8*) we found both up- and downregulated genes. Looking at known regulators of myelination we saw a tendency towards downregulation of *Egr2*, the master transcriptional regulator of myelination, in both ABKO and ABKO*flox* mice. We further found increased expression of negative regulators of myelination such as *Notch1*, *Hes1*, *Sox2*, and *Id2*. Additionally, myelin genes such as *Mbp* and *Mpz* were less expressed in ABKO and ABKO*flox* nerves. Interestingly, we observed an upregulation of some of the genes encoding cyclins, regulators of cell cycle progression, especially of the cyclin D family. Overall the transcriptomic data show that loss of both Rals leads to a more immature transcriptome profile of sciatic nerves with an upregulation of negative regulators of myelination and a downregulation of myelin genes. Furthermore, an upregulation of cyclins indicates that cell cycle progression may be disturbed in ABKO and ABKO*flox* mice.

5.4. ABKO Schwann cells show increased proliferation and normal rates of apoptosis

Ral GTPases have previously been implicated in cell cycle regulation as well as in the growth and transformation of tumor cells (Bodempudi et al., 2009; Rosse et al., 2003; Tazat et al., 2013). During radial sorting, SCs proliferate to match axon and SC numbers, and disturbances in SC proliferation can cause defects in radial sorting (Feltri et al., 2015). Since mRNA sequencing showed a deregulation of cyclin expression (Figure 9C) we hypothesized that Ral GTPases are important for the regulation of SC proliferation. To investigate this hypothesis, we injected P5 mice with 5-ethynyl-2'-deoxyuridine (EdU) one hour before euthanasia and performed immunohistochemistry to co-label EdU and Sox10, an established SC marker (Figure 10A). Overall cell numbers were increased in all three knockout genotypes compared to control mice (Figure 10B). Meanwhile, SC numbers were significantly increased in BKO,

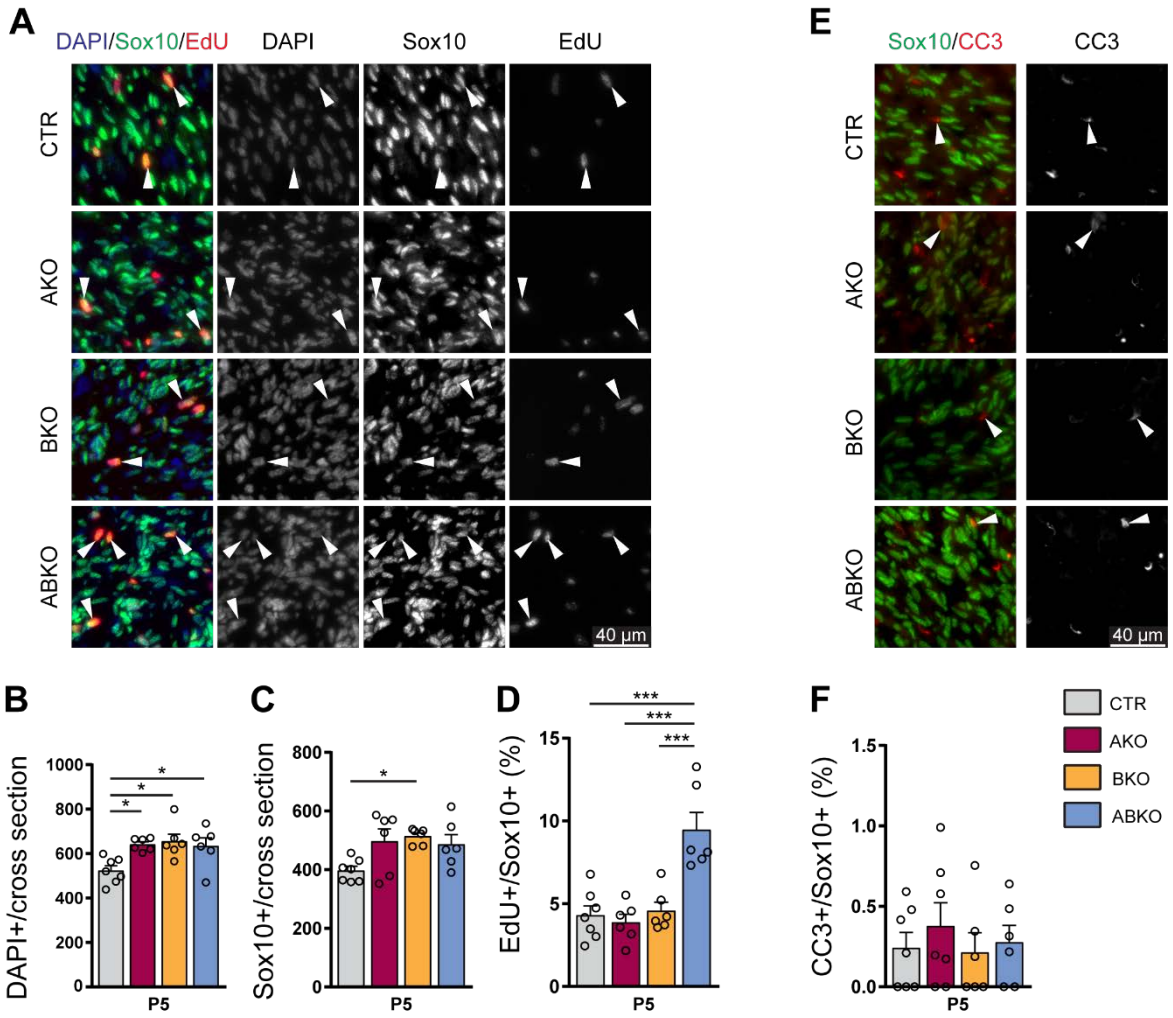

Figure 10: Schwann cell proliferation is increased in sciatic nerves of P5 ABKO mice. (**A**) EdU detection in sciatic nerves of P5 mice injected with EdU one hour prior to dissection. Nuclei were stained with DAPI and SCs labeled by immunostaining for Sox10. Arrowheads highlight EdU-positive Schwann cell nuclei. (**B, C**) Quantification of immunostaining showing all nuclei (B) and all Schwann cells (C) per cross section. n = 7 animals (CTR) or 6 animals (AKO, BKO, ABKO) per genotype, one-way Anova with Tukey's multiple comparisons test. (**D**) The number of proliferating Schwann cells (EdU+) is expressed as a fraction of all Schwann cells. n = 7 animals (CTR) or 6 animals (AKO, BKO, ABKO) per genotype, one-way Anova with Tukey's multiple comparisons test. (**E**) Immunostaining of cleaved caspase 3 (CC3) and Sox10. Arrowheads highlight CC3-positive Schwann cells. (**F**) Quantification of immunostaining showing the number of apoptotic Schwann cells (CC3+) as a fraction of all Schwann cells. n = 7 animals (CTR, AKO) or 6 animals (BKO, ABKO) per genotype. One-way Anova with Tukey's multiple comparisons test. All data are shown as mean ± SEM. *: $p < 0.05$; **: $p < 0.01$; ***: $p < 0.001$.

with a tendency to increase in AKO and ABKO nerves (Figure 10C). While AKO and BKO mice showed no differences in the number of proliferating SCs, we detected significantly more EdU-positive SCs in ABKO mice (Figure 10D). Since not only decreased proliferation but also increased apoptosis can impair radial sorting (Feltri et al., 2015), we stained sciatic nerve

cross sections for Sox10 and cleaved caspase 3 (Figure 10E). We did not detect significant differences in the number of apoptotic SCs for Ral single or double knockout mice (Figure 10F). Since the number of Schwann cells and the percentage of proliferating cells were not decreased, but rather increased, we conclude that the defects in our mutants cannot stem from a lower availability of Schwann cells for radial sorting.

5.5. ABKO Schwann cells show hallmarks of process extension deficits *in vivo* and *in vitro*

Radial sorting defects in a number of mouse models have been attributed to defects in SC process extension or stability, and the small GTPases Rac1, Cdc42, and Rho have been established as key regulators of process extension and radial sorting in SCs (Benninger et al., 2007; Montani et al., 2014; Nodari et al., 2007; Pereira et al., 2009). Since Ral GTPases can influence the activity of Rac1 and Cdc42 (Cantor et al., 1995; Jullien-Flores et al., 1995; Lee et al., 2014; Park and Weinberg, 1995; Zago et al., 2017) we hypothesized that Rals may contribute to the regulation of SC process extension during radial sorting. High resolution EM images of sciatic nerves of two-month-old ABKO mice showed that some of the bundles of unsorted axons that are present at this age were not fully surrounded by SC processes (Figure 11A). We also found loops of redundant basal lamina surrounding these bundles (Figure 11A), which were detached from the SC in some areas. We also observed not-myelinated axons that were incompletely surrounded by a SC and some of them were not visibly in contact with a SC (Figure 11B, C). These observations indicate that ABKO SCs indeed struggle with the formation or maintenance of their processes *in vivo*.

To further this point, we tried to confirm these findings *in vitro*. A number of previously published studies have correlated radial sorting defects with shorter processes due to impaired process extension or stability and impaired formation of lamellipodia in cultured primary SCs (Benninger et al., 2007; Guo et al., 2013; Guo et al., 2012; Jin et al., 2011; Montani et al., 2014; Ness et al., 2013; Nodari et al., 2007; Pereira et al., 2009). Therefore we isolated SCs from the sciatic nerves of P5 mice, plated them on laminin, and analyzed process extension.

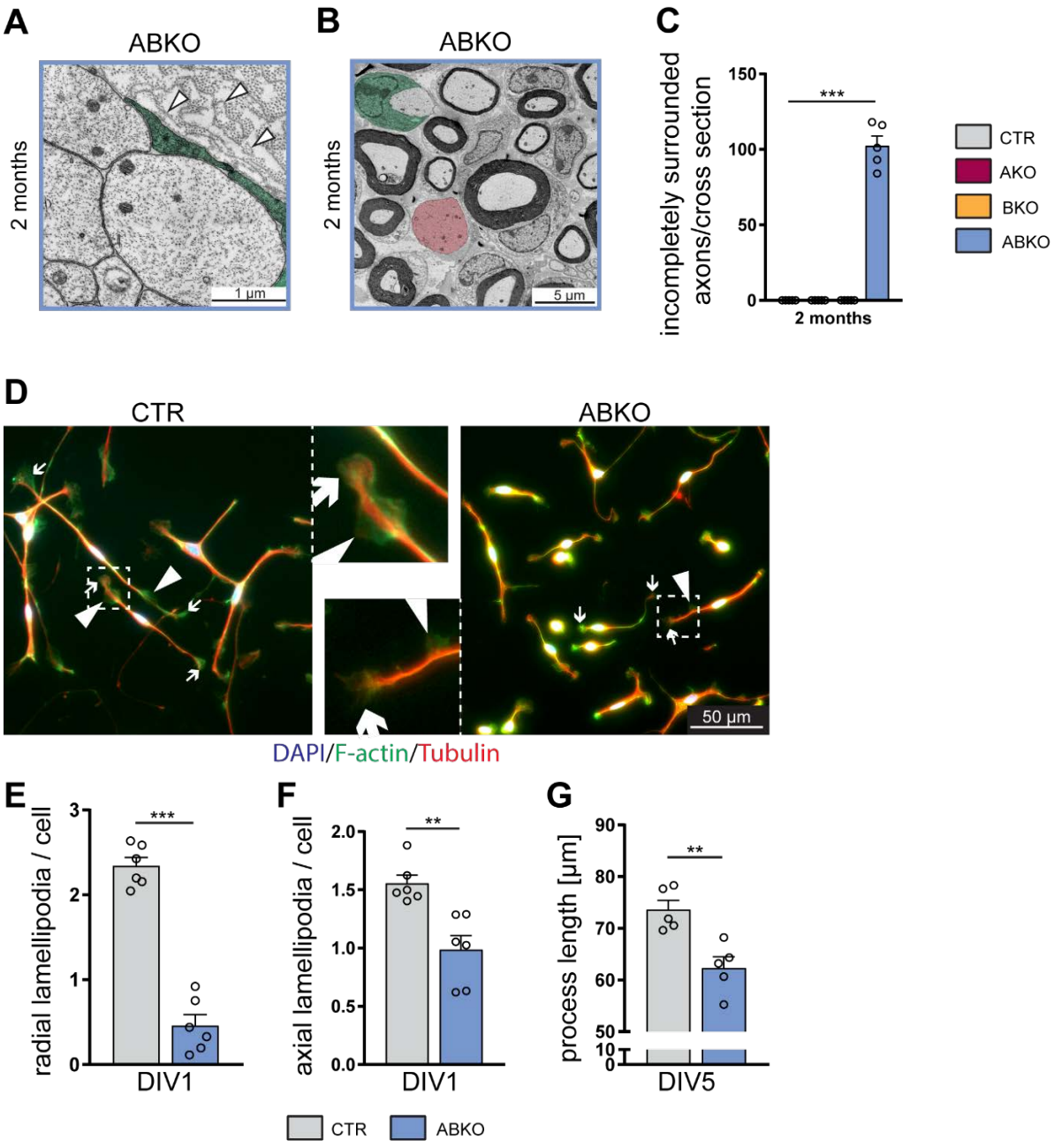

Figure 11: Schwann cells deficient in RalA and RalB show process extension defects *in vivo* and *in vitro*. (**A, B**) Exemplary high-resolution electron micrographs of sciatic nerves of two-month-old ABKO mice. Schwann cell processes that fail to fully surround a bundle (A) or individual axon (B) are highlighted in green. Arrowheads point to loops of basal lamina. An axon that is not visibly in contact with a Schwann cell process is highlighted in pink. (**C**) Quantification of the number of incompletely surrounded, not-myelinated axons with diameter > 1 µm per sciatic nerve cross section in two-month-old animals. n = 5 animals per genotype, one-sample t test. (**D**) Schwann cells isolated from P5 sciatic nerves of CTR and ABKO mice, grown in culture for 24 h on laminin (20 µg/mL). Processes and lamellipodia were visualized by immunostaining of α-tubulin (red) and F-actin (green), and nuclei were labelled with DAPI. Arrows point to axial lamellipodia, arrowheads point to radial lamellipodia. (**E, F**) Number of radial (E) and axial (F) lamellipodia per Schwann cell from P5 sciatic nerves after 24 h in culture on laminin. n = 6 animals per genotype; at least 100 cell per animal. Unpaired two-tailed t test. (**G**) Average process length of Schwann cells from P5 sciatic nerves after five days in culture, plated on laminin. n = 5 mice per genotype; at least 100 cells per animal. Unpaired two-tailed t test. All data are shown as mean ± SEM. *: $p < 0.05$; **: $p < 0.01$; ***: $p < 0.001$.

We visualized processes and lamellipodia by staining of α-Tubulin and F-Actin (Figure 11D). Cultured ABKO Schwann cells showed a reduction in the number of both radial and axial lamellipodia after one day in culture (DIV1; Figure 11E, F). We also assessed the overall length of the processes formed by the cells on DIV5. ABKO SCs had significantly shorter processes compared to control cells (Figure 11G). Given their described involvement in neurite branching (Lalli and Hall, 2005) and filopodia formation (Ohta et al., 1999; Sugihara et al., 2002) the *in vitro* data suggest that Ral GTPases could be important for the cytoskeletal rearrangements that underlie the formation of protrusions in SCs. We conclude that loss of RalA and RalB in SCs impairs the formation or maintenance of cellular processes *in vitro* and *in vivo*, which could account for the observed defect in the sorting of axons.

5.6. RalA promotes process extension in Schwann cells through the exocyst complex

Cellular signaling by small GTPases relies on stringent control of activity levels rather than protein expression levels. Ral GTPases interact with most of their described downstream effectors only in the GTP-bound active form. Four effectors of RalA that have been described in many different cell types are RalBP1 (Cantor et al., 1995), PLD1 (Jiang et al., 1995), and the exocyst complex components 2 and 8 (Brymora et al., 2001). Exchange of a single amino acid in the GTPase can not only interfere with its ability to be activated or inactivated, but can also specifically prevent the interaction with one of the downstream targets (Lalli and Hall, 2005). In order to investigate if the interaction of RalA with one of its known effectors is crucial for SC process extension we utilized lentivirus-mediated infection of cultured SCs to express six different RalA mutants in CTR and ABKO SCs, and analyzed the length of the processes on DIV5.

As proof of principle, we used lentivirus encoding a constitutively active RalA (CA-RalA; RalA72L) to successfully rescue the process length of ABKO Schwann cells (Figure 12A). In contrast, expression of a dominant negative RalA mutant (DN-RalA; RalA28N) did not increase the length of ABKO processes to CTR level (Figure 12B), indicating that RalA needs

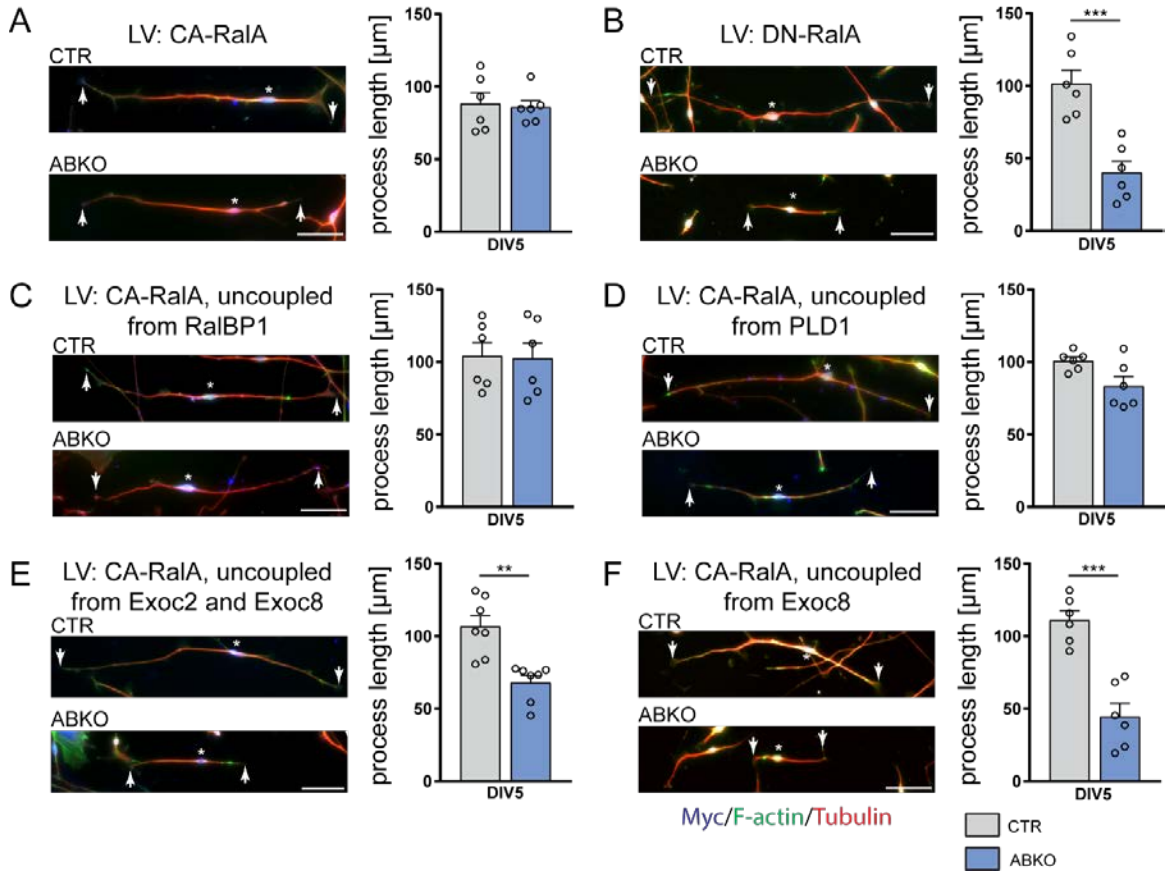

Figure 12: Interaction of RalA with the exocyst complex is crucial for *in vitro* Schwann cell process extension. Exemplary images of a control and ABKO Schwann cell from P5 sciatic nerves infected with lentivirus expressing myc-tagged RalA72L (**A**; constitutively active (CA) RalA), myc-tagged RalA28N (**B**; dominant negative (DN) RalA), myc-tagged RalA72L D49N (**C**; CA-RalA uncoupled from interaction with RalBP1), myc-tagged RalA72L ΔN11 (**D**; CA- RalA uncoupled from interaction with PLD1), myc-tagged RalA72L D49E (**E**; CA-RalA uncoupled from interaction with Exoc2 and Exoc8), myc-tagged RalA72L A48W (**F**; CA-RalA uncoupled from interaction with Exoc8). Processes and lamellipodia were visualized by immunostaining of α-tubulin (red) and F-actin (green), and infection was controlled by immunostaining for myc (blue). Arrows indicate the far ends of SC processes, asterisks mark the location of the SC nuclei along the SC length. Quantifications of average process length are depicted on the right. n = 6 mice per genotype; at least 100 cells per animal; multiple unpaired two-tailed t tests with Holm-Sidak method for multiple comparisons correction. All data are shown as mean ± SEM. *: $p < 0.05$; **: $p < 0.01$; ***: $p < 0.001$.

to be active to promote process extension in Schwann cells. Notably, expression of the dominant negative RalA mutant in control cells did not reduce the average process length when compared to the other control cells in this experiment, indicating that the activity of RalB is not impaired by expression of DN-RalA and is sufficient to maintain process length in agreement with absence of defects in RalA single knockout mice.

Lentiviral expression of RalA72L D49N, a CA-RalA that is unable to interact with RalBP1, was able to rescue the process extension deficit of ABKO Schwann cells (Figure 12C). We also observed a rescue by expressing RalA72L ΔN11, a CA-RalA uncoupled from interaction with PLD1 (Figure 12D), indicating that the interactions of RalA with RalBP1 and PLD1 are not essential for SC process extension *in vitro*. In contrast, expression of RalA72L D49E, which encodes a CA-RalA unable to interact with the exocyst complex subunits Exoc2 and Exoc8, was not able to improve the process length of ABKO Schwann cells to CTR levels (Figure 12E). Similarly, we did not observe a rescue when expressing RalA72L A48W, a CA-RalA uncoupled only from Exoc8 (Figure 12F). These results show that RalA promotes process extension in SCs through interaction with the exocyst complex components Exoc2 and Exoc8, suggesting that the exocyst complex could also play a role in radial sorting.

5.7. RalA is activated by growth factors in cultured rat Schwann cells

Defective radial sorting due to impaired process extension has almost exclusively been attributed to two signaling cascades downstream of the laminin receptor integrin β1 (Feltri et al., 2002): ILK-Rho-ROCK-Pfn and LCK-Paxillin-CrkII-Rac1. We therefore thought it possible that Rals also act downstream of laminin and laminin receptors such as integrins, an idea that is not completely new in the context of Ral GTPase function. A previous study reported that RalA was activated when sympathetic superior cervical ganglia neurons were plated on laminin (Lalli and Hall, 2005). A different study found that RalA and the exocyst complex mediate integrin-dependent membrane raft exocytosis upon re-plating of MEFs (Balasubramanian et al., 2010). Canonically, activation of Rals occurs downstream of Ras, since RalGEFs are direct effectors of active Ras (Hofer et al., 1994; Kikuchi et al., 1994; Peterson et al., 1996; Shao and Andres, 2000; Spaargaren and Bischoff, 1994). Ras itself is activated by receptor tyrosine kinases, thus responding to a variety of growth factors, e.g. EGF and insulin-like growth factor (IGF) (Alberts et al., 2015).

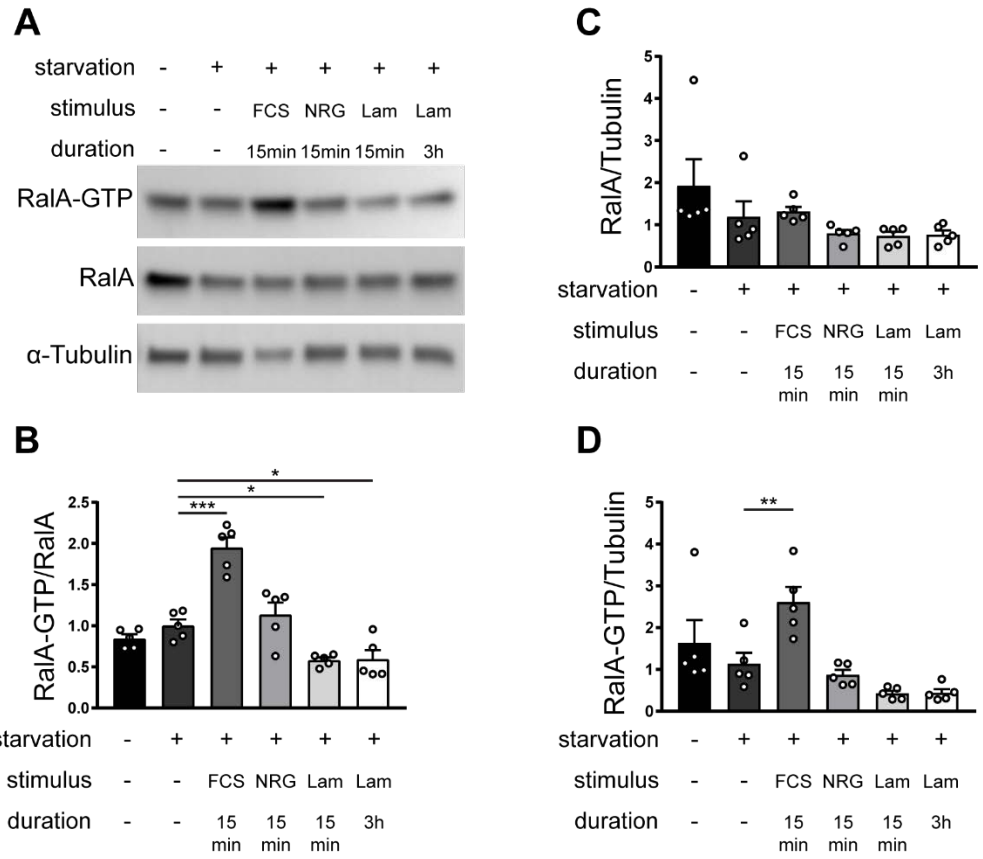

Figure 13: RalA is activated by growth factors in cultured Schwann cells. Primary rat SCs were serum-starved for 24 h and treated with the indicated stimuli. GTP-bound RalA was precipitated using the GST-coupled Ral-binding-domain of RalBP1 and detected by immunoblot. (**A**) Representative immunoblot showing GTP-bound RalA, total RalA, and housekeeper. (**B-D**) Densitometric quantification of immunoblots. n = 5 technical replicates. One-way Anova with Dunnett's multiple comparisons test; all data are shown as mean ± SEM. *: $p < 0.05$; **: $p < 0.01$; ***: $p < 0.001$.

In order to determine if RalA responds to laminin signaling in Schwann cells, we treated serum-starved primary SCs from neonatal rats with 10 µg/mL soluble Laminin111 for 15 min or 3 h. As a positive control, we treated cells for 15 min with 10% fetal calf serum (FCS), which contains many different growth factors that rapidly activate both Ras and Ral (Hofer et al., 1998). We also included cells stimulated with 10 ng/mL NRG1, which is known to regulate many aspects of SC development (Birchmeier and Bennett, 2016). We assessed activity of RalA by precipitating GTP-bound RalA with a GST-coupled Ral-binding-domain of RalBP1 (Hofer et al., 1998) and subsequent immunoblotting (Figure 13A). We saw a robust increase in RalA activity after 15 min stimulation with FCS, while NRG1 did not have a detectable effect (Figure 13B). Stimulation for 15 min or 3 h with Laminin111 led to a small but reproducible

reduction in RalA activity (Figure 13B). Neither condition reliably affected the total level of RalA expression (Figure 13C, D). Our results show that in cultured rat SCs, RalA is activated in response to growth factors and inhibited by Laminin111, while NRG1 does not influence RalA activity.

5.8. Long-term loss of RalA in Schwann cells and RalB in all cell types leads to demyelination

As the radial sorting defects observed in ABKO mice improved between P5 and two months (Figure 7), we wondered if radial sorting would eventually be completed in mutant mice at an even later time point. We therefore performed morphological analysis of sciatic nerves of one-year-old CTR, AKO, BKO, and ABKO mice. The analysis revealed that radial sorting was not completed in one-year-old ABKO mice, since bundles of unsorted axons were still present at this age (Figure 14A, lower panel). We also observed a persistent reduction in the number of both myelinated and sorted axons (Figure 14B, C). Interestingly, the number of myelinated and of sorted axons decreased from two months to one year, suggesting loss of axons (Figure 14B, C). In addition, ABKO mice showed hypomyelination of large caliber axons at both two months and one year (Figure 14D, E). Small caliber axons were hyper-myelinated in two-month-old mice but not anymore in one-year-old mice (Figure 14D, E). We did not detect morphological changes in one-year-old AKO mice. However, one-year-old BKO mice displayed hypermyelination across all axonal sizes (Figure 14E). This surprising finding indicates a potential role for RalB in the homeostasis of mature myelin. Overall these observations show that radial sorting is not completed in adult ABKO mice. In addition, there is evidence of ongoing de- and remyelination in the deregulation of the g-ratio as well as axonal loss, indicating a potential role for Ral GTPases in the long-term maintenance of myelin and axons.

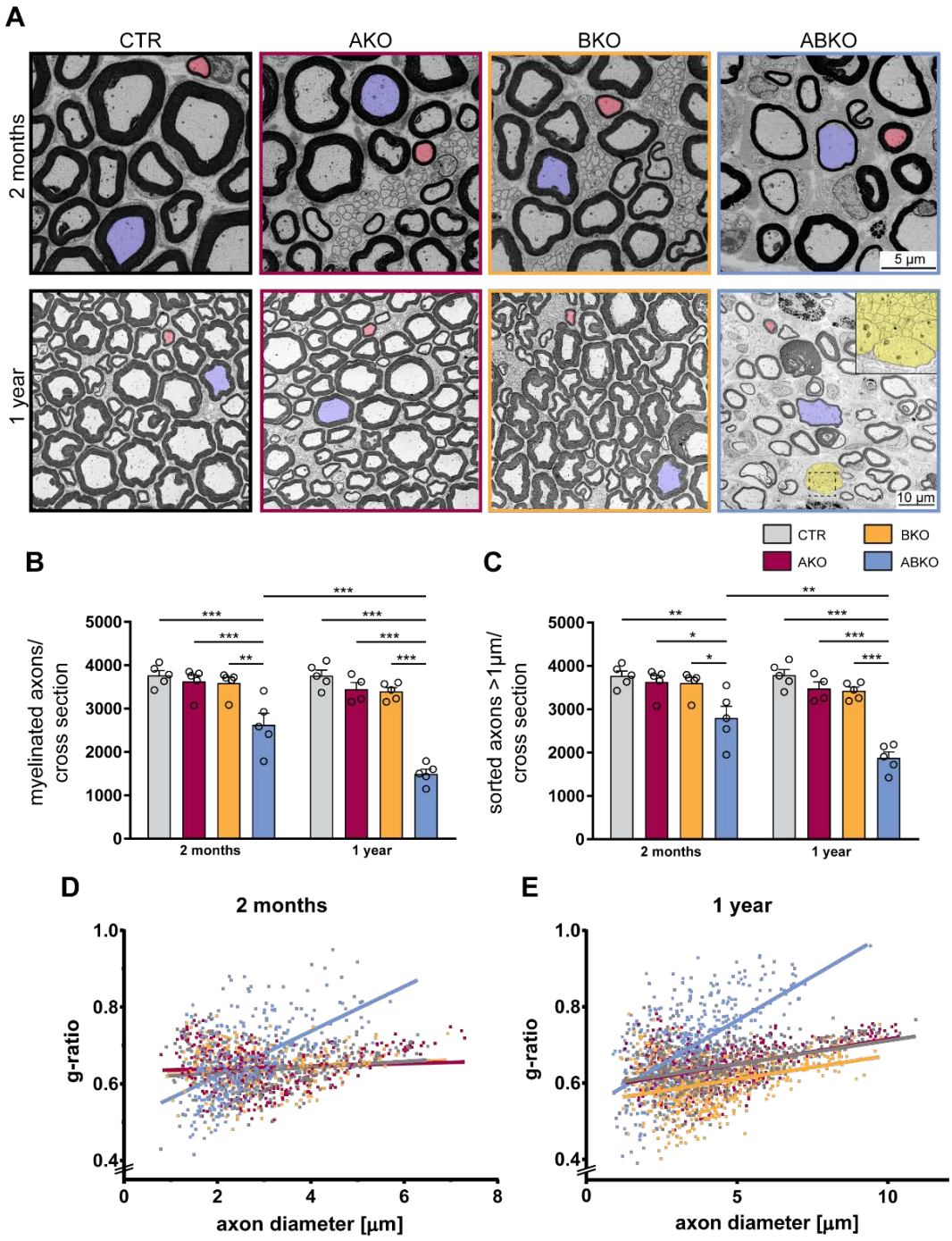

Figure 14: Long-term loss of RalA in Schwann cells and RalB in all cells leads to demyelination and potential axonal loss. (**A**) Electron micrographs of sciatic nerves of Control, AKO, BKO, and ABKO mice at two months (upper panel) and one year (lower panel) of age. Bundles of unsorted axons in one-year-old mice are highlighted in yellow. A small and large axon are marked in red and blue, respectively. (**B, C**) Quantification of myelinated axons (B; shown also in Figure 7F) and all sorted axons with a diameter > 1 µm (C; shown also in Figure 7G) per sciatic nerve cross section in mice at ages two months and one year. n = 5 mice (CTR, BKO, ABKO; AKO at two months) or 4 mice (AKO at one year). Two-way Anova with Tukey's multiple comparisons test. Data are shown as mean ± SEM. *: $p < 0.05$; **: $p < 0.01$; ***: $p < 0.001$. (**D, E**) Distribution of g-ratio versus axon diameter in mice at two months (D) and one year (E). Each dot represents the measurement for an individual axon. n = 5 mice (CTR, BKO, ABKO; AKO at two months) or 4 mice (AKO at one year). Lines show linear regression.

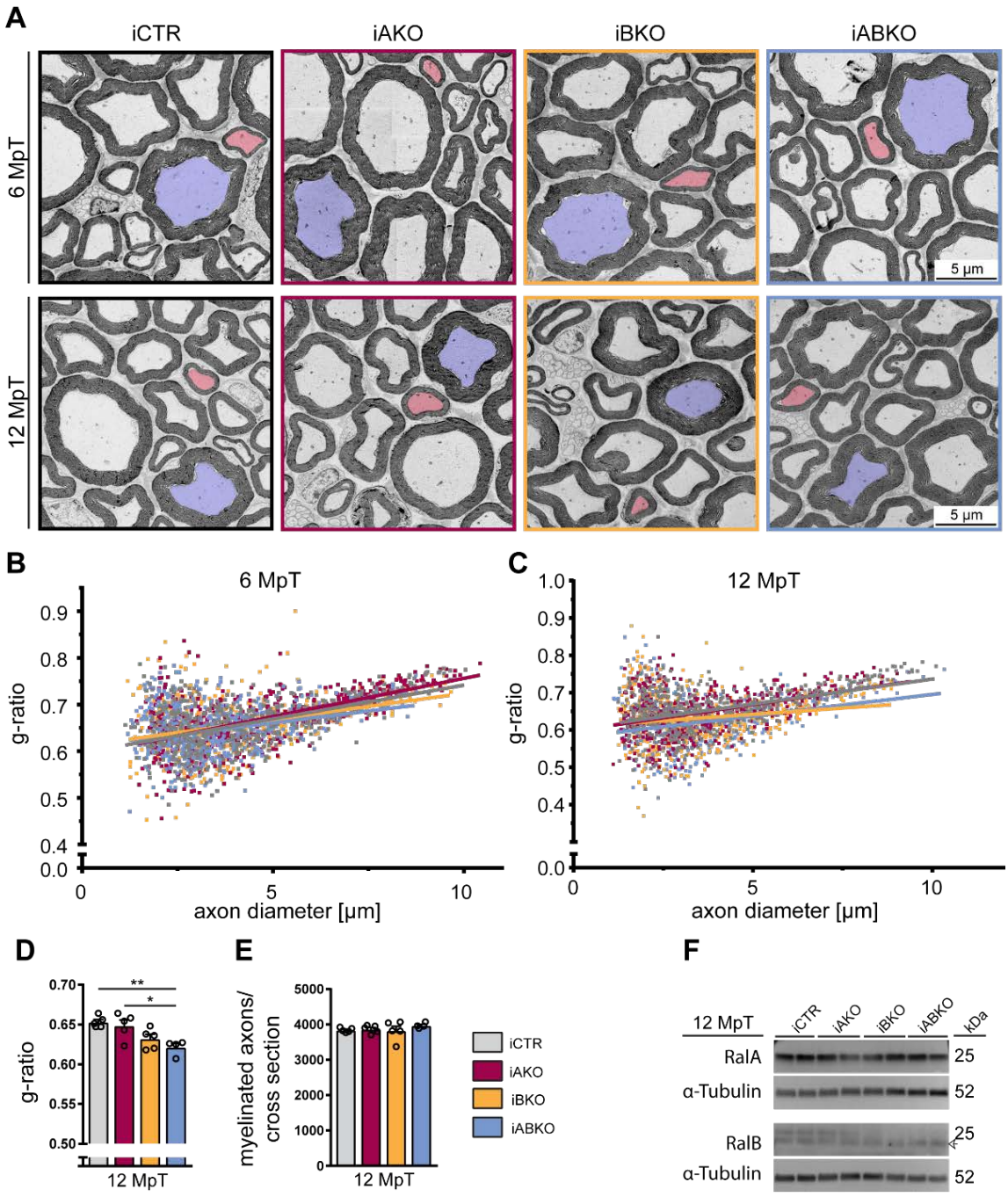

Figure 15: Ral GTPases are potentially dispensable for the maintenance of myelin and axons in the sciatic nerve. (**A**) Electron micrographs of sciatic nerves of iCTR, iAKO, iBKO, and iABKO mice at age 6 MpT (upper panel) and 12 MpT (lower panel). A small and large axon are marked in red and blue, respectively. (**B, C**) Distribution of g-ratio versus axon diameter in mice at 6 MpT (B) and 12 MpT (C). Each dot represents the measurement for an individual axon. Lines show linear regression. (**D**) Average g-ratio in the sciatic nerve at 12 MpT. (**E**) Quantification of myelinated axons per sciatic nerve cross section at 12 MpT. For B-E: n = 5 mice (Control, iAKO, iBKO) or 4 mice (iABKO) per genotype; For D-E: one-way Anova with Tukey's multiple comparisons test. (**F**) Representative immunoblots detecting RalA and RalB in sciatic nerve lysates at 12 MpT. Arrow indicates unspecific binding of the RalB antibody. All data are shown as mean ± SEM. *: $p < 0.05$; **: $p < 0.01$; ***: $p < 0.001$.

5.9. RalA and RalB are potentially dispensable for myelin maintenance after developmental myelination

As reported in the previous section, adult mice that had lost RalA and RalB early on in SC development showed hallmarks of demyelination and axonal loss. Therefore we hypothesized that Rals could be important for the long-term stability of myelin and maintenance of axons. However, the developmental defects of ABKO mice persisted up to one year of age, as indicated by bundles of unsorted axons. With our developmental mouse model it was therefore impossible to determine if the not-myelinated axons present at this age were due to still ongoing radial sorting or to demyelination, although the reduction in the number of myelinated axons between two months and one year suggested the latter (Figure 14B). Similarly, the reduced number of sorted fibers from two months to one year suggests that axons are degenerating (Figure 14C). However we cannot exclude the possibility that these axons are still present in the bundles of unsorted axons. In addition it is possible that these observations are merely long-term effects resulting from the absence of Rals during developmental myelination.

We therefore decided to investigate specifically the function of Rals in the maintenance of the adult nerve. To this end we crossed *Rala*$^{fl/fl}$ *Ralb*$^{-/-}$ mice with a strain harboring a tamoxifen-inducible CreERT2 recombinase under the control of the glia-specific proteolipid protein (*Plp*) promoter (Leone et al., 2003). We thus obtained mice with an inducible deletion of RalA on the background of constitutive RalB deletion (*Plp*$^{CreERT2/+}$ *Rala*$^{fl/fl}$ *Ralb*$^{-/-}$; hereafter iABKO). We also obtained mice with inducible knockout of RalA alone (*Plp*$^{CreERT2/+}$ *Rala*$^{fl/fl}$; hereafter iAKO). Recombination was induced by tamoxifen injections at 10 weeks of age. To account for effects of the tamoxifen injection, control (*Rala*$^{fl/fl}$; hereafter iCTR) and RalB single knockout mice (*Ralb*$^{-/-}$; hereafter iBKO) were injected with tamoxifen as well.

We analyzed sciatic nerves six and 12 months post tamoxifen injection (MpT) by scanning electron microscopy (Figure 15A). For both time-points, we did not observe major alterations of the sciatic nerve morphology. At 6 MpT, myelin thickness was not changed for any of the

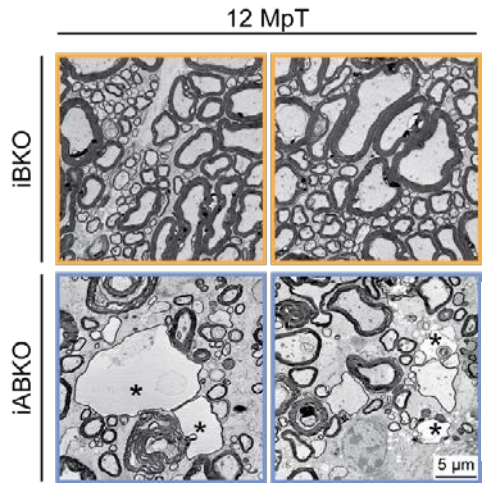

Figure 16: Tamoxifen injection leads to morphological abnormalities in spinal cords of iABKO mice. Representative electron micrographs of the ventral lumbar spinal cord of iBKO and iABKO mice at 12 MpT. Asterisks mark areas of vacuolation.

analyzed genotypes (Figure 15B). However at 12 MpT we observed thicker myelin sheaths in iBKO and iABKO animals (Figure 15C, D). We had already observed hypermyelination in one-year-old BKO mice (Figure 14E), indicating that this is due to the loss of RalB specifically. We were surprised that iABKO mice did not have a stronger phenotype than iBKO mice, indicating that RalA does not play a role in myelin maintenance or axonal stability. To confirm that recombination had actually occurred in these mice we analyzed protein levels of RalA and RalB in sciatic nerves at 12MpT (Figure 15F). Surprisingly, we were unable to detect a reduction in RalA expression in iAKO and iABKO nerve lysates, while RalB was not detectable in iBKO and iABKO nerves. Again of note is the unspecific binding of the RalB antibody (Figure 15F).

As we were unable to show loss of RalA by protein analysis we sought other means to determine if recombination had happened in the mice. Since *Plp*^{CreERT2} also recombines in oligodendrocytes, we analyzed spinal cords of the same mice for defects in the CNS as part of a different project. Spinal cords from iABKO mice were clearly different from iBKO mice, showing large areas of vacuolation and possibly fewer myelinated axons (Figure 16). This observation suggests that recombination of the *Rala* locus has happened in oligodendrocytes; however analysis of protein expression of mRNA levels of RalA would be necessary to validate this point. Taken together our data show that in the PNS, loss of RalB leads to long-term

hypermyelination while RalA may be dispensable for myelin maintenance after developmental myelination.

6. Discussion

Small GTPases of the Ras and Rho families are well established regulators of essential Schwann cell functions. Rac1 activity is required for the formation of lamellipodia downstream of integrin signaling (Benninger et al., 2007; Nodari et al., 2007), thus being an important player in radial sorting. Cdc42 has been reported as a regulator of Schwann cell proliferation during early development (Benninger et al., 2007). Data on Rho points to a potential role in regulating cell morphology, actin stress fiber formation, and substrate adhesion (Melendez-Vasquez et al., 2004). Furthermore, increased Ras activity due to loss of NF1 can lead to malignant transformation of Schwann cells (Durbin et al., 2016), a process that was reported to involve RalA (Bodempudi et al., 2009).

The small Ras-like GTPases RalA and RalB have been implicated in a variety of cellular events including proliferation (Kashatus et al., 2011), receptor-mediated endocytosis (Jullien-Flores et al., 2000), mTOR signaling (Xu et al., 2011), vesicle targeting (Teodoro et al., 2013), and autophagy (Bodemann et al., 2011). We know from previous studies that Ral GTPases are expressed and active in SCs (Bodempudi et al., 2009), that RalA mRNA expression increases during early PNS development (Patzig et al., 2011), and that both GTPases are present in pseudopods (Poitelon et al., 2015), small and temporary cytoplasmic projections that cells form in response to a stimulus. We therefore hypothesized that Ral GTPases could be important regulators of SC development.

In the present study we demonstrate that the small GTPases RalA and RalB are required for radial sorting and exert redundant or compensatory functions. In fact, loss of a single Ral GTPase is compatible with normal SC development, while loss of both Rals leads to a partial block in radial sorting. A thorough analysis of SC morphology *in vivo* and *in vitro* revealed that the impaired radial sorting is likely due to defects in the extension of processes. Furthermore we showed, by utilizing mutants of RalA that are unable to interact with one of the downstream

effectors, that the interaction of RalA with the exocyst complex is necessary to promote process extension in cultured SCs.

6.1. Expression of one Ral GTPase is sufficient for PNS development

RalA and RalB are highly similar proteins, sharing 85% of their amino acid sequence and identical effector binding regions (Chardin and Tavitian, 1989). Thus, they are regulated by the same set of GEFs and GAPs and utilize the same downstream effectors. Still, reports on functional redundancy between the two GTPases vary depending on the system that is studied. In a mouse model of Ras-driven non-small cell lung carcinoma it was shown that expression of either RalA or RalB is sufficient to drive tumorigenesis (Peschard et al., 2012). Meanwhile, multiple studies reported that in various human cancer cell lines, Ras-driven transformation depends solely on RalA and not RalB (Chien and White, 2003; Lim et al., 2005; Lim et al., 2006; Sablina et al., 2007). We found that in our mouse model, expression of only one Ral GTPase was sufficient for normal radial sorting, indicating that during PNS development Rals are either functionally redundant or can compensate for the loss of the other.

While qPCR data showed an upregulation of RalB mRNA upon loss of RalA, we did not observe this on the protein level. However, a compensation could involve other mechanisms besides transcription and translation. There is evidence suggesting that divergent functions of the two Ral GTPases are mediated by distinct intracellular localization (Shipitsin and Feig, 2004), which is largely dependent on lipid-modifications of the C-terminal region (Falsetti et al., 2007). While RalA was reported to associate with the plasma membrane as well as endosomes, RalB was shown to localize predominantly to endosomes (Shipitsin and Feig, 2004). Shifts in the localization of the remaining GTPase could be sufficient to compensate for the loss of the other. Thus, it would be interesting to analyze the intracellular localization of the two Ral GTPases in wild-type and single Ral knockout Schwann cells. In addition, the activity levels of Ral GTPases can be flexibly regulated by RalGEFs and RalGAPs, providing yet another mechanism how SCs could compensate for the loss of one Ral GTPase (Peschard

et al., 2012). This issue could be addressed by assessing the levels of active RalA in sciatic nerve lysates in the absence of RalB and vice versa by precipitation of GTP-bound Ral with the Ral-binding domain of RalBP1, comparing single knockout nerves to controls.

6.2. Loss of Rals increases proliferation in SCs

RalGEFs are direct targets of active Ras and the Ras-RalGEF-Ral axis was previously shown to drive malignant transformation of SCs, leading to the formation of malignant peripheral nerve sheath tumors (Bodempudi et al., 2009). In cultured MPNST cells, a decrease in Ral activity led to reduced proliferation and invasiveness (Bodempudi et al., 2009). We therefore hypothesized that loss of Ral GTPases during SC development would likewise impair SC proliferation, which can result in a radial sorting defect as has been demonstrated in mice lacking FAK (Grove et al., 2007) or the small GTPase Cdc42 (Benninger et al., 2007). Surprisingly we found the opposite, an increase in proliferation of SCs in P5 sciatic nerves of ABKO mice. At the same time we did not detect major differences in apoptosis while we only saw a mild and non-significant increase in the number of SCs per cross section in ABKO mice, which was also present in the single knockout nerves although those did not show increased proliferation. It is therefore possible that the Ras-RalGEF-Ral axis is involved in the fine-tuning of SC proliferation during development.

Follow-up experiments could be conducted to gain further insight into the role of Ral GTPases in SC proliferation and survival by looking at proliferation and apoptosis in adult nerves. Due to our observations in P5 sciatic nerves we would expect to see either an increase in the number of SCs or, if that is not the case, an increase in the number of apoptotic SCs. Notably we did not observe major differences in proliferation and survival of ABKO SCs compared to CTR while culturing primary SCs from sciatic nerves of P5 mice, although we did not specifically address this question. In sciatic nerves of wild-type mice, SC proliferation gradually decreases during the early postnatal days while radial sorting completes and myelination is ongoing (Brown and Asbury, 1981). It is therefore possible that the increase in proliferating SCs at P5 is a secondary effect, resulting from the delayed sorting of axons in ABKO mice.

6.3. Ral GTPases influence process extension in SCs, possibly downstream of laminin and growth factors

We were able to identify defects in process extension of Schwann cells *in vivo* and *in vitro* as the likely cause for the radial sorting defect in ABKO mice. On EM images we observed detached basal lamina and loops of redundant basal lamina, as well as sorted axons and bundles of unsorted axons that were only partially or not at all covered by a Schwann cell process. Notably, such features have been described for integrin β1 (Feltri et al., 2002) and Rac1 (Benninger et al., 2007; Nodari et al., 2007) knockout mice. Consistent with the findings of both of these studies, we observed shorter processes and less lamellipodia formed by ABKO Schwann cells in culture. Based on the observation that SCs lacking integrin β1 have defects in the formation of radial but not axial lamellipodia *in vitro*, it has been proposed that radial lamellipodia are especially important for radial sorting (Nodari et al., 2007). The authors also proposed a model in which lower levels of active Rac1 led to migration of SCs, formation and elongation of axial lamellipodia and processes along the axon, while an increase in Rac1 activity would induce the formation of radial lamellipodia, which are necessary for radial sorting and myelination (Nodari et al., 2007). Recently, live-imaging on cultured SCs showed that *in vitro*, the initial contact between SC and axon is preferentially formed by an axial lamellipodium of the SC, while radial lamellipodia are involved in stabilizing and maintaining contact over longer periods of time (Velasquez et al., 2018). Notably, ABKO SCs showed defects in the formation of both axial and radial lamellipodia, indicating that at least one other signaling cascade influencing the cytoskeleton, besides the ones downstream of integrin β1, is dysregulated in the absence of Ral GTPases.

Different studies have shown that ablation of the laminins α2, α4, or γ1 leads to radial sorting impairments, largely attributable to defects in proliferation and survival of SCs (Chen and Strickland, 2003; Occhi et al., 2005; Patton et al., 2008; Wallquist et al., 2005; Yang et al., 2005; Yu et al., 2005). Loss of integrin β1 also impedes proliferation (Berti et al., 2011) and causes a prominent defect in the extension of processes as discussed above (Feltri et al.,

2002; Nodari et al., 2007). Downstream of integrin β1 two parallel signaling cascades have been described that regulate process extension and lamellipodia formation in SCs (see Figure 17). On the one hand, integrin receptors activate ILK. As part of the ILK-PINCH-Parvin complex, ILK indirectly inhibits Rho and its downstream effector ROCK to promote the extension of processes (Pereira et al., 2009). Inhibition of ROCK also prevents the phosphorylation and inhibition of Profillin1 to promote lamellipodia formation (Montani et al., 2014). On the other hand, integrin β1 signaling activates lymphoid cell kinase (LCK) which, through involvement of Paxillin and CrkII, activates Rac1 to promote lamellipodia formation (Ness et al., 2013; Nodari et al., 2007). Active Rac1 also promotes the extension of processes, in part by inhibiting NF2/Merlin (Benninger et al., 2007; Guo et al., 2012).

We demonstrated that Rals are implicated in the regulation of process extension for radial sorting, similar to observations made for the signaling cascades downstream of integrin β1 (Benninger et al., 2007; Feltri et al., 2002; Guo et al., 2012; Montani et al., 2014; Ness et al., 2013; Nodari et al., 2007; Pereira et al., 2009). It is also known that Rals can influence the activity of Rac1, one of the downstream effectors of integrin β1, in other cell types (Lee et al., 2014). Although the canonical activation of Rals occurs downstream of Ras (Hofer et al., 1994; Kikuchi et al., 1994; Peterson et al., 1996; Shao and Andres, 2000; Spaargaren and Bischoff, 1994), and Ras itself is activated by receptor tyrosine kinases (Alberts et al., 2015), it has also been proposed that Rals play a role downstream of integrin signaling (Balasubramanian et al., 2010; Lalli, 2009). In mouse embryonic fibroblasts, RalA has been reported to mediate membrane raft exocytosis in response to integrin signaling through interaction with the exocyst complex (Balasubramanian et al., 2010). Furthermore it was shown that RalA activity increased when cortical neurons were plated on laminin (Lalli, 2009). We therefore thought it possible that Ral GTPases are also part of the signaling network that regulates cytoskeletal rearrangement downstream of integrin β1 in Schwann cells.

To address this question we analyzed RalA activity in cultured rat SCs that were exposed to different stimuli. Surprisingly we saw a small but consistent reduction of RalA activity in

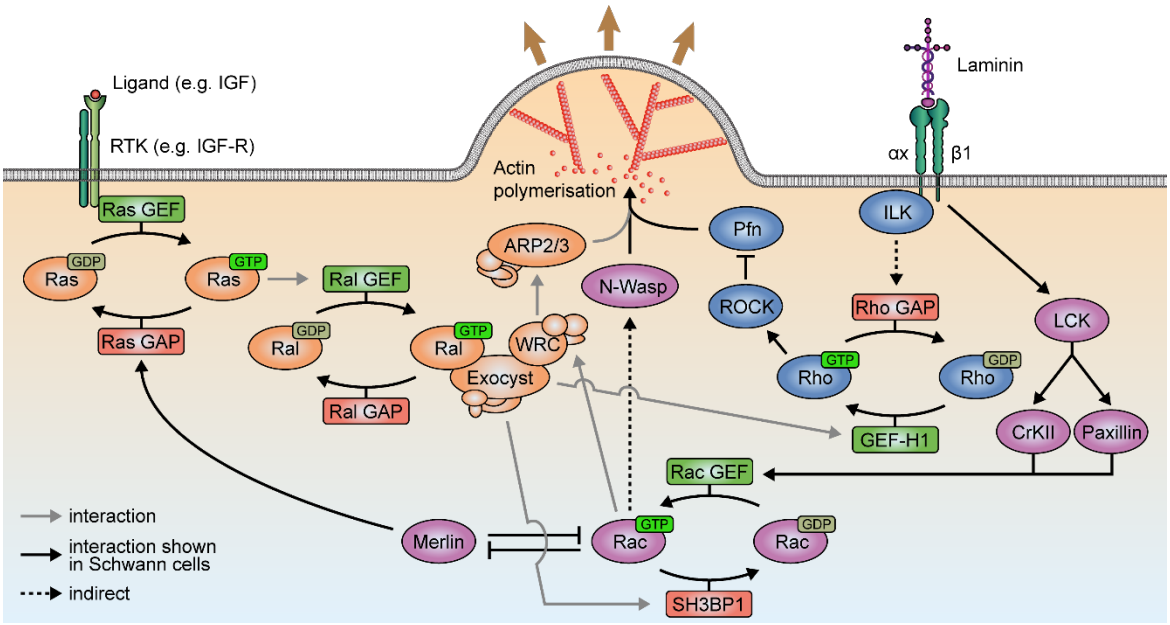

Figure 17: Integrating Ral GTPases into pathways that influence the actin cytoskeleton. Shown to the right are the integrin-ILK-Rho and integrin-LCK-Rac1 pathways that are established to control the actin cytoskeleton in SCs. Further shown to the left is the Ras-RalGEF-Ral pathway and how it could, through the exocyst complex, influence the actin cytoskeleton. All shown interactions are based on published literature. Black arrows indicate interactions that have been established in SCs. Dashed arrows indicate indirect interactions. Grey arrows indicate interactions that have been established in other cell types. Illustration by Dr. D.Gerber.

response to short-term stimulation with soluble laminin, contrary to what was reported previously (Lalli, 2009). To exclude that the incubation time was too short to permit binding of laminin to the integrin receptors, we also performed a longer stimulation for 3 h. Previous studies have shown that soluble laminin is bound to the SC membrane after 3 h incubation time (Pellegatta et al., 2013). We still observed a decrease of RalA activity. This was not only surprising because it was the opposite of what has been reported in the literature (Lalli, 2009), but also because loss of laminins α2, α4, or γ1, or of integrin β1, or of Ral GTPases all lead to similar radial sorting defects (Chen and Strickland, 2003; Feltri et al., 2002; Yang et al., 2005). As our results show that RalA was inhibited by laminin, the loss of laminin signaling in the laminin knockout mice or the integrin β1 knockout mice would conversely result in increased activation of RalA. While we show here that a loss of Rals leads to a radial sorting defect this does not necessarily mean that increased activity of Rals could not result in the same morphological abnormalities. However, overactivation of Rals has been associated with

malignant transformation of Schwann cells in a previous study (Bodempudi et al., 2009), which has not been reported for laminin or integrin β1 knockout mice (Chen and Strickland, 2003; Feltri et al., 2002; Yang et al., 2005). It is therefore likely that laminin signaling is not a main regulator of Ral activity in SCs. We suggest that Rals are instead controlled by a different signaling cascade, and that a cross-talk between those signaling cascades leads to decreased activity of RalA upon treatment with laminin.

Notably, SCs deficient for integrin β1 or ILK had impaired formation of radial lamellipodia specifically, while axial lamellipodia were unaffected (Nodari et al., 2007; Pereira et al., 2009). Furthermore, cells deficient for Profillin1 or Rac1, as well as our Ral-deficient SCs, additionally showed defects in the formation of axial lamellipodia (Montani et al., 2014; Nodari et al., 2007), indicating that other membrane receptors also participate in the regulation of the actin cytoskeleton. Possible candidates include dystroglycan (Berti et al., 2011) and GPR126 (Mogha et al., 2013; Monk et al., 2011), which can both be activated by laminin (Berti et al., 2011; Petersen et al., 2015). However, an involvement of the cytoskeleton has not been reported for the radial sorting defects that are cause by absence of these receptors. It is therefore likely that there are other receptors and downstream signaling cascades involved in the regulation of the SC cytoskeleton for radial sorting that have not yet been reported in this context.

As Ras is canonically activated by receptor tyrosine kinases we wanted to find out if RalA activity would increase in SCs in response to growth factors. We found that exposure to NRG1 did not have an effect on RalA activity, but we did observe a strong increase of RalA activity in response to stimulation with FCS. This indicates that the growth factors present in serum activate RalA, presumably through activation of Ras, as many growth factors are known to bind to receptor tyrosine kinases, e.g. EGF and IGF (Alberts et al., 2015). While not unexpected, this result shows a potential link from growth factor signaling to the regulation of the cytoskeleton in SCs.

Throughout SC development, their dependence on and response to growth factors undergoes a very substantial change. While SCPs depend on neuronal signals such as NRG1 for their survival, immature SCs are independent from axonal signals and instead ensure survival through an autocrine signaling loop (Meier et al., 1999). These autocrine signals include IGF, Neurotrophin 3, and platelet-derived growth factor (Meier et al., 1999). Since these growth factors bind to receptor tyrosine kinases, it is possible that these activate Ras-RalGEF-Ral signaling in SCs. Our data indicates that growth factor signaling could potentially influence the actin cytoskeleton in SCs and thus radial sorting through control of the Ras-RalGEF-Ral signaling axis. This is especially interesting considering that through such a mechanism, autocrine survival signals of immature SCs (Meier et al., 1999) could additionally function to promote radial sorting and thus lineage progression. As the activity of RalA was also influenced by laminin, Ral GTPases could potentially serve to integrate signaling from growth factors and the ECM to regulate radial sorting, since both pathways converge on Rals. To strengthen this hypothesis it would be helpful to identify the specific growth factors contained in serum that activate Ral signaling. Furthermore it would be necessary to show that Ral activation in this instance happens in response to Ras activation. Similarly, preventing Ras activation in SCs to analyze the impact on the actin cytoskeleton could yield valuable insight. Due to their role in regulating SC survival, investigating the role of growth factor signaling on process extension and lamellipodia formation in wild-type SCs could be challenging.

6.4. RalA promotes process extension in SCs through the exocyst complex

As we found that the activity of RalA was influenced by laminin signaling, and loss of Ral GTPases caused a phenotype reminiscent of those observed upon loss of components of the signaling cascade downstream of integrins, we wondered which of the Ral effector pathways would mediate the effect on the actin cytoskeleton. Looking at Rals and their known effectors, the most straightforward link to cytoskeletal regulation is via RalBP1, since it contains a RhoGAP domain and has been shown to have GAP activity towards Rac1 and Cdc42, but not RhoA (Cantor et al., 1995; Jullien-Flores et al., 1995; Park and Weinberg, 1995). Still, reports

showing that Ral GTPases influence the activity of Rac1 or Cdc42 through the GAP activity of RalBP1 are missing. It has however been reported that RalBP1 can bind to Arno, a GEF for Arf6, to modulate the activity of Rac1 and regulate cell spreading and motility in 3T3 fibroblasts (Lee et al., 2014). In the present work we show that in SCs the interaction between RalA and RalBP1 is not required for process extension *in vitro*. Instead it is the exocyst complex that seems to mediate the influence of Ral GTPases on the SC cytoskeleton.

The mammalian exocyst complex consists of 8 proteins and is involved in polarized membrane formation and targeted vesicle trafficking. To date, little is known about the function of the exocyst complex in Schwann cells. To our knowledge, a single study has addressed this issue (Bolis et al., 2009). The authors showed in myelinating co-cultures that interaction between the multidomain scaffolding protein Dlg1, the phospholipid phosphatase Mtmr2, and Exoc4 is crucial to achieve homeostatic control of myelination (Bolis et al., 2009). In this complex, which is localized to sites of membrane addition by the kinesin motor protein kif13B, Exoc4 positively regulates membrane addition, while Mtmr2 negatively regulates the process (Bolis et al., 2009). Consequently, the authors report that loss of Mtmr2 in Schwann cells results in excessive myelin folds which can be rescued by reducing Exoc4 expression in Schwann cells. Interestingly, Exoc4 has also been reported as a crucial component for membrane formation in oligodendrocytes (Anitei et al., 2006). Therefore it is possible that Rals and the exocyst complex regulate membrane addition at the leading edge of SC processes, thereby regulating process elongation.

A recent review has focused on the ability of Rals to connect the Ras, Rac, and Rho signaling pathways through the exocyst complex to control cell migration (Zago et al., 2017). Focusing on the Rho and Rac signaling cascades that are central to process extension in SCs, two major interactions are of note. First, Exoc2 can directly bind the RhoA-GEF GEF-H1 (Biondini et al., 2015). Second, Exoc4 and Exoc8 can interact with the RacGAP SH3BP1 and this interaction is important for the stability of the leading edge of processes (Parrini et al., 2011). Assuming a signaling cascade from Rals via the exocyst to Rho and Rac, loss of Rals would

decrease Rho activity, resulting in activation of Profillin1 and increased lamellipodia formation. With regards to SH3BP1, loss of Rals would increase Rac1 activity, also promoting both lamellipodia formation and process extension (see Figure 17). Thus both of these interactions would have effects opposite to those we observed, indicating that a simple model of Rals influencing the activity of Rac1 or Rho through the exocyst is not sufficient to explain our findings. Under physiological conditions the activation of GTPases can occur in a temporarily and spatially restricted manner. It has been shown that both the activation and inactivation of Rac1 specifically at the leading edge is necessary to promote the extension of cytoplasmic protrusions (Parrini et al., 2011). There are also other reports indicating that the cycling of GTPases, rather than their overall activation state, can be important to convey their cellular functions (Barale et al., 2006; Fidyk et al., 2006). Therefore, if process extension in SCs relies on a precise control of activation, inactivation, and localization of Rho, Rac, and their downstream targets, it is possible that Ral GTPases and the exocyst complex are involved in this regulation.

In addition to the interactors described above a major Rac effector, the WRC, can also bind to the exocyst complex (Biondini et al., 2016). It was shown that SH3BP1, WRC, and the exocyst all localize to the leading edge of migratory cells (Biondini et al., 2015; Parrini et al., 2011). In their literature review, Zago and colleagues proposed a model in which Rals and the exocyst work as a “molecular taxi” to physically transport signaling molecules to the sites of active process extension (Zago et al., 2017). Since the WRC acts downstream of Rac1, loss of Ral GTPases in this model would lead to an inability of Rac1 to promote process extension regardless of its activation status (see Figure 17). Interestingly, the WRC is not activated by Rac1 alone, but also requires activity of the small Ras GTPase Arf1 (Koronakis et al., 2011). As mentioned above, Rals can activate Arf6 through RalBP1 and Arno (Lee et al., 2014) to mediate anchorage independent growth in tumor cells downstream of integrins (Pawar et al., 2016). In addition, RalA and Arf1 or Arf6 cooperate to activate PLD1 (Kim et al., 1998; Luo et

al., 1998; Xu et al., 2003). It is therefore possible that Rals act in conjunction with the Arf GTPases to influence process extension in SCs.

In summary, we have shown that Ral GTPases and the exocyst complex are novel regulators of the SC cytoskeleton during radial sorting. While they are likely not directly involved in the established signaling cascades downstream of laminin/integrin β1, we propose that Rals and the exocyst recruit the WRC to sites of active protrusion formation. Further experiments will be needed to validate this hypothesis and analyze in depth the molecular signals that regulate Ral GTPases and the exocyst complex in SCs. To this end it would be interesting to specifically determine the activation state of Rac1 and Rho in ABKO SCs or nerves, as well as the activation state of Ras upon stimulation of SCs with FCS, by affinity purification of the GTP-bound form of the GTPases. Furthermore, Förster resonance energy transfer (FRET) constructs such as RAICHU-RalA and RAICHU-Rac1 (Graham et al., 2001; Takaya et al., 2004) could be introduced into wild-type SCs to determine when and where in the cell RalA and Rac1 are activated during active process extension. In addition, it may be possible to fluorescently label the WRC, Rals, and the exocyst complex to determine if the above hypothesis about WRC recruitment by Rals and the exocyst holds true. However, such an experiment is likely only feasible in cell lines that are easy to transfect. Furthermore, the role of the WRC and Arp2/3 complexes in SCs has not been addressed previously and would be worth investigating.

6.5. Ral GTPases are potentially dispensable for the maintenance of axons, but RalB controls myelination in adult nerves

In adult ABKO mice, we observed a reduction in the number of myelinated fibers between two months and one year of age. A concomitant reduction of the number of sorted fibers indicates that there could be axonal loss between these time points. Interestingly we detected decreased mRNA expression of MAG in P5 sciatic nerves of ABKO mice. It has been reported that MAG has an anti-apoptotic effect on motor neurons during PNS development (Palandri et al., 2015). It is possible that decreased MAG expression in ABKO Schwann cells could, over

time, lead to apoptosis of motor neurons, contributing to the morphological changes we observed in adult ABKO mice. Alternatively it is possible that demyelinated axons are clustered together to form what we think are bundles of unsorted axons. This idea stems from mice deficient for HDAC1 and HDAC2 (Jacob et al., 2011). In these mice, axons are sorted into a 1:1 relationship with SCs initially but massive SC apoptosis starting at P2 virtually depletes the nerves of SCs and leads to the formation of axon clusters that resemble bundles of unsorted axons, but are surrounded by perineurial cells and not SCs (Jacob et al., 2011). However, ABKO nerves are still populated by SCs at one year of age, showing that there is no similar apoptosis as in HDAC1 and HDAC2 knockout mice. Furthermore, we did not observe a major increase in the number and size of axonal bundles between two-month and one-year-old ABKO mice.

To determine if these observations were long-term consequences of the developmental deletion of Ral GTPases or can be attributed to a role of Rals in the maintenance of adult axons and myelin, we generated mice with a tamoxifen-inducible deletion of RalA in addition to constitutive deletion of RalB in all cells (*Plp*$^{CreERT2/+}$ *Rala*$^{fl/fl}$ *Ralb*$^{0/0}$). We induced recombination of RalA in adult mice to be sure that developmental myelination was completed. Analyzing sciatic nerves of these mice at six and 12 months post recombination we unexpectedly did not observe a reduction in the number of myelinated fibers. These findings indicate that RalA and RalB are indeed dispensable for the survival of the axon-SC unit.

We did however observe a hypermyelination across all axonal sizes in iBKO and iABKO mice at 12 MpT, comparable to the hypermyelination that we had observed in one-year-old BKO mice. This suggests that RalB but not RalA plays a role in preventing myelin growth past the optimal thickness. Notably the exocyst complex subunit Exoc4 has been implicated in homeostatic control of myelination alongside Dlg1 and Mtmr2 (Bolis et al., 2009). Mice deficient for Mtmr2 show focal hypermyelination (Berger et al., 2002; Bolino et al., 2004; Bolino et al., 2000), which, *in vitro* could be rescued by reduced Exoc4 expression (Bolis et al., 2009). While focal hypermyelination is different from the overall hypermyelination that we observed

in BKO, iBKO, and iABKO mice, it is possible that a similar mechanism causes both phenotypes, implicating RalB and the exocyst as important regulators of the extent of myelination. On the other hand it was reported that hyperactivation of mTORC1 after developmental myelination results in radial hypermyelination without focal hypermyelination (Figlia et al., 2017). Connections between the Ral and mTOR signaling pathways have been reported in different *in vitro* settings. In MEFs RalB was shown to directly associate with and activate mTOR independently of Rheb, while RalA did not share this function (Martin et al., 2014). In HeLa cells, RalA promotes the Rheb-dependent activation of mTORC1 in response to nutrients (Maehama et al., 2008). In addition, PLD1, which requires association with RalA for activation (Kim et al., 1998), facilitates activation of mTOR by Rheb through the metabolite phosphatidic acid (Xu et al., 2011). Although these reports differ with regards to which Ral GTPase regulates mTOR activity as well as the mechanism of mTOR activation by Rals, they agree on a positive influence of Ral activity on mTOR activity. Thus it is unlikely that loss of RalB in our knockout mice directly results in hyperactivity of mTOR that could explain the observed hypermyelination.

7. Material and Methods

7.1. Common buffers and solutions

Lysogeny broth (LB), Miller	10 g/L Tryptone, 10 g/L NaCl, 5 g/L Yeast Extract (ThermoFisher Scientific, Waltham, MA, USA; DF0446-07-5)
Phosphate buffer (PB)	0.4 M Na_2HPO_4, 0.4 M NaH_2PO_4
Phosphate buffered saline (PBS)	140 mM NaCl, 2.5 mM KCl, 6.5 mM Na_2HPO_4, 1.5 mM KH_2PO_4, pH 7.4
SDS-PAGE Running buffer	25 mM Tris-Base, 190 mM glycine, 1% SDS
Tris buffered saline with Tween-20 (TBS-T)	20 mM Tris-HCl pH 7.6, 150 mM NaCl, 0.05% Tween-20
Transfer buffer	25 mM Tris-Base, 190 mM glycine, 20% methanol

7.2. Mice

Mice with floxed alleles for *Rala* and null alleles for *Ralb* were generated previously (Peschard et al., 2012). These mice were received on a FVBN background and subsequently crossed with *Mpz*-Cre mice (Feltri et al., 1999) on a C57B6 background. Experimental mice were of mixed background between the 3rd and 6th generation of backcrosses into C57B6. For all experiments, age-matched mice derived from parallel breedings were used. Experimental genotypes are referred to with abbreviations as follows: *Mpz*-Cre$^{+/wt}$ *Rala*$^{fl/fl}$ (AKO); *Rala*$^{fl/fl}$

Ralb$^{0/0}$ (BKO); *Mpz*-Cre$^{+/wt}$ *Rala*$^{fl/fl}$ *Ralb*$^{0/0}$ (ABKO). Mice of the genotype *Rala*$^{fl/fl}$ served as controls (CTR).

To investigate the impact of deletion of RalB in cells other than Schwann cells, mice with floxed alleles for both *Rala* and *Ralb* were crossed with the *Mpz*-Cre driver line (Feltri et al., 1999). Experimental mice were age-matched and of C57B6 background for more than 10 generations of backcrosses. For all experiments, age-matched mice derived from parallel breedings were used. Experimental genotypes are referred to with abbreviations as follows: *Mpz*-Cre$^{+/wt}$ *Rala*$^{fl/fl}$ (AKO*flox*); *Mpz*-Cre$^{+/wt}$ *Ralb*$^{fl/fl}$ (BKO*flox*); *Mpz*-Cre$^{+/wt}$ *Rala*$^{fl/fl}$ *Ralb*$^{fl/fl}$ (ABKO*flox*). A mixture of mice carrying floxed alleles for RalA (*Rala*$^{fl/fl}$), RalB (*Ralb*$^{fl/fl}$), or both (*Rala*$^{fl/fl}$ *Ralb*$^{fl/fl}$) served as controls (CTR).

In order to study the effect of Ral deletion after developmental myelination, mice carrying floxed alleles for RalA and null alleles for RalB (Peschard et al., 2012) were crossed with the *Plp*-CreERT2 driver line (Leone et al., 2003). The resulting experimental mice were of mixed background (FVBN and C57B6) at the 5th generation of backcrosses into C57B6. To induce recombination, 10-weeks-old mice were injected for 5 consecutive days with 2 mg Tamoxifen (Sigma-Aldrich, St.Louis, MO; T5648) in 10% ethanol in sunflower seed oil from *Helianthus annuus* (Sigma-Aldrich, St.Louis, MO; S5007). For all experiments, age-matched animals from parallel breedings were used. Experimental genotypes are referred to with abbreviations as follows: *Plp*-CreERT2$^{+/wt}$ *Rala*$^{fl/fl}$ (iAKO); *Rala*$^{fl/fl}$ *Ralb*$^{0/0}$ (iBKO); *Plp*-CreERT2$^{+/wt}$ *Rala*$^{fl/fl}$ *Ralb*$^{0/0}$ (iABKO). Mice of the genotype *Rala*$^{fl/fl}$ served as controls (iCTR).

Genotypes were determined by genomic polymerase chain reaction (PCR) with the following primer sequences: Cre forward 5'-ACCAGGTTCGTTCACTCATGG-3', Cre reverse 5'-AGGCTAAGTGCCTTCTCTACA-3'; RalA forward 5'-GATGCCCTTAATGCAAATGACC-3', RalA reverse 5'-GCCATAGCAACGAGACAAGCC-3'; RalB forward 5'-GGAGGCATGGGAAGATTAGAAG-3', RalB null 5'-GTCTGCTTACACACCTGTGTAC-3', RalB reverse 5'-CCCAAGCCAGAGATGCCTCAC-3'. All mice were co-housed in cages with a maximum of 5 mice, kept in a 12 h light and dark cycle, and fed standard chow *ad libitum*.

All animal experiments were approved by and performed in accordance to the guidelines of the Zurich Cantonal Veterinary Office.

7.3. Motor behavior analysis (Catwalk)

For analysis of motor behavior of adult mice the CatWalk XT system (Noldus, Wageningen, Netherlands) was utilized. Mice were placed on the running field and left to traverse the field of their own accord. Per mouse, three compliant runs (run duration between 0.5 and 5 seconds, maximum allowed speed variation of 60%) were considered. Analysis was performed with CatWalk XT 10.6 software (Noldus, Wageningen, Netherlands). Stride length was measured as the distance between consecutive prints of the left hindlimb. Base of support was measured as the average distance between the hindlimbs and the support was calculated as the fraction of the step cycle that is spend on more than two paws.

7.4. Morphological analysis

To prepare for electron microscopy sectioning, sciatic nerves were fixed immediately after dissection and stored in 4% paraformaldehyde (PFA) in 0.1 M PB. Nerves were tied with surgical thread to EM embedding buckets and subsequently washed 3 times in 0.1 M PB. After incubation in 1% osmium tetroxide (EMS, Hatfield, PA, USA) in 0.1M PB overnight at 4°C on a rotator, samples were washed with PB 3 times for 20, 40, and 80 minutes. Dehydration was carried out by washes in increasing concentrations of acetone for 20 min each starting at 30% acetone, followed by 50%, 70%, 90%, 96%, and 100% acetone, followed by an incubation for 1h in 100% acetone. Spurr resin (EMS, Hatfield, PA, USA) was prepared as indicated in Table 2. Introduction of Spurr resin was performed through incubation of the samples with resin diluted in acetone in a ratio of 1:2, 1:1, and 2:1 for 1.5 hours each and finally with pure resin at 4°C overnight on a rotator. On the next morning the resin was replaced with freshly prepared resin and samples were incubated another 2 to 8 h at room temperature before embedding in molds and incubating overnight at 65°C to polymerize the Spurr resin.

Table 2: Preparation of Spurr resin for embedding. Twice the indicated amount was used for each round of embedding.

component	Electron Microscopy Sciences catalogue number	amount [g]
NSA	19050	29.5
ERL 4221	15004	20.5
DER 736	13000	7.15
DMAE	13300	0.5

To obtain representative high-resolution micrographs of basal lamina and SC processes, ultrathin sections (65 nm) were imaged with a Morgagni 268 transmission electron microscope (Field Electron and Ion Company, Hillsboro, OR, USA). To obtain reconstructions of the entire sciatic nerve, 99 nm thick sections were collected on ITO coverslips (Optics Balzers, Balzers, Liechtenstein) and imaged with either a Zeiss Gemini Leo 1530 FEG or a Zeiss Merlin FEG scanning electron microscope attached to ATLAS modules (Zeiss, Jena, Germany). Image alignment and processing was performed with Photoshop CS6 or CC (Adobe, San Jose, CA, USA). To determine the numbers of myelinated, not-myelinated, and sorted fibers as well as the area of sciatic nerve occupied by bundles, the whole endoneurial area was taken into account. For g-ratio calculations, the axon diameter was derived from the axon area and the fiber diameter was obtained by adding twice the average myelin thickness measured at different locations. Per animal, a total of at least 100 fibers in 3 different regions of the sciatic nerve were measured.

7.5. Preparation and culture of primary SCs

Sciatic nerves were isolated from P5 mice, the perineurium was removed, and nerves were digested with 1.25 mg/mL trypsin (Sigma-Aldrich, St.Louis, MO; T9201) and 2 mg/mL collagenase (Sigma-Aldrich, St.Louis, MO; C0130) in HBSS (Life Technologies, Carlsbad, CA, USA) for 1h in a 37°C waterbath. The enzymatic digestion was stopped by addition of DMEM

GlutaMAX + 10% FCS (Life Technologies, Carlsbad, CA, USA) containing 100 U/mL penicillin and 100 µg/mL streptomycin. Cells were pelleted by centrifugation for 5 min at 600 x g, resuspended in DMEM GlutaMAX +10% FCS (Life Technologies, Carlsbad, CA, USA) containing 100 U/mL penicillin and 100 µg/mL streptomycin and seeded in 24-well plates on coverslips coated with 20 µg/mL laminin111 (Sigma-Aldrich, St.Louis, MO; L2020). Laminin-coating was performed prior by incubation of coverslips for at least 3h at 37°C with laminin111 diluted in PBS. 16 h after seeding, the medium was changed to N2 SC medium (N2 supplement (Life Technologies, Carlsbad, CA, USA), 10 ng/mL recombinant human EGF domain of neuregulin-1 β1 (R&D Systems, Minneapolis, MN, USA), 2.5 µM Forskolin (Sigma-Aldrich, St.Louis, MO) in Advanced DMEM/F-12 (Life Technologies, Carlsbad, CA, USA), 100 U/mL penicillin and 100 µg/mL streptomycin). For analysis of lamellipodia, cells were fixed 24 h after plating. For virus infection, 10 µL of concentrated virus were added per well to the N2 SC medium 16 h after plating and cells were fixed on DIV5.

For all experiments, cells from individual animals were kept separate to provide biological replicates. To account for technical reproducibility, each experiment was repeated twice with cells from 2 - 4 animals at a time.

7.6. Lentiviral vectors and virus production

The following myc-tagged RalA mutants were kindly provided by Dr. G.Lalli (Lalli and Hall, 2005): RalA72L (constitutively active), RalA28N (dominant negative), RalA72L ΔN11 (constitutively active, uncoupled from PLD1), RalA72L D49E (constitutively active, uncoupled from Exoc2 and Exoc8), RalA72L D49N (constitutively active, uncoupled from RalBP1), and RalA72L A48W (constitutively active, uncoupled from Exoc8). All constructs were amplified by PCR and inserted into pSicoR-Δ3'-loxP (modified version of pSicoR (Ventura et al., 2004) with deleted 3'-loxP site) between the NheI and EcoRI restriction sites under control of the CMV promotor.

For production of concentrated viruses, two 15 cm dishes of mycoplasma-free HEK293T cells were transfected per construct with the lentiviral vector and the packaging plasmids psPAX2 and pCMV-VSV-G using Lipofectamine 2000 (Life Technologies, Carlsbad, CA, USA) according to the manufacturer's instructions (see Table 3). Supernatants were collected 72 h after transfection, filtered through a 45 µm sterile filter to remove cellular debris, and viruses were concentrated by ultracentrifugation at 21000 rpm and 11°C for 2 h using a Sorvall WX 80+ ultracentrifuge and a Sorvall SureSpin 630 Swinging Bucket Rotor (ThermoFisher Scientific, Waltham, MA, USA). The pelleted viruses were resuspended in 500 µL PBS and used as indicated above.

Table 3: Detailed procotol for transfection of HEK239T cells using Lipofectamine 2000.

Transfection mix for 2 x 15 cm dish	**OptiMeM [mL]**	**Lipofectamine 2000 [µL]**	**packaging plasmids [µg]**		**lentiviral vector [µg]**
			pCMV-VSV-G	psPAX2	
Tube 1	7.2	172.8	-	-	-
Tube 2	7.2	-	14.4	14.4	28.8

7.7. Pull-down assay to determine RalA activity

7.7.1. Expression of recombinant protein

The pGEX-RalBD construct encoding the Ral-binding-domain of RalBP1 fused to gluthathion-S-transferase (GST) was a kind gift from Dr. G.Lalli. The plasmid was introduced into E.Coli bacteria of the BL21 strain by standard heat-shock transformation. The bacteria were plated on LB-Agar plates containing ampicillin (200 µg/µL) and incubated overnight at 37°C. A single colony was transferred into 50 mL LB medium + ampicillin (0.1 mg/mL) and cultured overnight at 37°C while shaking. On the following day, 400 mL LB medium + ampicillin (0.1 mg/mL) were added and the culture was incubated until the optic density at 600 nm (OD_{600}) ranged between 0.5 and 0.7. To induce protein expression, isopropyl β-D-1-thiogalactopyranoside (IPTG; 1

mM) was added and the culture was incubated for 4 h at 37°C. The bacteria were then pelleted by centrifugation, washed once with PBS, and frozen at -80°C overnight. After thawing on ice the pellet was resuspended in PBS supplemented with protease inhibitors (Roche, Basel, Switzerland) and bacteria were lysed with lysozyme (10 mg/mL; Sigma-Aldrich, St.Louis, MO; L6876) and additionally by sonication for 5x10 sec with 10 sec breaks on ice (U200S; IKA Labortechnik, Stauffen im Breisgau, Germany). Bacterial debris was pelleted by centrifugation for 1 h at 4°C and the supernatant was aliquoted and stored at -80°C until further use.

7.7.2. Pull-down assay

For the pull-down assay, all steps were carried out at 4°C and all samples were kept on ice at all times. For each pull-down sample, 20 µL glutathione magnetic agarose beads (Pierce™, ThermoFisher Scientific, Waltham, MA, USA; 78602) were washed and incubated for 1 h with 400 µL bacterial lysate containing recombinant protein to allow coupling of recombinant protein to the beads. Beads were washed 3 times with wash buffer (125 mM Tris, 150 mM NaCl, 40 mM $MgCl_2$, pH 8.0) before further use.

Cultured cells were washed 2x with ice cold PBS and lysed using 600 µL lysis buffer (50 mM Tris-HCl pH 7.2, 1% Triton X-100, 500 mM NaCl, 10 mM $MgCl_2$, protease and phosphatase inhibitors (Roche, Basel, Switzerland)). Samples were centrifuged for 10 min to clear the lysates of cellular debris and incubated for 30 min with 10 µL uncoupled glutathione magnetic agarose beads (Pierce™, ThermoFisher Scientific, Waltham, MA, USA; 78602) for preclearing. From the supernatant, a fraction was removed to serve as input while the remainder was transferred to magnetic beads coupled with recombinant protein as described before and incubated for 1 h. Following 5 washes with wash buffer the beads were collected, excess liquid was removed and samples were prepared for SDS-PAGE as described in section 7.13.

7.7.3. Treatment of primary rat Schwann cells for RalA activity assay

Primary rat Schwann cells (rSCs) were a gift from Dr. D. Gerber and Dr. G. Figlia. The cells were plated on PLL-coated (0.1 mg/mL; Sigma-Aldrich, St.Louis, MO; P5899) dishes in rSC growth medium (DMEM GlutaMAX, 10% FCS, 5 µg/mL bovine pituitary extract (Life Technologies, Carlsbad, CA, USA; 13028-014), 2 µM forskolin (Sigma-Aldrich, St.Louis, MO; F6886)). 24 h prior to lysis the medium was exchanged to starvation medium (DMEM GlutaMAX, 2 µM forskolin), except for non-starved control cells. Cells were then treated with 10% FCS or 10 ng/mL NRG1 (recombinant human EGF domain of neuregulin-1 β1, R&D Systems, Minneapolis, MN, USA) or 10 µg / mL laminin111 (Sigma-Aldrich, St.Louis, MO; L2020) for 15 min or 3 h.

7.8. Antibodies

Table 4: List of primary antibodies. For immunoblot (IB) antibodies were diluted in 5% milk in TBS-T, and for immunostaining (IS) in blocking buffer (1% BSA, 10% donkey serum, 0.1% Triton X-100 in PBS).

target	company	catalogue no.	species	dilution	
				IB	IS
RalA	BD Biosciences	610221	mouse	1:1000	-
RalB	R&D Systems	MAB3920	rat	1:1000	-
α-tubulin	Sigma-Aldrich	T5168	mouse	1:1000	-
α-tubulin	Abcam	ab18251	rabbit	-	1:500
Sox10	R&D Systems	AF2864	goat	-	1:200
cleaved caspase 3	Cell Signaling Technology	9664	rabbit	-	1:500
myc-tag	Abcam	ab32	mouse	-	1:500

Alexa488-coupled Phalloidin (used 1:40) was purchased from Life Technologies (Carlsbad, CA, USA; A12379). HRP- and fluorophore-coupled secondary antibodies (used 1:200 for immunostainings and 1:10000 for immunoblots) were obtained from Life Technologies (Carlsbad, CA, USA) or Jackson ImmunoResearch (West Grove, PA, USA).

7.9. Immunostaining

Sciatic nerves were fixed with 4% PFA in PBS for 1 h at 4°C, incubated for 1 h in 10% sucrose followed by overnight incubation in 20% sucrose at 4°C. Nerves were embedded in OCT (Tissue Tek, Torrance, CA, USA) and 8 µm thick sections were cut and stored at -80°C until further processing. Frozen slides were fixed for 10 min in 4% PFA and permeabilized for 20 min in 0.25% Triton X-100 in PBS. Slides were blocked for 30 min in blocking buffer (1% BSA, 10% donkey serum, 0.1% Triton X-100 in PBS), incubated overnight with primary antibodies (see Table 4), washed 3x with PBS, for 1 h with secondary antibodies, and counterstained with DAPI (Life Technologies, Carlsbad, CA, USA). Finally, slides were mounted with Vectashield (Vector Laboratories, Burlingame, CA, USA).

To analyze proliferation, P5 pups were injected with 50 µg EdU (Life Technologies, Carlsbad, CA, USA) per gram of body weight one hour prior to sacrificing. For EdU detection, the Click-iT EdU Alexa647 kit (Life Technologies, Carlsbad, CA, USA) was used according to the manufacturer's instructions. Briefly, frozen sections were washed twice with 3% BSA in PBS and permeabilized with 0.5% Triton X-100 and 3% BSA in PBS. Following three washes with 3% BSA in PBS, slides were incubated for 45 min at RT with the reaction cocktail containing reaction buffer, $CuSO_4$, Alexa Fluor azide, and reaction buffer additive. Slides were washed once with 3% BSA in PBS and subsequently stained with antibodies as described before.

To visualize the cytoskeleton of primary mouse SCs cultured on coverslips, cells were fixed with 4% PFA in microtubule protection buffer (65 mM PIPES, 25 mM HEPES, 10 mM EGTA, 3 mM $MgCl_2$, pH 6.9) for 10 min. Cells were permeabilized for 5 min with 0.1% Triton X-100 in PBS, incubated for 30 min with blocking buffer (10% goat serum, 1% BSA in PBS) and

overnight with primary antibodies. Coverslips were incubated with secondary antibodies and Phalloidin-Alexa488 (Life Technologies, Carlsbad, CA, USA) for one hour, counterstained with DAPI (Life Technologies, Carlsbad, CA, USA), and mounted with ImmuMount (ThermoFisher Scientific, Waltham, MA, USA).

All Immunostainings were imaged with an Axio Imager.M2 (Zeiss, Jena, Germany) with a monochromatic CCD camera (sCMOS, pco.edge; PCO AG, Kelheim, Germany) and automatic stage to reconstruct full coverslips. For analysis of sciatic nerve sections, at least one representative section per animal was imaged and analyzed.

To analyze lamellipodia of cultured mouse SCs, a total of at least 100 cells per animal from 2 coverslips (4-6 representative fields per coverslip) were imaged and lamellipodia were counted using Photoshop CC (Adobe, San Jose, CA, USA). We considered lamellipodia at the far ends of the main processes of a SC as axial and those along the length of the processes or SC cell body as radial. The numbers of lamellipodia per cell were averaged for each replicate, and shown (in Figure 11E and F) are the averages for each animal.

To determine process length of cultured mouse SCs, two full coverslips per biological replicate were imaged. Process length was measured from the nucleus to the tip of the process using Fiji version 2.0.0-rc-8/1.49c (Schindelin et al., 2012; Schneider et al., 2012) on at least 50 cells per coverslip. Only processes originating directly from the cell body were considered as individual processes, and for each such process the longest branch was measured. For each animal, the length of all measured processes was averaged and depicted (in Figure 11G and Figure 12) are the averages for each animal.

Primary mouse SCs had to be seeded at a high density to ensure survival for five days in culture during viral infection experiments. It was therefore not possible to reliably quantify the number of lamellipodia per cell on DIV5. Measurement of process length was however possible since infection rates were generally low and myc-staining of infected cells was sufficient to discriminate the processes of infected cells. For lentiviral constructs with very low

infection rate, 50 infected cells per coverslip were randomly selected. For non-infected cells and lentiviral constructs with higher infection rates 2 areas at the edge of each coverslip were selected and 25 cells were measured per area.

7.10. RNA extraction

Sciatic nerves from P5 mice were extracted and placed in cold PBS. The epineurium was peeled off using two forceps, then nerves were snap frozen in liquid nitrogen and stored at -80°C until further use. To isolate total RNA for mRNA sequencing, an RNeasy kit (Qiagen, Hilden, Germany) was used according to the manufacturer's instructions. Briefly, frozen nerves were placed on dry ice and mechanically dissociated using pestles. Per sample, 50 µL buffer RLT with β-mercaptoethanol (1:100) were added to the frozen tissue and again grinded with the pestle. Another 300 µL supplemented RLT buffer were added and the semi-frozen sample was grinded until thawed. Samples were then subjected to purification using spin columns. To isolate RNA for quantitative real-time PCR analysis, QIAzol (Qiagen, Hilden, Germany) was used according to the manufacturer's instructions. In brief, samples were placed on dry ice and mechanically disrupted using pestles. Per sample, 1 mL of trizol was added and the tissue was grinded until the trizol melted. The homogenized samples were incubated for 5 min at room temperature (RT). 200 µL chloroform were added and the tubes were shaken and incubated 2-3 min at RT. The samples were centrifuged at 12000 x g for 15 min at 4°C to separate the solution into three phases. The upper aquaeous phase containing RNA was carefully removed and transferred to a new tube and an equal volume of isopropanol was added along with 2 µL BlycoBlue coprecipitant (ThermoFisher Scientific, Waltham, MA, USA; AM9516). To precipitate the RNA, samples were incubated 10 min at RT and subsequently centrifuged at 12000 x g for 10 min at 4°C. The supernatant was removed leaving the RNA pellet, which was washed twice with 500 µL 75% ethanol. After the second wash, the pellet was air dried to remove residual ethanol and resuspended in 15 µL ultra-pure water (ThermoFisher Scientific, Waltham, MA, USA; 10977035). RNA concentration was

measured using a NanoDrop spectrophotometer (ThermoFisher Scientific, Waltham, MA, USA) and samples were stored at -80°C until further use.

7.11. Reverse transcription and quantitative real-time PCR analysis

For reverse transcription, 190 ng of total RNA were transcribed using the Maxima First Strand cDNA Synthesis Kit (Life Technologies, Carlsbad, CA, USA; K1641) according to the manufacturer's instructions. Briefly, the reaction mix was prepared as indicated in Table 5 and samples were incubated for 10 min at 25°C followed by 15 min at 50°C. For termination of the reaction the samples were incubated at 85°C for 5 min and the resulting cDNA was diluted 1:40 with ultra-pure water and stored at -20°C.

Table 5: Reaction mix for reverse transcription.

Reagent	**per reaction**
5x Reaction Buffer	4 µL
Maxima Enzyme Mix	2 µL
RNA	190 ng
H_2O	adjust volume to 20 µL

qPCR was performed using the FastStart Essential DNA Green Master as indicated in Table 6 (Roche, Basel, Switzerland) and Light Cycler 480 II (Roche, Basel, Switzerland). The following primers, all targeting mouse genes, were used: β-Actin forward 5'-GTCCACACCCGCCACC-3', reverse 5'-GGCCTCGTCACCCACATAG-3'; RalA forward 5'-TTCCGAAGTGGGGAGGGATT-3', reverse 5'-TGCCTCTTCTACAGAAACCTGC-3'; RalB forward 5'-GGTTGTGCGCATAGCCAGA-3', reverse 5'-GAAGCGTCAGGGCTGATTTG-3'. Each sample was run in triplicate to account for technical variability. The results were quantified according to the $2^{-\Delta\Delta Ct}$ method to obtain relative mRNA fold changes normalized to β-Actin expression.

Table 6: Reaction mix for quantitative real-time PCR.

Reagent	**per reaction**
forward primer (5 µM)	0.5 µL
reverse primer (5 µM)	0.5 µL
FastStart Essential DNA Green Master 2x	5 µL
cDNA template (diluted 1:40)	4 µL

7.12. RNA-sequencing

The quality of the isolated RNA was determined with a Qubit® (1.0) Fluorometer (Life Technologies**,** Carlsbad, CA, USA) and a Bioanalyzer 2100 (Agilent, Waldbronn, Germany). Only those samples with a 260 nm/280 nm ratio between 1.8–2.1 and a 28S/18S ratio within 1.5–2 were further processed. The TruSeq RNA Sample Prep Kit v2 (Illumina, San Diego, CA, USA) was used in the succeeding steps. Briefly, total RNA samples (100-1000 ng) were poly A enriched and then reverse-transcribed into double-stranded cDNA. The cDNA samples were fragmented, end-repaired and polyadenylated before ligation of TruSeq adapters containing the index for multiplexing. Fragments containing TruSeq adapters on both ends were selectively enriched with PCR. The quality and quantity of the enriched libraries were validated using a Qubit® (1.0) Fluorometer and the Caliper GX LabChip® GX (Caliper Life Sciences, Waltham, MA, USA). The product is a smear with an average fragment size of approximately 260 bp. The libraries were normalized to 10 nM in Tris-HCl 10 mM, pH8.5, 0.1% Tween 20. The TruSeq PE Cluster Kit HS4000 or TruSeq SR Cluster Kit HS4000 (Illumina, San Diego, CA, USA) was used for cluster generation using 10 pM of pooled normalized libraries on the cBOT. Sequencing was performed on the Illumina HiSeq 4000 single end 125 bp using the TruSeq SBS Kit HS4000 (Illumina, San Diego, CA, USA).

For data analysis, the raw reads were first cleaned by removing adapter sequences, trimming low quality ends, and filtering reads with low quality (phred quality <20) using Trimmomatic, version 0.36 (Bolger et al., 2014). Sequence alignment of the resulting high-quality reads to the Mouse reference genome (build GRCm38.p5) and quantification of gene level expression was carried out using RSEM, version 1.3.0 (Li and Dewey, 2011). To detect differentially expressed genes we applied a count based negative binomial model implemented in the software package EdgeR (R version: 3.5.0, EdgeR version: 3.22.1) (Robinson et al., 2010). The differential expression was assessed using an exact test adapted for over-dispersed data. Genes showing altered expression with adjusted (Benjamini and Hochberg method) p-value < 0.05 were considered differentially expressed. The obtained sequencing data will be publicly available on NCBI Gene Expression Omnibus upon publication of the corresponding manuscript that is currently in preparation.

7.13. Western Blot

For protein analysis, sciatic nerves were extracted, immediately transferred to ice-cold PBS, and the epineurium was removed. Nerves were snap frozen in liquid nitrogen and stored at -80°C until further use. The frozen samples were mechanically disrupted using a small pestle and mixed with PN2 lysis buffer (25 mM Tris-HCl pH 7.4, 95 mM NaCl, 10 mM EDTA, 2% SDS, protease and phosphatase inhibitors (Roche, Basel, Switzerland)). Samples were centrifuged for 15 min and protein concentration was measured with a Micro BCA protein assay kit (ThermoFisher Scientific, Waltham, MA, USA) according to the manufacturer's instructions.

For SDS-PAGE, 10 – 15 µg of protein were diluted with PN2 and 4 x sample buffer (200 mM Tris-HCl pH 6.8, 40% glycerol, 8% SDS, 20% β-mercaptoethanol, 0.4% bromophenol blue). Samples were run on 4-15% polyacrylamide gradient gels (BioRad, Hercules, CA, USA) at constant 15 mA per gel for 1.5 h and transferred onto PVDF membranes (Millipore, Burlington, MA, USA) at constant 90 V for 1h at 4°C. Membranes were blocked for 1 h in 5% non-fat dry milk in TBS-T, incubated overnight at 4°C with primary antibodies diluted in 5% BSA in TBS-

T (see Table 4), washed 3 times with TBS-T and incubated for 1 h with HRP-conjugated secondary antibodies. Blots were incubated with ECL or ECL Prime (GE Healthcare, Chicago, IL, USA) to produce chemiluminescent signals that were detected with Fusion FX7 (Vilber Lourmat, Collégien, France). Densitometric quantification was performed with Fiji, version 2.0.0-rc-8/1.49c (Schindelin et al., 2012; Schneider et al., 2012).

7.14. Statistics

Statistical analyses were performed with GraphPad Prism (version 7.03) and Microsoft Excel (version 15.0). Normal distribution and equal variances were assumed for all data but not formally tested due to low number of replicates. Sample sizes were chosen in accordance to what is generally employed in the field. For all quantifications on microscopy images, the investigators were blinded to the genotype of the mice or cells. All data is shown as mean ± standard error of mean (SEM). The number of biological replicates, the statistical test used for each figure, as well as mean, SEM, and exact p-values are as follows:

7.14.1. Figure 5

B: n = 4 (CTR), 5 (AKO, ABKO), or 6 (BKO) mice per genotype; one-way Anova, Tukey's multiple comparisons test; mean ± SEM: CTR = 1.0 ± 0.045, AKO = 0.048 ± 0.007, BKO = 0.780 ± 0.106, ABKO = 0.089 ± 0.008; $F_{(3, 16)} = 48.72$, $p < 0.0001$, $p_{CTR\ vs.\ AKO} < 0.0001$, $p_{CTR\ vs.\ BKO} = 0.1494$, $p_{CTR\ vs.\ ABKO} < 0.0001$, $p_{AKO\ vs.\ BKO} < 0.0001$, $p_{AKO\ vs.\ ABKO} = 0.9737$, $p_{BKO\ vs.\ ABKO} < 0.0001$;

C: n = 5 animals per genotype; one-way Anova, Tukey's multiple comparisons test; mean ± SEM: CTR = 1.0 ± 0.121, AKO = 1.477 ± 0.163, BKO = 0.002 ± 0.001, ABKO = 0.004 ± 0.003; $F_{(3,\ 16)RalB} = 52.88$, $p_{RalB} < 0.0001$, $p_{CTR\ vs.\ AKO} = 0.0204$, $p_{CTR\ vs.\ BKO} < 0.0001$, $p_{CTR\ vs.\ ABKO} < 0.0001$, $p_{AKO\ vs.\ BKO} < 0.0001$, $p_{AKO\ vs.\ ABKO} < 0.0001$, $p_{BKO\ vs.\ ABKO} > 0.9999$;

E: n = 6 animals per genotype; one-way Anova, Dunnett's multiple comparisons test; mean ± SEM: CTR = 1.0 ± 0.075, AKO = 0.501 ± 0.031, BKO = 1.14 ± 0.118, ABKO = 0.723 ± 0.048;

RalA: $F_{(3, 20)} = 14.31$, $p < 0.0001$, $p_{CTR\ vs.\ AKO} = 0.0004$, $p_{CTR\ vs.\ BKO} = 0.4347$, $p_{CTR\ vs.\ ABKO} = 0.0446$;

F: n = 4 animals per genotype: one-way Anova, Dunnett's multiple comparisons test; mean ± SEM: CTR = 1.0 ± 0.279, AKO = 0.939 ± 0.222, BKO = 0.075 ± 0.013, ABKO = 0.051 ± 0.011; $F_{(3, 12)} = 8.648$, $p = 0.0025$, $p_{CTR\ vs.\ AKO} = 0.9898$, $p_{CTR\ vs.\ BKO} = 0.0085$, $p_{CTR\ vs.\ ABKO} = 0.0071$;

H: n = 9 animals (CTR) or 10 animals (AKO, BKO, ABKO); one-way Anova, Tukey's multiple comparisons test; mean ± SEM: CTR = 2.866 ± 0.1, AKO = 2.982 ± 0.086, BKO = 2.652 ± 0.095, ABKO = 2.142 ± 0.153; $F_{(3, 35)} = 11.17$, $p < 0.0001$, $p_{CTR\ vs.\ AKO} = 0.8878$, $p_{CTR\ vs.\ BKO} = 0.5507$, $p_{CTR\ vs.\ ABKO} = 0.0004$, $p_{AKO\ vs.\ BKO} = 0.1706$, $p_{AKO\ vs.\ ABKO} < 0.0001$, $p_{BKO\ vs.\ ABKO} = 0.0126$;

I: n = 9 animals (CTR) or 10 animals (AKO, BKO, ABKO); one-way Anova, Tukey's multiple comparisons test; mean ± SEM: CTR = 15.49 ± 2.457, AKO = 14.19 ± 3.338, BKO = 23.67 ± 3.777, ABKO = 35.04 ± 3.762; $F_{(3, 35)} = 7.931$, $p = 0.0004$, $p_{CTR\ vs.\ AKO} = 0.9934$, $p_{CTR\ vs.\ BKO} = 0.3562$, $p_{CTR\ vs.\ ABKO} = 0.0018$, $p_{AKO\ vs.\ BKO} = 0.2134$, $p_{AKO\ vs.\ ABKO} = 0.0006$, $p_{BKO\ vs.\ ABKO} = 0.1$;

J: n = 9 animals (CTR) or 10 animals (AKO, BKO, ABKO); one-way Anova, Tukey's multiple comparisons test; mean ± SEM: CTR = 9.043 ± 0.258, AKO = 9.483 ± 0.249, BKO = 8.792 ± 0.211, ABKO = 7.904 ± 0.209; $F_{(3, 35)} = 8.432$, $p = 0.0002$, $p_{CTR\ vs.\ AKO} = 0.5527$, $p_{CTR\ vs.\ BKO} = 0.8747$, $p_{CTR\ vs.\ ABKO} = 0.0082$, $p_{AKO\ vs.\ BKO} = 0.1615$, $p_{AKO\ vs.\ ABKO} = 0.0001$, $p_{BKO\ vs.\ ABKO} = 0.0446$;

7.14.2. Figure 6

A: n = at least 20 mice per genotype;

B: n = at least 30 mice per genotype;

7.14.3. Figure 7

B: n = 4 animals per genotype; one-way Anova, Tukey's multiple comparisons test; mean ± SEM: CTR = 1611 ± 210.6, AKO = 2061 ± 140.1, BKO = 1541 ± 113.7, ABKO = 196.8 ± 68.73;

$F_{(3, 12)} = 31.68$, $p < 0.0001$, $p_{CTR\ vs.\ AKO} = 0.1713$, $p_{CTR\ vs.\ BKO} = 0.9849$, $p_{CTR\ vs.\ ABKO} < 0.0001$, $p_{AKO\ vs.\ BKO} = 0.0978$, $p_{AKO\ vs.\ ABKO} < 0.0001$, $p_{BKO\ vs.\ ABKO} = 0.0001$;

C: n = 4 animals per genotype; one-way Anova, Tukey's multiple comparisons test; mean ± SEM: CTR = 1001 ± 98.53, AKO = 1098 ± 146.2, BKO = 1323 ± 163.9, ABKO = 1063 ± 210.8; $F_{(3, 12)} = 0.7678$, $p = 0.5338$ $p_{CTR\ vs.\ AKO} = 0.9722$, $p_{CTR\ vs.\ BKO} = 0.5102$, $p_{CTR\ vs.\ ABKO} = 0.9923$, $p_{AKO\ vs.\ BKO} = 0.7565$, $p_{AKO\ vs.\ ABKO} = 0.9986$, $p_{BKO\ vs.\ ABKO} = 0.6692$;

D: n = 4 animals per genotype; one-way Anova, Tukey's multiple comparisons test; mean ± SEM: CTR = 2612 ± 251, AKO = 3159 ± 82.61, BKO = 2863 ± 177.5, ABKO = 1260 ± 279.2; $F_{(3, 12)} = 15.72$, $p = 0.0002$, $p_{CTR\ vs.\ AKO} = 0.3083$, $p_{CTR\ vs.\ BKO} = 0.8346$, $p_{CTR\ vs.\ ABKO} = 0.0034$, $p_{AKO\ vs.\ BKO} = 0.7594$, $p_{AKO\ vs.\ ABKO} = 0.0002$, $p_{BKO\ vs.\ ABKO} = 0.0009$;

E: n = 4 animals per genotype; one-way Anova, Tukey's multiple comparisons test; mean ± SEM: CTR = 4.55 ± 0.46, AKO = 4.64 ± 0.42, BKO = 5.88 ± 0.66, ABKO = 18.21 ± 2.94; $F_{(3, 12)} = 18.53$, $p < 0.0001$, $p_{CTR\ vs.\ AKO} > 0.9999$, $p_{CTR\ vs.\ BKO} = 0.9258$, $p_{CTR\ vs.\ ABKO} = 0.0002$, $p_{AKO\ vs.\ BKO} = 0.9385$, $p_{AKO\ vs.\ ABKO} = 0.0002$, $p_{BKO\ vs.\ ABKO} = 0.0005$;

F: n = 5 animals per genotype; one-way Anova, Tukey's multiple comparisons test; mean ± SEM: CTR = 3767 ± 111.4, AKO = 3628 ± 143.1, BKO = 3590 ± 127.6, ABKO = 2624 ± 270.1; $F_{(3, 16)} = 9.004$, $p = 0.001$, $p_{CTR\ vs.\ AKO} = 0.9417$, $p_{CTR\ vs.\ BKO} = 0.8905$, $p_{CTR\ vs.\ ABKO} = 0.0014$, $p_{AKO\ vs.\ BKO} = 0.9987$, $p_{AKO\ vs.\ ABKO} = 0.0045$, $p_{BKO\ vs.\ ABKO} = 0.0061$;

G: n = 5 animals per genotype; one-way Anova, Tukey's multiple comparisons test; mean ± SEM: CTR = 2 ± 1.304, AKO = 4.8 ± 2.035, BKO = 10.2 ± 3.089, ABKO = 174.6 ± 20.02; $F_{(3, 16)} = 68.66$, $p < 0.0001$, $p_{CTR\ vs.\ AKO} = 0.9973$, $p_{CTR\ vs.\ BKO} = 0.9401$, $p_{CTR\ vs.\ ABKO} < 0.0001$, $p_{AKO\ vs.\ BKO} = 0.9815$, $p_{AKO\ vs.\ ABKO} < 0.0001$, $p_{BKO\ vs.\ ABKO} < 0.0001$;

H: n = 5 animals per genotype; one-way Anova, Tukey's multiple comparisons test; mean ± SEM: CTR = 3769 ± 111.8, AKO = 3632 ± 144.1, BKO = 3601 ± 129, ABKO = 2798 ± 271.7; $F_{(3, 16)} = 6.271$, $p = 0.0051$, $p_{CTR\ vs.\ AKO} = 0.9459$, $p_{CTR\ vs.\ BKO} = 0.9049$, $p_{CTR\ vs.\ ABKO} = 0.0063$, $p_{AKO\ vs.\ BKO} = 0.9992$, $p_{AKO\ vs.\ ABKO} = 0.0190$, $p_{BKO\ vs.\ ABKO} = 0.0245$;

I: n = 5 animals per genotype; one-way Anova, Tukey's multiple comparisons test; mean ± SEM: CTR = 0.0 ± 0.0, AKO = 0.0 ± 0.0, BKO = 0.0 ± 0.0, ABKO = 2.68 ± 1.116; $F_{(3, 16)} = 5.763$, $p = 0.0072$, $p_{CTR\ vs.\ AKO} > 0.9999$, $p_{CTR\ vs.\ BKO} > 0.9999$, $p_{CTR\ vs.\ ABKO} = 0.0175$, $p_{AKO\ vs.\ BKO} > 0.9999$, $p_{AKO\ vs.\ ABKO} = 0.0175$, $p_{BKO\ vs.\ ABKO} = 0.0175$;

7.14.4. Figure 8

B: n = 5 animals per genotype; one-way Anova, Tukey's multiple comparisons test; mean ± SEM: CTR = 2599 ± 67.55, AKO = 2304 ± 186.9, BKO = 2493 ± 50.49, ABKO = 349.6 ± 54.96; $F_{(3, 16)} = 100.7$, $p < 0.0001$, $p_{CTR\ vs.\ AKO} = 0.2435$, $p_{CTR\ vs.\ BKO} = 0.8952$, $p_{CTR\ vs.\ ABKO} < 0.0001$, $p_{AKO\ vs.\ BKO} = 0.6003$, $p_{AKO\ vs.\ ABKO} < 0.0001$, $p_{BKO\ vs.\ ABKO} < 0.0001$;

C: n = 5 animals per genotype; one-way Anova, Tukey's multiple comparisons test; mean ± SEM: CTR = 694 ± 60.83, AKO = 905.6 ± 88.37, BKO = 677.8 ± 45.93, ABKO = 740.6 ± 125; $F_{(3, 16)} = 1.484$, $p = 0.2565$, $p_{CTR\ vs.\ AKO} = 0.332$, $p_{CTR\ vs.\ BKO} = 0.9991$, $p_{CTR\ vs.\ ABKO} = 0.9799$, $p_{AKO\ vs.\ BKO} = 0.2735$, $p_{AKO\ vs.\ ABKO} = 0.5380$, $p_{BKO\ vs.\ ABKO} = 0.9532$;

D: n = 5 animals per genotype; one-way Anova, Tukey's multiple comparisons test; mean ± SEM: CTR = 3293 ± 78.16, AKO = 3255 ± 93.5, BKO = 3206 ± 54.21, ABKO = 1090 ± 177.7; $F_{(3, 16)} = 94.65$, $p < 0.0001$, $p_{CTR\ vs.\ AKO} = 0.9948$, $p_{CTR\ vs.\ BKO} = 0.9445$, $p_{CTR\ vs.\ ABKO} < 0.0001$, $p_{AKO\ vs.\ BKO} = 0.9892$, $p_{AKO\ vs.\ ABKO} < 0.0001$, $p_{BKO\ vs.\ ABKO} < 0.0001$;

E n = 5 animals per genotype; one-way Anova, Tukey's multiple comparisons test; mean ± SEM: CTR = 7.61 ± 0.297, AKO = 6.021 ± 0.603, BKO = 6.377 ± 0.449, ABKO = 26.37 ± 1.992; $F_{(3, 16)} = 84.36$, $p < 0.0001$, $p_{CTR\ vs.\ AKO} = 0.7263$, $p_{CTR\ vs.\ BKO} = 0.8484$, $p_{CTR\ vs.\ ABKO} < 0.0001$, $p_{AKO\ vs.\ BKO} = 0.9953$, $p_{AKO\ vs.\ ABKO} < 0.0001$, $p_{BKO\ vs.\ ABKO} < 0.0001$;

F: n = 5 animals per genotype; one-way Anova, Tukey's multiple comparisons test; mean ± SEM: CTR = 4009 ± 134.6, AKO = 4212 ± 70.03, BKO = 4038 ± 69.99, ABKO = 2202 ± 280.3; $F_{(3, 16)} = 33.65$, $p < 0.0001$, $p_{CTR\ vs.\ AKO} = 0.8144$, $p_{CTR\ vs.\ BKO} = 0.9993$, $p_{CTR\ vs.\ ABKO} < 0.0001$, $p_{AKO\ vs.\ BKO} = 0.8725$, $p_{AKO\ vs.\ ABKO} < 0.0001$, $p_{BKO\ vs.\ ABKO} < 0.0001$;

G: n = 5 animals per genotype; one-way Anova, Tukey's multiple comparisons test; mean ± SEM: CTR = 0.2 ± 0.2, AKO = 0.2 ± 0.2, BKO = 0.4 ± 0.245, ABKO = 160.6 ± 15.62; $F_{(3, 16)} = 105.4$, $p < 0.0001$, $p_{CTR\ vs.\ AKO} > 0.9999$, $p_{CTR\ vs.\ BKO} > 0.9999$, $p_{CTR\ vs.\ ABKO} < 0.0001$, $p_{AKO\ vs.\ BKO} > 0.9999$, $p_{AKO\ vs.\ ABKO} < 0.0001$, $p_{BKO\ vs.\ ABKO} < 0.0001$;

H: n = 5 animals per genotype; one-way Anova, Tukey's multiple comparisons test; mean ± SEM: CTR = 4009 ± 134.5, AKO = 4213 ± 70.05, BKO = 4038 ± 69.81, ABKO = 2362 ± 290.2; $F_{(3, 16)} = 26.81$, $p < 0.0001$, $p_{CTR\ vs.\ AKO} = 0.8254$, $p_{CTR\ vs.\ BKO} = 0.9993$, $p_{CTR\ vs.\ ABKO} < 0.0001$, $p_{AKO\ vs.\ BKO} = 0.8809$, $p_{AKO\ vs.\ ABKO} < 0.0001$, $p_{BKO\ vs.\ ABKO} < 0.0001$;

I: n = 5 animals per genotype; one-way Anova, Tukey's multiple comparisons test; mean ± SEM: CTR = 0.0 ± 0.0, AKO = 0.0 ± 0.0, BKO = 0.0 ± 0.0, ABKO = 8.639 ± 2.288; $F_{(3, 16)} = 14.25$, $p < 0.0001$, $p_{CTR\ vs.\ AKO} > 0.9999$, $p_{CTR\ vs.\ BKO} > 0.9999$, $p_{CTR\ vs.\ ABKO} = 0.0003$, $p_{AKO\ vs.\ BKO} > 0.9999$, $p_{AKO\ vs.\ ABKO} = 0.0003$, $p_{BKO\ vs.\ ABKO} = 0.0003$;

7.14.5. Figure 9

A: n = 3 (BKO) or 4 (CTR, AKO, ABKO) mice per genotype;

B: n = 4 mice per genotype;

C: n = 4 mice per genotype;

7.14.6. Figure 10

B: n = 6 animals (AKO, BKO, ABKO) or 7 animals (CTR) per genotype; one-way Anova, Tukey's multiple comparisons test; mean ± SEM: CTR = 523.4 ± 21.79, AKO = 641.2 ± 11.56, BKO = 655.4 ± 32.16, ABKO = 633.6 ± 36.94; $F_{(3, 21)} = 5.402$, $p = 0.0065$, $p_{CTR\ vs.\ AKO} = 0.0241$, $p_{CTR\ vs.\ BKO} = 0.0103$, $p_{CTR\ vs.\ ABKO} = 0.0371$, $p_{AKO\ vs.\ BKO} = 0.9828$, $p_{AKO\ vs.\ ABKO} = 0.9973$, $p_{BKO\ vs.\ ABKO} = 0.9429$;

C: n = 6 animals (AKO, BKO, ABKO) or 7 animals (CTR) per genotype; one-way Anova, Tukey's multiple comparisons test; mean ± SEM: CTR = 397± 14.52, AKO = 496.7 ± 42.4, BKO = 514.2 ± 11.01, ABKO = 486.5 ± 33.34; $F_{(3, 21)} = 3.852$, $p = 0.0243$, $p_{CTR\ vs.\ AKO} = 0.0733$,

$p_{CTR\ vs.\ BKO} = 0.0284$, $p_{CTR\ vs.\ ABKO} = 0.1222$, $p_{AKO\ vs.\ BKO} = 0.9709$, $p_{AKO\ vs.\ ABKO} = 0.9940$, $p_{BKO\ vs.\ ABKO} = 0.8978$;

D: n = 6 animals (AKO, BKO, ABKO) or 7 animals (CTR) per genotype; one-way Anova, Tukey's multiple comparisons test; mean ± SEM: CTR = 4.304 ± 0.566, AKO = 3.886 ± 0.477, BKO = 4.583 ± 0.509, ABKO = 9.47 ± 1.046; $F_{(3, 21)} = 14.41$, $p < 0.0001$, $p_{CTR\ vs.\ AKO} = 0.9705$, $p_{CTR\ vs.\ BKO} = 0.9909$, $p_{CTR\ vs.\ ABKO} = 0.0001$, $p_{AKO\ vs.\ BKO} = 0.8925$, $p_{AKO\ vs.\ ABKO} < 0.0001$, $p_{BKO\ vs.\ ABKO} = 0.0003$;

F: n = 7 animals (CTR, AKO) or 6 animals (BKO, ABKO) per genotype; one-way Anova, Tukey's multiple comparisons test; mean ± SEM: CTR = 0.243 ± 0.096, AKO = 0.378 ± 0.145, BKO = 0.215 ± 0.122, ABKO = 0.276 ± 0.105; $F_{(3, 22)} = 0.3682$, $p = 0.7767$, $p_{CTR\ vs.\ AKO} = 0.8389$, $p_{CTR\ vs.\ BKO} = 0.9984$, $p_{CTR\ vs.\ ABKO} = 0.9971$, $p_{AKO\ vs.\ BKO} = 0.7719$, $p_{AKO\ vs.\ ABKO} = 0.9310$, $p_{BKO\ vs.\ ABKO} = 0.9850$;

7.14.7. Figure 11

C: n = 5 animals per genotype; one-sample t test; mean ± SEM: CTR = 0.0 ± 0.0, AKO = 0.0 ± 0.0, BKO = 0.0 ± 0.0, ABKO = 102.4 ± 6.547; t = 15.64, df = 4; $p < 0.0001$;

E: n = 6 animals, at least 100 cells per animal; unpaired two-tailed t test; mean ± SEM: CTR = 2.342 ± 0.099, ABKO = 0.459 ± 0.130; t = 11.5; df = 10; $p < 0.0001$;

F: n = 6 animals, at least 100 cells per animal; unpaired two-tailed t test; mean ± SEM: CTR = 1.555 ± 0.072, ABKO = 0.985 ± 0.122; t = 4.018; df = 10; $p = 0.0024$;

G: n = 5 animals, at least 100 cells per animal; unpaired two-tailed t test; mean ± SEM: CTR = 73.6 ± 1.832, ABKO = 62.32 ± 2.151; t = 4; df = 8; $p = 0.004$;

7.14.8. Figure 12

A: n = 6 animals, at least 100 cells per animal; multiple unpaired two-tailed t tests, Holm-Sidak method for multiple comparisons correction; mean ± SEM: CTR = 88.22 ± 7.766, ABKO = 85.76 ± 4.69; t = 0.2282; df = 62; $p = 0.9677$;

B: n = 6 animals, at least 100 cells per animal; multiple unpaired two-tailed t tests, Holm-Sidak method for multiple comparisons correction; mean ± SEM: CTR = 101.6 ± 9.305, ABKO = 40.26 ± 7.82; t = 5.703; df = 62; $p < 0.0001$;

C: n = 6 animals, at least 100 cells per animal; multiple unpaired two-tailed t tests, Holm-Sidak method for multiple comparisons correction; mean ± SEM: CTR = 104.1 ± 9.359, ABKO = 102.6 ± 10.61; t = 0.1397; df = 62; $p = 0.9677$;

D: n = 6 animals, at least 100 cells per animal; multiple unpaired two-tailed t tests, Holm-Sidak method for multiple comparisons correction; mean ± SEM: CTR = 100.8 ± 2.609, ABKO = 83.49 ± 6.586; t = 1.611; df = 62; $p = 0.3005$;

E: n = 7 animals, at least 100 cells per animal; multiple unpaired two-tailed t tests, Holm-Sidak method for multiple comparisons correction; mean ± SEM: CTR = 106.8 ± 7.568, ABKO = 68.14 ± 4.856; t = 3.881; df = 62; $p = 0.001$;

F: n = 6 animals, at least 100 cells per animal; multiple unpaired two-tailed t tests, Holm-Sidak method for multiple comparisons correction; mean ± SEM: CTR = 111.2 ± 6.548, ABKO = 44.69 ± 9.007; t = 6.179; df = 62; $p < 0.0001$;

7.14.9. Figure 13

B: n = 5 independent experiments for each condition; One-way Anova, Dunnett's multiple comparisons test; mean ± SEM: not starved = 0.846 ± 0.051, no stimulus = 1.004 ± 0.075, FCS = 1.952 ± 0.122, NRG = 1.137 ± 0.145, Lam 15 min = 0.583 ± 0.032, Lam 3 h = 0.594 ± 0.109; $F_{(5, 24)} = 27.03$, $p < 0.0001$, $p_{\text{no stimulus vs. not starved}} = 0.6757$, $p_{\text{no stimulus vs. FCS}} = 0.0001$, $p_{\text{no stimulus vs. NRG}} = 0.7973$, $p_{\text{no stimulus vs. Lam 15 min}} = 0.0226$, $p_{\text{no stimulus vs. Lam 3 h}} = 0.0273$;

C: n = 5 independent experiments for each condition; One-way Anova, Dunnett's multiple comparisons test; mean ± SEM: not starved = 1.927 ± 0.628, no stimulus = 1.194 ± 0.365, FCS = 1.317 ± 0.111, NRG = 0.797 ± 0.086, Lam 15 min = 0.738 ± 0.099, Lam 3 h = 0.767 ± 0.104; $F_{(5, 24)} = 2.27$, $p = 0.0803$;

D: n = 5 independent experiments for each condition; One-way Anova, Dunnett's multiple comparisons test; mean ± SEM: not starved = 1.636 ± 0.546, no stimulus = 1.134 ± 0.264, FCS = 2.611 ± 0.362, NRG = 0.875 ± 0.115, Lam 15 min = 0.429 ± 0.063, Lam 3 h = 0.441 ± 0.086; $F_{(5, 24)} = 7.936$, $p = 0.0002$, $p_{\text{no stimulus vs. not starved}} = 0.6382$, $p_{\text{no stimulus vs. FCS}} = 0.0073$, $p_{\text{no stimulus vs. NRG}} = 0.9559$, $p_{\text{no stimulus vs. Lam 15 min}} = 0.334$, $p_{\text{no stimulus vs. Lam 3 h}} = 0.3484$;

7.14.10. Figure 14

B: n = 5 animals (CTR, BKO, ABKO at two months and one year; and AKO at two months) or 4 animals (AKO at one year) per genotype, two-way Anova, Tukey's multiple comparisons test; mean ± SEM: $CTR_{(2\ months)} = 3767 \pm 111.4$, $AKO_{(2\ months)} = 3628 \pm 143.1$, $BKO_{(2\ months)} = 3590 \pm 127.6$, $ABKO_{(2\ months)} = 2624 \pm 270.1$, $CTR_{(1\ year)} = 3762 \pm 127.6$, $AKO_{(1\ year)} = 3449 \pm 154.5$, $BKO_{(1\ year)} = 3398 \pm 88.73$, $ABKO_{(1\ year)} = 1495 \pm 105.5$; $p_{CTR(2\ months)\ vs.\ AKO(2\ months)} = 0.9975$, $p_{CTR(2\ months)\ vs.\ BKO(2\ months)} = 0.9894$, $p_{CTR(2\ months)\ vs.\ ABKO(2\ months)} = 0.0002$, $p_{AKO(2\ months)\ vs.\ BKO(2\ months)} > 0.9999$, $p_{AKO(2\ months)\ vs.\ ABKO(2\ months)} = 0.001$, $p_{BKO(2\ months)\ vs.\ ABKO(2\ months)} = 0.0016$; $p_{CTR(1\ year)\ vs.\ AKO(1\ year)} = 0.8501$, $p_{CTR(1\ year)\ vs.\ BKO(1\ year)} = 0.6699$, $p_{CTR(1\ year)\ vs.\ ABKO(1\ year)} < 0.0001$, $p_{AKO(1\ year)\ vs.\ BKO(1\ year)} > 0.9999$, $p_{AKO(1\ year)\ vs.\ ABKO(1\ year)} < 0.0001$, $p_{BKO(1\ year)\ vs.\ ABKO(1\ year)} < 0.0001$; $p_{CTR(2\ months)\ vs.\ CTR(1\ year)} > 0.9999$, $p_{AKO(2\ months)\ vs.\ AKO(1\ year)} = 0.992$, $p_{BKO(2\ months)\ vs.\ BKO(1\ year)} = 0.9825$, $p_{ABKO(2\ months)\ vs.\ ABKO(1\ year)} = 0.0002$;

C: n = 5 animals (CTR, BKO, ABKO at two months and one year; and AKO at two months) or 4 animals (AKO at one year) per genotype, two-way Anova, Tukey's multiple comparisons test; mean ± SEM: $CTR_{(2\ months)} = 3769 \pm 111.8$, $AKO_{(2\ months)} = 3632 \pm 144.1$, $BKO_{(2\ months)} = 3601 \pm 129$, $ABKO_{(2\ months)} = 2798 \pm 271.7$, $CTR_{(1\ year)} = 3785 \pm 128.9$, $AKO_{(1\ year)} = 3478 \pm 152.1$, $BKO_{(1\ year)} = 3422 \pm 87.22$, $ABKO_{(1\ year)} = 1875 \pm 140.8$; $p_{CTR(2\ months)\ vs.\ AKO(2\ months)} = 0.9981$, $p_{CTR(2\ months)\ vs.\ BKO(2\ months)} = 0.9932$, $p_{CTR(2\ months)\ vs.\ ABKO(2\ months)} = 0.0021$, $p_{AKO(2\ months)\ vs.\ BKO(2\ months)} > 0.9999$, $p_{AKO(2\ months)\ vs.\ ABKO(2\ months)} = 0.0114$, $p_{BKO(2\ months)\ vs.\ ABKO(2\ months)} = 0.0165$; $p_{CTR(1\ year)\ vs.\ AKO(1\ year)} = 0.8764$, $p_{CTR(1\ year)\ vs.\ BKO(1\ year)} = 0.7009$, $p_{CTR(1\ year)\ vs.\ ABKO(1\ year)} < 0.0001$, $p_{AKO(1\ year)\ vs.\ BKO(1\ year)} > 0.9999$, $p_{AKO(1\ year)\ vs.\ ABKO(1\ year)} < 0.0001$, $p_{BKO(1\ year)\ vs.\ ABKO(1\ year)} < 0.0001$;

$p_{CTR(2\ months)\ vs.\ CTR(1\ year)} > 0.9999$, $p_{AKO(2\ months)\ vs.\ AKO(1\ year)} = 0.9972$, $p_{BKO(2\ months)\ vs.\ BKO(1\ year)} = 0.9903$, $p_{ABKO(2\ months)\ vs.\ ABKO(1\ year)} = 0.0039$;

7.14.11. Figure 15

B: n = 5 animals per genotype, at least 100 axons per animal; linear regression; $R^2_{CTR} = 0.2946$, $R^2_{AKO} = 0.3576$, $R^2_{BKO} = 0.1532$, $R^2_{ABKO} = 0.0922$;

C: n = 5 (CTR, AKO, BKO) or 4 (ABKO) animals per genotype, at least 100 axons per animal; linear regression; $R^2_{CTR} = 0.2006$, $R^2_{AKO} = 0.1844$, $R^2_{BKO} = 0.0286$, $R^2_{ABKO} = 0.0658$;

D: n = 5 (CTR, AKO, BKO) or 4 (ABKO) animals per genotype, at least 100 axons per animal; one-way Anova, Tukey's multiple comparisons test; mean ± SEM: CTRi = 0.653 ± 0.003, AKOi = 0.648 ± 0.007, BKOi = 0.632 ± 0.006, ABKOi = 0.621 ± 0.005; $F_{(3, 21)} = 6.736$, $p = 0.0043$, $p_{CTRi\ vs.\ AKOi} = 0.9289$, $p_{CTRi\ vs.\ BKOi} = 0.0626$, $p_{CTRi\ vs.\ ABKOi} = 0.0064$, $p_{AKOi\ vs.\ BKOi} = 0.1804$, $p_{AKOi\ vs.\ ABKOi} = 0.0197$, $p_{BKOi\ vs.\ ABKOi} = 0.5574$;

E: n = 5 (CTR, AKO, BKO) or 4 (ABKO) animals per genotype; one-way Anova, Tukey's multiple comparisons test; mean ± SEM: CTRi = 3841 ± 28.35, AKOi = 3866 ± 50.47, BKOi = 3823 ± 125.3, ABKOi = 3969 ± 37.74; $F_{(3, 15)} = 0.6844$, $p = 0.5753$.

8. References

Ackerman, S.D., R. Luo, Y. Poitelon, A. Mogha, B.L. Harty, M. D'Rozario, N.E. Sanchez, A.K.K. Lakkaraju, P. Gamble, J. Li, J. Qu, M.R. MacEwan, W.Z. Ray, A. Aguzzi, M.L. Feltri, X. Piao, and K.R. Monk. 2018. GPR56/ADGRG1 regulates development and maintenance of peripheral myelin. *The Journal of experimental medicine*. 215:941-961.

Alberts, B., A. Johnson, J. Lewis, D. Morgan, M. Raff, K. Roberts, P. Walter, J. with problems by Wilson, and T. Hunt. 2015. Molecular Biology of the Cell. Garland Science, New York.

Albright, C.F., B.W. Giddings, J. Liu, M. Vito, and R.A. Weinberg. 1993. Characterization of a guanine nucleotide dissociation stimulator for a *ras*-related GTPase. *The EMBO journal*. 12:339 - 347.

Anitei, M., M. Ifrim, M.A. Ewart, A.E. Cowan, J.H. Carson, R. Bansal, and S.E. Pfeiffer. 2006. A role for Sec8 in oligodendrocyte morphological differentiation. *Journal of cell science*. 119:807-818.

Atanasoski, S., S.S. Scherer, E. Sirkowski, D. Leone, A.N. Garratt, C. Birchmeier, and U. Suter. 2006. ErbB2 signaling in Schwann cells is mostly dispensable for maintenance of myelinated peripheral nerves and proliferation of adult Schwann cells after injury. *The Journal of neuroscience : the official journal of the Society for Neuroscience*. 26:2124-2131.

Awasthi, S., J. Cheng, S.S. Singhal, M.K. Saini, U. Pandya, S. Pikula, J. Bandorowicz-Pikula, S.V. Singh, P. Zimniak, and Y.C. Awasthi. 2000. Novel function of human RLIP76: ATP-dependent transport of glutathione conjugates and doxorubicin. *Biochemistry*. 39:9327-9334.

Awasthi, S., J.Z. Cheng, S.S. Singhal, U. Pandya, R. Sharma, S.V. Singh, P. Zimniak, and Y.C. Awasthi. 2001. Functional reassembly of ATP-dependent xenobiotic transport by the N- and C-terminal domains of RLIP76 and identification of ATP binding sequences. *Biochemistry*. 40:4159-4168.

Balasubramanian, N., J.A. Meier, D.W. Scott, A. Norambuena, M.A. White, and M.A. Schwartz. 2010. RalA-exocyst complex regulates integrin-dependent membrane raft exocytosis and growth signaling. *Current biology : CB*. 20:75-79.

Barale, S., D. McCusker, and R.A. Arkowitz. 2006. Cdc42p GDP/GTP cycling is necessary for efficient cell fusion during yeast mating. *Molecular biology of the cell*. 17:2824-2838.

Bear, M.F., B.W. Connors, and M.A. Paradiso. 2007. Neuroscience: Exploring the Brain. Lippincott Williams & Wilkins.

Beirowski, B., E. Babetto, J.P. Golden, Y.J. Chen, K. Yang, R.W. Gross, G.J. Patti, and J. Milbrandt. 2014. Metabolic regulator LKB1 is crucial for Schwann cell-mediated axon maintenance. *Nature neuroscience*. 17:1351-1361.

Beirowski, B., K.M. Wong, E. Babetto, and J. Milbrandt. 2017. mTORC1 promotes proliferation of immature Schwann cells and myelin growth of differentiated Schwann cells. *Proceedings of the National Academy of Sciences of the United States of America*. 114:E4261-E4270.

Benninger, Y., T. Thurnherr, J.A. Pereira, S. Krause, X. Wu, A. Chrostek-Grashoff, D. Herzog, K.A. Nave, R.J. Franklin, D. Meijer, C. Brakebusch, U. Suter, and J.B. Relvas. 2007. Essential and distinct roles for cdc42 and rac1 in the regulation of Schwann cell biology during peripheral nervous system development. *The Journal of cell biology*. 177:1051-1061.

Berger, P., S. Bonneick, S. Willi, M. Wymann, and U. Suter. 2002. Loss of phosphatase activity in myotubularin-related protein 2 is associated with Charcot-Marie-Tooth disease type 4B1. *Human molecular genetics*. 11:1569-1579.

Berti, C., L. Bartesaghi, M. Ghidinelli, D. Zambroni, G. Figlia, Z.L. Chen, A. Quattrini, L. Wrabetz, and M.L. Feltri. 2011. Non-redundant function of dystroglycan and beta1 integrins in radial sorting of axons. *Development*. 138:4025-4037.

Bhattacharya, M., A.V. Babwah, C. Godin, P.H. Anborgh, L.B. Dale, M.O. Poulter, and S.S. Ferguson. 2004. Ral and phospholipase D2-dependent pathway for constitutive metabotropic glutamate receptor endocytosis. *The Journal of neuroscience : the official journal of the Society for Neuroscience*. 24:8752-8761.

Biondini, M., G. Duclos, N. Meyer-Schaller, P. Silberzan, J. Camonis, and M.C. Parrini. 2015. RalB regulates contractility-driven cancer dissemination upon TGFbeta stimulation via the RhoGEF GEF-H1. *Scientific reports*. 5:11759.

Biondini, M., A. Sadou-Dubourgnoux, P. Paul-Gilloteaux, G. Zago, M.D. Arslanhan, F. Waharte, E. Formstecher, M. Hertzog, J. Yu, R. Guerois, A. Gautreau, G. Scita, J. Camonis, and M.C. Parrini. 2016. Direct interaction between exocyst and Wave complexes promotes cell protrusions and motility. *Journal of cell science*. 129:3756-3769.

Birchmeier, C., and D.L.H. Bennett. 2016. Chapter Four - Neuregulin/ErbB Signaling in Developmental Myelin Formation and Nerve Repair. *In* Current Topics in Developmental Biology. Vol. 116. P.M. Wassarman, editor. Academic Press. 45-64.

Bodemann, B.O., A. Orvedahl, T. Cheng, R.R. Ram, Y.H. Ou, E. Formstecher, M. Maiti, C.C. Hazelett, E.M. Wauson, M. Balakireva, J.H. Camonis, C. Yeaman, B. Levine, and M.A. White. 2011. RalB and the exocyst mediate the cellular starvation response by direct activation of autophagosome assembly. *Cell*. 144:253-267.

Bodempudi, V., F. Yamoutpoor, W. Pan, A.Z. Dudek, T. Esfandyari, M. Piedra, D. Babovick-Vuksanovic, R.A. Woo, V.F. Mautner, L. Kluwe, D.W. Clapp, G.H. De Vries, S.L. Thomas, A. Kurtz, L.F. Parada, and F. Farassati. 2009. Ral overactivation in malignant peripheral nerve sheath tumors. *Molecular and cellular biology*. 29:3964-3974.

Bolger, A.M., M. Lohse, and B. Usadel. 2014. Trimmomatic: a flexible trimmer for Illumina sequence data. *Bioinformatics*. 30:2114-2120.

Bolino, A., A. Bolis, S.C. Previtali, G. Dina, S. Bussini, G. Dati, S. Amadio, U. Del Carro, D.D. Mruk, M.L. Feltri, C.Y. Cheng, A. Quattrini, and L. Wrabetz. 2004. Disruption of Mtmr2 produces CMT4B1-like neuropathy with myelin outfolding and impaired spermatogenesis. *The Journal of cell biology*. 167:711-721.

Bolino, A., M. Muglia, F.L. Conforti, E. LeGuern, M.A. Salih, D.M. Georgiou, K. Christodoulou, I. Hausmanowa-Petrusewicz, P. Mandich, A. Schenone, A. Gambardella, F. Bono, A. Quattrone, M. Devoto, and A.P. Monaco. 2000. Charcot-Marie-Tooth type 4B is caused by mutations in the gene encoding myotubularin-related protein-2. *Nature genetics*. 25:17-19.

Bolis, A., S. Coviello, I. Visigalli, C. Taveggia, A. Bachi, A.H. Chishti, T. Hanada, A. Quattrini, S.C. Previtali, A. Biffi, and A. Bolino. 2009. Dlg1, Sec8, and Mtmr2 regulate membrane homeostasis in Schwann cell myelination. *The Journal of neuroscience : the official journal of the Society for Neuroscience*. 29:8858-8870.

Brennan, A., C.H. Dean, A.L. Zhang, D.T. Cass, R. Mirsky, and K.R. Jessen. 2000. Endothelins control the timing of Schwann cell generation in vitro and in vivo. *Developmental biology*. 227:545-557.

Brinkmann, B.G., A. Agarwal, M.W. Sereda, A.N. Garratt, T. Muller, H. Wende, R.M. Stassart, S. Nawaz, C. Humml, V. Velanac, K. Radyushkin, S. Goebbels, T.M. Fischer, R.J. Franklin, C. Lai, H. Ehrenreich, C. Birchmeier, M.H. Schwab, and K.A. Nave. 2008. Neuregulin-1/ErbB signaling serves distinct functions in myelination of the peripheral and central nervous system. *Neuron*. 59:581-595.

Britsch, S., D.E. Goerich, D. Riethmacher, R.I. Peirano, M. Rossner, K.A. Nave, C. Birchmeier, and M. Wegner. 2001. The transcription factor Sox10 is a key regulator of peripheral glial development. *Genes & development*. 15:66-78.

Brown, M.J., and A.K. Asbury. 1981. Schwann cell proliferation in the postnatal mouse: timing and topography. *Experimental neurology*. 74:170-186.

Brugger, V., S. Engler, J.A. Pereira, S. Ruff, M. Horn, H. Welzl, E. Munger, A. Vaquie, P.N. Sidiropoulos, B. Egger, P. Yotovski, L. Filgueira, C. Somandin, T.C. Luhmann, M. D'Antonio, T. Yamaguchi, P. Matthias, U. Suter, and C. Jacob. 2015. HDAC1/2-Dependent P0 Expression Maintains Paranodal and Nodal Integrity Independently of Myelin Stability through Interactions with Neurofascins. *PLoS biology*. 13:e1002258.

Brymora, A., I.G. Duggin, L.A. Berven, E.M. van Dam, B.D. Roufogalis, and P.J. Robinson. 2012. Identification and characterisation of the RalA-ERp57 interaction: evidence for GDI activity of ERp57. *PloS one*. 7:e50879.

Brymora, A., V.A. Valova, M.R. Larsen, B.D. Roufogalis, and P.J. Robinson. 2001. The brain exocyst complex interacts with RalA in a GTP-dependent manner: identification of a novel mammalian Sec3 gene and a second Sec15 gene. *The Journal of biological chemistry*. 276:29792-29797.

Cantor, S.B., T. Urano, and L.A. Feig. 1995. Identification and characterization of Ral-binding protein 1, a potential downstream target of Ral GTPases. *Molecular and cellular biology*. 15:4578-4584.

Cascone, I., R. Selimoglu, C. Ozdemir, E. Del Nery, C. Yeaman, M. White, and J. Camonis. 2008. Distinct roles of RalA and RalB in the progression of cytokinesis are supported by distinct RalGEFs. *The EMBO journal*. 27:2375-2387.

Castelfranco, A.M., and D.K. Hartline. 2016. Evolution of rapid nerve conduction. *Brain research*. 1641:11-33.

Ceriani, M., C. Scandiuzzi, L. Amigoni, R. Tisi, G. Berruti, and E. Martegani. 2007. Functional analysis of RalGPS2, a murine guanine nucleotide exchange factor for RalA GTPase. *Experimental cell research*. 313:2293-2307.

Chan, J.R., C. Jolicoeur, J. Yamauchi, J. Elliott, J.P. Fawcett, B.K. Ng, and M. Cayouette. 2006. The polarity protein Par-3 directly interacts with p75NTR to regulate myelination. *Science*. 314:832-836.

Chardin, P., and A. Tavitian. 1986. The ral gene: a new ras related gene isolated by the use of a synthetic probe. *The EMBO journal*. 5:2203-2208.

Chardin, P., and A. Tavitian. 1989. Coding sequences of human ralA and ralB cDNAs. *Nucleic acids research*. 17:4380.

Chen, Q., C. Quan, B. Xie, L. Chen, S. Zhou, R. Toth, D.G. Campbell, S. Lu, R. Shirakawa, H. Horiuchi, C. Li, Z. Yang, C. MacKintosh, H.Y. Wang, and S. Chen. 2014. GARNL1, a major RalGAP alpha subunit in skeletal muscle, regulates insulin-stimulated RalA activation and GLUT4 trafficking via interaction with 14-3-3 proteins. *Cellular signalling*. 26:1636-1648.

Chen, X.W., M. Inoue, S.C. Hsu, and A.R. Saltiel. 2006. RalA-exocyst-dependent recycling endosome trafficking is required for the completion of cytokinesis. *The Journal of biological chemistry*. 281:38609-38616.

Chen, X.W., D. Leto, S.H. Chiang, Q. Wang, and A.R. Saltiel. 2007. Activation of RalA is required for insulin-stimulated Glut4 trafficking to the plasma membrane via the exocyst and the motor protein Myo1c. *Developmental cell*. 13:391-404.

Chen, X.W., D. Leto, T. Xiong, G. Yu, A. Cheng, S. Decker, and A.R. Saltiel. 2011. A Ral GAP complex links PI 3-kinase/Akt signaling to RalA activation in insulin action. *Molecular biology of the cell*. 22:141-152.

Chen, X.W., and A.R. Saltiel. 2011. Ral's engagement with the exocyst: breaking up is hard to do. *Cell cycle*. 10:2299-2304.

Chen, Z.L., and S. Strickland. 2003. Laminin gamma1 is critical for Schwann cell differentiation, axon myelination, and regeneration in the peripheral nerve. *The Journal of cell biology*. 163:889-899.

Chien, Y., S. Kim, R. Bumeister, Y.M. Loo, S.W. Kwon, C.L. Johnson, M.G. Balakireva, Y. Romeo, L. Kopelovich, M. Gale, Jr., C. Yeaman, J.H. Camonis, Y. Zhao, and M.A. White. 2006. RalB GTPase-mediated activation of the IkappaB family kinase TBK1 couples innate immune signaling to tumor cell survival. *Cell*. 127:157-170.

Chien, Y., and M.A. White. 2003. RAL GTPases are linchpin modulators of human tumour-cell proliferation and survival. *EMBO Rep*. 4:800-806.

Corrotte, M., A.P. Nyguyen, M.L. Harlay, N. Vitale, M.F. Bader, and N.J. Grant. 2010. Ral isoforms are implicated in Fc gamma R-mediated phagocytosis: activation of phospholipase D by RalA. *Journal of immunology*. 185:2942-2950.

Cullis, D.N., B. Philip, J.D. Baleja, and L.A. Feig. 2002. Rab11-FIP2, an adaptor protein connecting cellular components involved in internalization and recycling of epidermal growth factor receptors. *The Journal of biological chemistry*. 277:49158-49166.

Czikora, A., N. Kedei, H. Kalish, and P.M. Blumberg. 2017. Importance of the REM (Ras exchange) domain for membrane interactions by RasGRP3. *Biochimica et biophysica acta*. 1859:2350-2360.

D'Adamo, D.R., S. Novick, J.M. Kahn, P. Leonardi, and A. Pellicer. 1997. rsc: a novel oncogene with structural and functional homology with the gene family of exchange factors for Ral. *Oncogene*. 14:1295 - 1305.

D'Antonio, M., A. Droggiti, M.L. Feltri, J. Roes, L. Wrabetz, R. Mirsky, and K.R. Jessen. 2006. TGFbeta type II receptor signaling controls Schwann cell death and proliferation in developing nerves. *The Journal of neuroscience : the official journal of the Society for Neuroscience*. 26:8417-8427.

da Silva, T.F., J. Eira, A.T. Lopes, A.R. Malheiro, V. Sousa, A. Luoma, R.L. Avila, R.J. Wanders, W.W. Just, D.A. Kirschner, M.M. Sousa, and P. Brites. 2014. Peripheral nervous system plasmalogens regulate Schwann cell differentiation and myelination. *J Clin Invest*. 124:2560-2570.

Das, A., S. Gajendra, K. Falenta, M.J. Oudin, P. Peschard, S. Feng, B. Wu, C.J. Marshall, P. Doherty, W. Guo, and G. Lalli. 2014. RalA promotes a direct exocyst-Par6 interaction to regulate polarity in neuronal development. *Journal of cell science*. 127:686-699.

de Bruyn, K.M., J. de Rooij, R.M. Wolthuis, H. Rehmann, J. Wesenbeek, R.H. Cool, A.H. Wittinghofer, and J.L. Bos. 2000. RalGEF2, a pleckstrin homology domain containing guanine nucleotide exchange factor for Ral. *The Journal of biological chemistry*. 275:29761-29766.

de Leeuw, H.P., M. Fernandez-Borja, E.A. Reits, T. Romani de Wit, P.M. Wijers-Koster, P.L. Hordijk, J. Neefjes, J.A. van Mourik, and J. Voorberg. 2001. Small GTP-binding protein Ral modulates regulated exocytosis of von Willebrand factor by endothelial cells. *Arterioscler Thromb Vasc Biol*. 21:899-904.

Deng, Y., L.M.N. Wu, S. Bai, C. Zhao, H. Wang, J. Wang, L. Xu, M. Sakabe, W. Zhou, M. Xin, and Q.R. Lu. 2017. A reciprocal regulatory loop between TAZ/YAP and G-protein Galphas regulates Schwann cell proliferation and myelination. *Nature communications*. 8:15161.

Dong, Z., A. Brennan, N. Liu, Y. Yarden, G. Lefkowitz, R. Mirsky, and K.R. Jessen. 1995. Neu differentiation factor is a neuron-glia signal and regulates survival, proliferation, and maturation of rat Schwann cell precursors. *Neuron*. 15:585-596.

Duband, J.-L. 2006. Neural Crest Delamination and Migration: Integrating Regulations of Cell Interactions, Locomotion, Survival and Fate. *In* Neural Crest Induction and Differentiation. J.-P. Saint-Jeannet, editor. Springer Science+Business media, New York.

Durbin, A.D., D.H. Ki, S. He, and A.T. Look. 2016. Malignant Peripheral Nerve Sheath Tumors. *Advances in experimental medicine and biology*. 916:495-530.

Eckfeldt, C.E., E.J. Pomeroy, R.D. Lee, K.S. Hazen, L.A. Lee, B.S. Moriarity, and D.A. Largaespada. 2016. RALB provides critical survival signals downstream of Ras in acute myeloid leukemia. *Oncotarget*. 7:65147-65156.

Einheber, S., M.J. Hannocks, C.N. Metz, D.B. Rifkin, and J.L. Salzer. 1995. Transforming growth factor-beta 1 regulates axon/Schwann cell interactions. *The Journal of cell biology*. 129:443-458.

Emkey, R., S. Freedman, and L.A. Feig. 1991. Characterization of a GTPase-activating protein for the Ras-related Ral protein. *The Journal of biological chemistry*. 266:9703-9706.

Essers, M.A., S. Weijzen, A.M. de Vries-Smits, I. Saarloos, N.D. de Ruiter, J.L. Bos, and B.M. Burgering. 2004. FOXO transcription factor activation by oxidative stress mediated by the small GTPase Ral and JNK. *The EMBO journal*. 23:4802-4812.

Etienne-Manneville, S., and A. Hall. 2002. Rho GTPases in cell biology. *Nature*. 420:629-635.

Exton, J.H. 1990. Signaling through phosphatidylcholine breakdown. *The Journal of biological chemistry*. 265:1-4.

Falsetti, S.C., D.A. Wang, H. Peng, D. Carrico, A.D. Cox, C.J. Der, A.D. Hamilton, and S.M. Sebti. 2007. Geranylgeranyltransferase I inhibitors target RalB to inhibit anchorage-dependent growth and

induce apoptosis and RalA to inhibit anchorage-independent growth. *Molecular and cellular biology*. 27:8003-8014.

Feltri, M.L., M. D'Antonio, S. Previtali, M. Fasolini, A. Messing, and L. Wrabetz. 1999. P0-Cre transgenic mice for inactivation of adhesion molecules in Schwann cells. *Annals of the New York Academy of Sciences*. 883:116-123.

Feltri, M.L., D. Graus Porta, S.C. Previtali, A. Nodari, B. Migliavacca, A. Cassetti, A. Littlewood-Evans, L.F. Reichardt, A. Messing, A. Quattrini, U. Mueller, and L. Wrabetz. 2002. Conditional disruption of beta 1 integrin in Schwann cells impedes interactions with axons. *The Journal of cell biology*. 156:199-209.

Feltri, M.L., Y. Poitelon, and S.C. Previtali. 2015. How Schwann Cells Sort Axons: New Concepts. *The Neuroscientist : a review journal bringing neurobiology, neurology and psychiatry*.

Feltri, M.L., and L. Wrabetz. 2005. Laminins and their receptors in Schwann cells and hereditary neuropathies. *Journal of the peripheral nervous system : JPNS*. 10:128-143.

Fidyk, N., J.B. Wang, and R.A. Cerione. 2006. Influencing cellular transformation by modulating the rates of GTP hydrolysis by Cdc42. *Biochemistry*. 45:7750-7762.

Figlia, G., D. Gerber, and U. Suter. 2018. Myelination and mTOR. *Glia*. 66:693-707.

Figlia, G., C. Norrmen, J.A. Pereira, D. Gerber, and U. Suter. 2017. Dual function of the PI3K-Akt-mTORC1 axis in myelination of the peripheral nervous system. *eLife*. 6.

Frankel, P., A. Aronheim, E. Kavanagh, M.S. Balda, K. Matter, T.D. Bunney, and C.J. Marshall. 2005. RalA interacts with ZONAB in a cell density-dependent manner and regulates its transcriptional activity. *The EMBO journal*. 24:54-62.

Fratta, P., P. Saveri, D. Zambroni, C. Ferri, E. Tinelli, A. Messing, M. D'Antonio, M.L. Feltri, and L. Wrabetz. 2011. P0S63del impedes the arrival of wild-type P0 glycoprotein to myelin in CMT1B mice. *Human molecular genetics*. 20:2081-2090.

Fuhrmann, D., M. Mernberger, A. Nist, T. Stiewe, and H.P. Elsasser. 2018. Miz1 Controls Schwann Cell Proliferation via H3K36(me2) Demethylase Kdm8 to Prevent Peripheral Nerve Demyelination. *The Journal of neuroscience : the official journal of the Society for Neuroscience*. 38:858-877.

Fukai, S., H.T. Matern, J.R. Jagath, R.H. Scheller, and A.T. Brunger. 2003. Structural basis of the interaction between RalA and Sec5, a subunit of the sec6/8 complex. *The EMBO journal*. 22:3267-3278.

Furlan, A., and I. Adameyko. 2018. Schwann cell precursor: a neural crest cell in disguise? *Developmental biology*.

Garratt, A.N., O. Voiculescu, P. Topilko, P. Charnay, and C. Birchmeier. 2000. A dual role of erbB2 in myelination and in expansion of the schwann cell precursor pool. *The Journal of cell biology*. 148:1035-1046.

Gentry, L.R., T.D. Martin, D.J. Reiner, and C.J. Der. 2014. Ral small GTPase signaling and oncogenesis: More than just 15minutes of fame. *Biochimica et biophysica acta*. 1843:2976-2988.

Gentry, L.R., A. Nishimura, A.D. Cox, T.D. Martin, D. Tsygankov, M. Nishida, T.C. Elston, and C.J. Der. 2015. Divergent roles of CAAX motif-signaled posttranslational modifications in the regulation and subcellular localization of Ral GTPases. *The Journal of biological chemistry*. 290:22851-22861.

Ghidinelli, M., Y. Poitelon, Y.K. Shin, D. Ameroso, C. Williamson, C. Ferri, M. Pellegatta, K. Espino, A. Mogha, K. Monk, P. Podini, C. Taveggia, K.A. Nave, L. Wrabetz, H.T. Park, and M.L. Feltri. 2017. Laminin 211 inhibits protein kinase A in Schwann cells to modulate neuregulin 1 type III-driven myelination. *PLoS biology*. 15:e2001408.

Graham, D.L., P.N. Lowe, and P.A. Chalk. 2001. A method to measure the interaction of Rac/Cdc42 with their binding partners using fluorescence resonance energy transfer between mutants of green fluorescent protein. *Anal Biochem*. 296:208-217.

Gridley, S., J.A. Chavez, W.S. Lane, and G.E. Lienhard. 2006. Adipocytes contain a novel complex similar to the tuberous sclerosis complex. *Cellular signalling*. 18:1626-1632.

Grigoryan, T., S. Stein, J. Qi, H. Wende, A.N. Garratt, K.A. Nave, C. Birchmeier, and W. Birchmeier. 2013. Wnt/Rspondin/beta-catenin signals control axonal sorting and lineage progression in Schwann cell development. *Proceedings of the National Academy of Sciences of the United States of America*. 110:18174-18179.

Grove, M., and P.J. Brophy. 2014. FAK is required for Schwann cell spreading on immature basal lamina to coordinate the radial sorting of peripheral axons with myelination. *The Journal of neuroscience : the official journal of the Society for Neuroscience*. 34:13422-13434.

Grove, M., H. Kim, M. Santerre, A.J. Krupka, S.B. Han, J. Zhai, J.Y. Cho, R. Park, M. Harris, S. Kim, B.E. Sawaya, S.H. Kang, M.F. Barbe, S.H. Cho, M.A. Lemay, and Y.J. Son. 2017. YAP/TAZ initiate and maintain Schwann cell myelination. *eLife*. 6.

Grove, M., N.H. Komiyama, K.A. Nave, S.G. Grant, D.L. Sherman, and P.J. Brophy. 2007. FAK is required for axonal sorting by Schwann cells. *The Journal of cell biology*. 176:277-282.

Guo, L., A.A. Lee, T.A. Rizvi, N. Ratner, and L.S. Kirschner. 2013. The protein kinase A regulatory subunit R1A (Prkar1a) plays critical roles in peripheral nerve development. *The Journal of neuroscience : the official journal of the Society for Neuroscience*. 33:17967-17975.

Guo, L., C. Moon, K. Niehaus, Y. Zheng, and N. Ratner. 2012. Rac1 controls Schwann cell myelination through cAMP and NF2/merlin. *The Journal of neuroscience : the official journal of the Society for Neuroscience*. 32:17251-17261.

Hanani, M. 2005. Satellite glial cells in sensory ganglia: from form to function. *Brain Res Brain Res Rev*. 48:457-476.

Henry, D.O., S.A. Moskalenko, K.J. Kaur, M. Fu, R.G. Pestell, J.H. Camonis, and M.A. White. 2000. Ral GTPases contribute to regulation of cyclin D1 through activation of NF-kappaB. *Molecular and cellular biology*. 20:8084-8092.

Hinoi, T., S. Kishida, S. Koyama, M. Ikeda, Y. Matsuura, and A. Kikuchi. 1996. Post-translational modifications of Ras and Ral are important for the action of Ral GDP dissociation stimulator. *The Journal of biological chemistry*. 271:19710-19716.

Hofer, F., R. Berdeaux, and G.S. Martin. 1998. Ras-independent activation of Ral by a Ca(2+)-dependent pathway. *Current biology : CB*. 8:839-842.

Hofer, F., S. Fields, C. Schneider, and G.S. Martin. 1994. Activated Ras interacts with the Ral guanine nucleotide dissociation stimulator. *Proceedings of the National Academy of Sciences of the United States of America*. 91:11089-11093.

Hu, X., H. Hou, C. Bastian, W. He, S. Qiu, Y. Ge, X. Yin, G.J. Kidd, S. Brunet, B.D. Trapp, S. Baltan, and R. Yan. 2017. BACE1 regulates the proliferation and cellular functions of Schwann cells. *Glia*. 65:712-726.

Ikeda, M., O. Ishida, T. Hinoi, S. Kishida, and A. Kikuchi. 1998. Identification and characterization of a novel protein interacting with Ral-binding protein 1, a putative effector protein of Ral. *The Journal of biological chemistry*. 273:814-821.

Jacob, C., C.N. Christen, J.A. Pereira, C. Somandin, A. Baggiolini, P. Lotscher, M. Ozcelik, N. Tricaud, D. Meijer, T. Yamaguchi, P. Matthias, and U. Suter. 2011. HDAC1 and HDAC2 control the transcriptional program of myelination and the survival of Schwann cells. *Nature neuroscience*. 14:429-436.

Jacob, C., P. Lotscher, S. Engler, A. Baggiolini, S. Varum Tavares, V. Brugger, N. John, S. Buchmann-Moller, P.L. Snider, S.J. Conway, T. Yamaguchi, P. Matthias, L. Sommer, N. Mantei, and U. Suter. 2014. HDAC1 and HDAC2 control the specification of neural crest cells into peripheral glia. *The Journal of neuroscience : the official journal of the Society for Neuroscience*. 34:6112-6122.

Jang, S.Y., Y.K. Shin, S.Y. Park, J.Y. Park, S.H. Rha, J.K. Kim, H.J. Lee, and H.T. Park. 2015. Autophagy is involved in the reduction of myelinating Schwann cell cytoplasm during myelin maturation of the peripheral nerve. *PloS one*. 10:e0116624.

Jessen, K.R., and R. Mirsky. 2005. The origin and development of glial cells in peripheral nerves. *Nature reviews. Neuroscience*. 6:671-682.

Jessen, K.R., R. Mirsky, and A.C. Lloyd. 2015. Schwann Cells: Development and Role in Nerve Repair. *Cold Spring Harbor perspectives in biology*. 7:a020487.

Jiang, H., J.Q. Luo, T. Urano, P. Frankel, Z. Lu, D.A. Foster, and L.A. Feig. 1995. Involvement of Ral GTPase in v-Src-induced phospholipase D activation. *Nature*. 378:409-412.

Jiang, Y., M.S. Sverdlov, P.T. Toth, L.S. Huang, G. Du, Y. Liu, V. Natarajan, and R.D. Minshall. 2016. Phosphatidic Acid Produced by RalA-activated PLD2 Stimulates Caveolae-mediated Endocytosis and Trafficking in Endothelial Cells. *The Journal of biological chemistry*. 291:20729-20738.

Jin, F., B. Dong, J. Georgiou, Q. Jiang, J. Zhang, A. Bharioke, F. Qiu, S. Lommel, M.L. Feltri, L. Wrabetz, J.C. Roder, J. Eyer, X. Chen, A.C. Peterson, and K.A. Siminovitch. 2011. N-WASp is required for Schwann cell cytoskeletal dynamics, normal myelin gene expression and peripheral nerve myelination. *Development*. 138:1329-1337.

Jin, R., J.R. Junutula, H.T. Matern, K.E. Ervin, R.H. Scheller, and A.T. Brunger. 2005. Exo84 and Sec5 are competitive regulatory Sec6/8 effectors to the RalA GTPase. *The EMBO journal*. 24:2064-2074.

Jullien-Flores, V., O. Dorseuil, F. Romero, F. Letourneur, S. Saragosti, R. Berger, A. Tavitian, G. Gacon, and J.H. Camonis. 1995. Bridging Ral GTPase to Rho pathways. RLIP76, a Ral effector with CDC42/Rac GTPase-activating protein activity. *The Journal of biological chemistry*. 270:22473-22477.

Jullien-Flores, V., Y. Mahe, G. Mirey, C. Leprince, B. Meunier-Bisceuil, A. Sorkin, and J.H. Camonis. 2000. RLIP76, an effector of the GTPase Ral, interacts with the AP2 complex: involvement of the Ral pathway in receptor endocytosis. *Journal of cell science*. 113 (Pt 16):2837-2844.

Kandel, E.R., J.H. Schwartz, and T.M. Jessell. 2012. Principles of Neural Science. Mcgraw-Hill Professional.

Karunanithi, S., T. Xiong, M. Uhm, D. Leto, J. Sun, X.W. Chen, and A.R. Saltiel. 2014. A Rab10:RalA G protein cascade regulates insulin-stimulated glucose uptake in adipocytes. *Molecular biology of the cell*. 25:3059-3069.

Kashatus, D.F., K.H. Lim, D.C. Brady, N.L. Pershing, A.D. Cox, and C.M. Counter. 2011. RALA and RALBP1 regulate mitochondrial fission at mitosis. *Nature cell biology*. 13:1108-1115.

Kawato, M., R. Shirakawa, H. Kondo, T. Higashi, T. Ikeda, K. Okawa, S. Fukai, O. Nureki, T. Kita, and H. Horiuchi. 2008. Regulation of platelet dense granule secretion by the Ral GTPase-exocyst pathway. *The Journal of biological chemistry*. 283:166-174.

Kikuchi, A., S.D. Demo, Z.H. Ye, Y.W. Chen, and L.T. Williams. 1994. ralGDS Family Members Interact with the Effector Loop of *ras* p21. *Molecular and cellular biology*:7483 - 7491.

Kim, J.H., S.D. Lee, J.M. Han, T.G. Lee, Y. Kim, J.B. Park, J.D. Lambeth, P.G. Suh, and S.H. Ryu. 1998. Activation of phospholipase D1 by direct interaction with ADP-ribosylation factor 1 and RalA. *FEBS letters*. 430:231-235.

Kinsella, B.T., R.A. Erdman, and W.A. Maltese. 1991. Carboxyl-terminal isoprenylation of ras-related GTP-binding proteins encoded by rac1, rac2, and ralA. *The Journal of biological chemistry*. 266:9786-9794.

Koronakis, V., P.J. Hume, D. Humphreys, T. Liu, O. Horning, O.N. Jensen, and E.J. McGhie. 2011. WAVE regulatory complex activation by cooperating GTPases Arf and Rac1. *Proceedings of the National Academy of Sciences of the United States of America*. 108:14449-14454.

Kuhlbrodt, K., B. Herbarth, E. Sock, I. Hermans-Borgmeyer, and M. Wegner. 1998. Sox10, a novel transcriptional modulator in glial cells. *The Journal of neuroscience : the official journal of the Society for Neuroscience*. 18:237-250.

Lallemand, Y., V. Luria, R. Haffner-Krausz, and P. Lonai. 1998. Maternally expressed PGK-Cre transgene as a tool for early and uniform activation of the Cre site-specific recombinase. *Transgenic Res*. 7:105-112.

Lalli, G. 2009. RalA and the exocyst complex influence neuronal polarity through PAR-3 and aPKC. *Journal of cell science*. 122:1499-1506.

Lalli, G., and A. Hall. 2005. Ral GTPases regulate neurite branching through GAP-43 and the exocyst complex. *The Journal of cell biology*. 171:857-869.

Lee, S., J.G. Wurtzel, and L.E. Goldfinger. 2014. The RLIP76 N-terminus binds ARNO to regulate PI 3-kinase, Arf6 and Rac signaling, cell spreading and migration. *Biochem Biophys Res Commun*. 454:560-565.

Leone, D.P., S. Genoud, S. Atanasoski, R. Grausenburger, P. Berger, D. Metzger, W.B. Macklin, P. Chambon, and U. Suter. 2003. Tamoxifen-inducible glia-specific Cre mice for somatic mutagenesis in oligodendrocytes and Schwann cells. *Molecular and cellular neurosciences*. 22:430-440.

Leto, D., M. Uhm, A. Williams, X.W. Chen, and A.R. Saltiel. 2013. Negative regulation of the RalGAP complex by 14-3-3. *The Journal of biological chemistry*. 288:9272-9283.

Levi, A.D., R.P. Bunge, J.A. Lofgren, L. Meima, F. Hefti, K. Nikolics, and M.X. Sliwkowski. 1995. The influence of heregulins on human Schwann cell proliferation. *The Journal of neuroscience : the official journal of the Society for Neuroscience*. 15:1329-1340.

Li, B., and C.N. Dewey. 2011. RSEM: accurate transcript quantification from RNA-Seq data with or without a reference genome. *BMC bioinformatics*. 12:323.

Li, G., L. Han, T.C. Chou, Y. Fujita, L. Arunachalam, A. Xu, A. Wong, S.K. Chiew, Q. Wan, L. Wang, and S. Sugita. 2007. RalA and RalB function as the critical GTP sensors for GTP-dependent exocytosis. *The Journal of neuroscience : the official journal of the Society for Neuroscience*. 27:190-202.

Li, H., H. Yang, Y. Liu, W. Huan, S. Zhang, G. Wu, Q. Lu, Q. Wang, and Y. Wang. 2011. The cyclin-dependent kinase inhibitor p27(Kip1) is a positive regulator of Schwann cell differentiation in vitro. *Journal of molecular neuroscience : MN*. 45:277-283.

Lim, K.H., A.T. Baines, J.J. Fiordalisi, M. Shipitsin, L.A. Feig, A.D. Cox, C.J. Der, and C.M. Counter. 2005. Activation of RalA is critical for Ras-induced tumorigenesis of human cells. *Cancer cell*. 7:533-545.

Lim, K.H., D.C. Brady, D.F. Kashatus, B.B. Ancrile, C.J. Der, A.D. Cox, and C.M. Counter. 2010. Aurora-A phosphorylates, activates, and relocalizes the small GTPase RalA. *Molecular and cellular biology*. 30:508-523.

Lim, K.H., K. O'Hayer, S.J. Adam, S.D. Kendall, P.M. Campbell, C.J. Der, and C.M. Counter. 2006. Divergent roles for RalA and RalB in malignant growth of human pancreatic carcinoma cells. *Current biology : CB*. 16:2385-2394.

Logan, A.M., A.E. Mammel, D.C. Robinson, A.L. Chin, A.F. Condon, and F.L. Robinson. 2017. Schwann cell-specific deletion of the endosomal PI 3-kinase Vps34 leads to delayed radial sorting of axons, arrested myelination, and abnormal ErbB2-ErbB3 tyrosine kinase signaling. *Glia*. 65:1452-1470.

Lopez-Anido, C., Y. Poitelon, C. Gopinath, J.J. Moran, K.H. Ma, W.D. Law, A. Antonellis, M.L. Feltri, and J. Svaren. 2016. Tead1 regulates the expression of Peripheral Myelin Protein 22 during Schwann cell development. *Human molecular genetics*. 25:3055-3069.

Lopez, J.A., E.P. Kwan, L. Xie, Y. He, D.E. James, and H.Y. Gaisano. 2008. The RalA GTPase is a central regulator of insulin exocytosis from pancreatic islet beta cells. *The Journal of biological chemistry*. 283:17939-17945.

Luo, J.Q., X. Liu, P. Frankel, T. Rotunda, M. Ramos, J. Flom, H. Jiang, L.A. Feig, A.J. Morris, R.A. Kahn, and D.A. Foster. 1998. Functional association between Arf and RalA in active phospholipase D complex. *Proceedings of the National Academy of Sciences of the United States of America*. 95:3632-3637.

Lyons, D.A., H.M. Pogoda, M.G. Voas, I.G. Woods, B. Diamond, R. Nix, N. Arana, J. Jacobs, and W.S. Talbot. 2005. erbb3 and erbb2 are essential for schwann cell migration and myelination in zebrafish. *Current biology : CB*. 15:513-524.

Maehama, T., M. Tanaka, H. Nishina, M. Murakami, Y. Kanaho, and K. Hanada. 2008. RalA functions as an indispensable signal mediator for the nutrient-sensing system. *The Journal of biological chemistry*. 283:35053-35059.

Maro, G.S., M. Vermeren, O. Voiculescu, L. Melton, J. Cohen, P. Charnay, and P. Topilko. 2004. Neural crest boundary cap cells constitute a source of neuronal and glial cells of the PNS. *Nature neuroscience*. 7:930-938.

Martin-Urdiroz, M., M.J. Deeks, C.G. Horton, H.R. Dawe, and I. Jourdain. 2016. The Exocyst Complex in Health and Disease. *Front Cell Dev Biol*. 4:24.

Martin, T.D., X.W. Chen, R.E. Kaplan, A.R. Saltiel, C.L. Walker, D.J. Reiner, and C.J. Der. 2014. Ral and Rheb GTPase activating proteins integrate mTOR and GTPase signaling in aging, autophagy, and tumor cell invasion. *Molecular cell*. 53:209-220.

Martin, T.D., N. Mitin, A.D. Cox, J.J. Yeh, and C.J. Der. 2012. Phosphorylation by protein kinase Calpha regulates RalB small GTPase protein activation, subcellular localization, and effector utilization. *The Journal of biological chemistry*. 287:14827-14836.

Masaki, T. 2012. Polarization and myelination in myelinating glia. *ISRN Neurol*. 2012:769412.

Meier, C., E. Parmantier, A. Brennan, R. Mirsky, and K.R. Jessen. 1999. Developing Schwann cells acquire the ability to survive without axons by establishing an autocrine circuit involving insulin-like growth factor, neurotrophin-3, and platelet-derived growth factor-BB. *The Journal of neuroscience : the official journal of the Society for Neuroscience*. 19:3847-3859.

Melendez-Vasquez, C.V., S. Einheber, and J.L. Salzer. 2004. Rho kinase regulates schwann cell myelination and formation of associated axonal domains. *The Journal of neuroscience : the official journal of the Society for Neuroscience*. 24:3953-3963.

Michailov, G.V., M.W. Sereda, B.G. Brinkmann, T.M. Fischer, B. Haug, C. Birchmeier, L. Role, C. Lai, M.H. Schwab, and K.A. Nave. 2004. Axonal neuregulin-1 regulates myelin sheath thickness. *Science*. 304:700-703.

Mogha, A., A.E. Benesh, C. Patra, F.B. Engel, T. Schoneberg, I. Liebscher, and K.R. Monk. 2013. Gpr126 functions in Schwann cells to control differentiation and myelination via G-protein activation. *The Journal of neuroscience : the official journal of the Society for Neuroscience*. 33:17976-17985.

Monk, K.R., M.L. Feltri, and C. Taveggia. 2015. New insights on Schwann cell development. *Glia*. 63:1376-1393.

Monk, K.R., K. Oshima, S. Jors, S. Heller, and W.S. Talbot. 2011. Gpr126 is essential for peripheral nerve development and myelination in mammals. *Development*. 138:2673-2680.

Montani, L., T. Buerki-Thurnherr, J.P. de Faria, J.A. Pereira, N.G. Dias, R. Fernandes, A.F. Goncalves, A. Braun, Y. Benninger, R.T. Bottcher, M. Costell, K.A. Nave, R.J. Franklin, D. Meijer, U. Suter, and J.B. Relvas. 2014. Profilin 1 is required for peripheral nervous system myelination. *Development*. 141:1553-1561.

Morgan, L., K.R. Jessen, and R. Mirsky. 1991. The effects of cAMP on differentiation of cultured Schwann cells: progression from an early phenotype (04+) to a myelin phenotype (P0+, GFAP-, N-CAM-, NGF-receptor-) depends on growth inhibition. *The Journal of cell biology*. 112:457-467.

Morinaka, K., S. Koyama, S. Nakashima, T. Hinoi, K. Okawa, A. Iwamatsu, and A. Kikuchi. 1999. Epsin binds to the EH domain of POB1 and regulates receptor-mediated endocytosis. *Oncogene*. 18:5915-5922.

Moskalenko, S., D.O. Henry, C. Rosse, G. Mirey, J.H. Camonis, and M.A. White. 2002. The exocyst is a Ral effector complex. *Nature cell biology*. 4:66-72.

Moskalenko, S., C. Tong, C. Rosse, G. Mirey, E. Formstecher, L. Daviet, J. Camonis, and M.A. White. 2003. Ral GTPases regulate exocyst assembly through dual subunit interactions. *The Journal of biological chemistry*. 278:51743-51748.

Mukouyama, Y.S., H.P. Gerber, N. Ferrara, C. Gu, and D.J. Anderson. 2005. Peripheral nerve-derived VEGF promotes arterial differentiation via neuropilin 1-mediated positive feedback. *Development*. 132:941-952.

Nakashima, S., K. Morinaka, S. Koyama, M. Ikeda, M. Kishida, K. Okawa, A. Iwamatsu, S. Kishida, and A. Kikuchi. 1999. Small G protein Ral and its downstream molecules regulate endocytosis of EGF and insulin receptors. *The EMBO journal*. 18:3629-3642.

Nave, K.A., and H.B. Werner. 2014. Myelination of the nervous system: mechanisms and functions. *Annual review of cell and developmental biology*. 30:503-533.

Neel, N.F., K.L. Rossman, T.D. Martin, T.K. Hayes, J.J. Yeh, and C.J. Der. 2012. The RalB small GTPase mediates formation of invadopodia through a GTPase-activating protein-independent function of the RalBP1/RLIP76 effector. *Molecular and cellular biology*. 32:1374-1386.

Ness, J.K., K.M. Snyder, and N. Tapinos. 2013. Lck tyrosine kinase mediates beta1-integrin signalling to regulate Schwann cell migration and myelination. *Nature communications*. 4:1912.

Newbern, J., and C. Birchmeier. 2010. Nrg1/ErbB signaling networks in Schwann cell development and myelination. *Semin Cell Dev Biol*. 21:922-928.

Neyraud, V., V.N. Aushev, A. Hatzoglou, B. Meunier, I. Cascone, and J. Camonis. 2012. RalA and RalB proteins are ubiquitinated GTPases, and ubiquitinated RalA increases lipid raft exposure at the plasma membrane. *The Journal of biological chemistry*. 287:29397-29405.

Nguyen, T., N.R. Mehta, K. Conant, K.J. Kim, M. Jones, P.A. Calabresi, G. Melli, A. Hoke, R.L. Schnaar, G.L. Ming, H. Song, S.C. Keswani, and J.W. Griffin. 2009. Axonal protective effects of the myelin-associated glycoprotein. *The Journal of neuroscience : the official journal of the Society for Neuroscience*. 29:630-637.

Nicely, N.I., J. Kosak, V. de Serrano, and C. Mattos. 2004. Crystal structures of Ral-GppNHp and Ral-GDP reveal two binding sites that are also present in Ras and Rap. *Structure*. 12:2025-2036.

Niemann, A., M. Ruegg, V. La Padula, A. Schenone, and U. Suter. 2005. Ganglioside-induced differentiation associated protein 1 is a regulator of the mitochondrial network: new implications for Charcot-Marie-Tooth disease. *The Journal of cell biology*. 170:1067-1078.

Nishimura, A., and M.E. Linder. 2013. Identification of a novel prenyl and palmitoyl modification at the CaaX motif of Cdc42 that regulates RhoGDI binding. *Molecular and cellular biology*. 33:1417-1429.

Nitzan, E., E.R. Pfaltzgraff, P.A. Labosky, and C. Kalcheim. 2013. Neural crest and Schwann cell progenitor-derived melanocytes are two spatially segregated populations similarly regulated by Foxd3. *Proceedings of the National Academy of Sciences of the United States of America*. 110:12709-12714.

Nodari, A., D. Zambroni, A. Quattrini, F.A. Court, A. D'Urso, A. Recchia, V.L. Tybulewicz, L. Wrabetz, and M.L. Feltri. 2007. Beta1 integrin activates Rac1 in Schwann cells to generate radial lamellae during axonal sorting and myelination. *The Journal of cell biology*. 177:1063-1075.

Norrmen, C., G. Figlia, F. Lebrun-Julien, J.A. Pereira, M. Trotzmuller, H.C. Kofeler, V. Rantanen, C. Wessig, A.L. van Deijk, A.B. Smit, M.H. Verheijen, M.A. Ruegg, M.N. Hall, and U. Suter. 2014. mTORC1 controls PNS myelination along the mTORC1-RXRgamma-SREBP-lipid biosynthesis axis in Schwann cells. *Cell reports*. 9:646-660.

Norton, W.T., and S.E. Poduslo. 1973. Myelination in rat brain: changes in myelin composition during brain maturation. *Journal of neurochemistry*. 21:759-773.

Novak, N., V. Bar, H. Sabanay, S. Frechter, M. Jaegle, S.B. Snapper, D. Meijer, and E. Peles. 2011. N-WASP is required for membrane wrapping and myelination by Schwann cells. *The Journal of cell biology*. 192:243-250.

Obremski, V.J., P.M. Wood, and M.B. Bunge. 1993. Fibroblasts promote Schwann cell basal lamina deposition and elongation in the absence of neurons in culture. *Developmental biology*. 160:119-134.

Occhi, S., D. Zambroni, U. Del Carro, S. Amadio, E.E. Sirkowski, S.S. Scherer, K.P. Campbell, S.A. Moore, Z.L. Chen, S. Strickland, A. Di Muzio, A. Uncini, L. Wrabetz, and M.L. Feltri. 2005. Both laminin and Schwann cell dystroglycan are necessary for proper clustering of sodium channels at nodes of Ranvier. *The Journal of neuroscience : the official journal of the Society for Neuroscience*. 25:9418-9427.

Oeckinghaus, A., T.S. Postler, P. Rao, H. Schmitt, V. Schmitt, Y. Grinberg-Bleyer, L.I. Kuhn, C.W. Gruber, G.E. Lienhard, and S. Ghosh. 2014. kappaB-Ras proteins regulate both NF-kappaB-dependent inflammation and Ral-dependent proliferation. *Cell reports*. 8:1793-1807.

Ohta, Y., N. Suzuki, S. Nakamura, J.H. Hartwig, and T.P. Stossel. 1999. The small GTPase RalA targets filamin to induce filopodia. *Proceedings of the National Academy of Sciences of the United States of America*. 96:2122-2128.

Osei-Sarfo, K., L. Martello, S. Ibrahim, and A. Pellicer. 2011. The human Rgr oncogene is overexpressed in T-cell malignancies and induces transformation by acting as a GEF for Ras and Ral. *Oncogene*. 30:3661-3671.

Oxford, G., C.R. Owens, B.J. Titus, T.L. Foreman, M.C. Herlevsen, S.C. Smith, and D. Theodorescu. 2005. RalA and RalB: antagonistic relatives in cancer cell migration. *Cancer research*. 65:7111-7120.

Ozcelik, M., L. Cotter, C. Jacob, J.A. Pereira, J.B. Relvas, U. Suter, and N. Tricaud. 2010. Pals1 is a major regulator of the epithelial-like polarization and the extension of the myelin sheath in peripheral nerves. *The Journal of neuroscience : the official journal of the Society for Neuroscience*. 30:4120-4131.

Palandri, A., V.R. Salvador, J. Wojnacki, A.L. Vivinetto, R.L. Schnaar, and P.H. Lopez. 2015. Myelin-associated glycoprotein modulates apoptosis of motoneurons during early postnatal development via NgR/p75(NTR) receptor-mediated activation of RhoA signaling pathways. *Cell death & disease*. 6:e1876.

Park, S.H., and R.A. Weinberg. 1995. A putative effector of Ral has homology to Rho/Rac GTPase activating proteins. *Oncogene*. 11:2349-2355.

Parkinson, D.B., Z. Dong, H. Bunting, J. Whitfield, C. Meier, H. Marie, R. Mirsky, and K.R. Jessen. 2001. Transforming growth factor beta (TGFbeta) mediates Schwann cell death in vitro and in vivo: examination of c-Jun activation, interactions with survival signals, and the relationship of TGFbeta-mediated death to Schwann cell differentiation. *The Journal of neuroscience : the official journal of the Society for Neuroscience*. 21:8572-8585.

Parmantier, E., B. Lynn, D. Lawson, M. Turmaine, S.S. Namini, L. Chakrabarti, A.P. McMahon, K.R. Jessen, and R. Mirsky. 1999. Schwann cell-derived Desert hedgehog controls the development of peripheral nerve sheaths. *Neuron*. 23:713-724.

Parrini, M.C., A. Sadou-Dubourgnoux, K. Aoki, K. Kunida, M. Biondini, A. Hatzoglou, P. Poullet, E. Formstecher, C. Yeaman, M. Matsuda, C. Rosse, and J. Camonis. 2011. SH3BP1, an exocyst-associated RhoGAP, inactivates Rac1 at the front to drive cell motility. *Molecular cell*. 42:650-661.

Patton, B.L., B. Wang, Y.S. Tarumi, K.L. Seburn, and R.W. Burgess. 2008. A single point mutation in the LN domain of LAMA2 causes muscular dystrophy and peripheral amyelination. *Journal of cell science*. 121:1593-1604.

Patzig, J., O. Jahn, S. Tenzer, S.P. Wichert, P. de Monasterio-Schrader, S. Rosfa, J. Kuharev, K. Yan, I. Bormuth, J. Bremer, A. Aguzzi, F. Orfaniotou, D. Hesse, M.H. Schwab, W. Mobius, K.A. Nave, and H.B. Werner. 2011. Quantitative and integrative proteome analysis of peripheral nerve myelin identifies novel myelin proteins and candidate neuropathy loci. *The Journal of neuroscience : the official journal of the Society for Neuroscience*. 31:16369-16386.

Pawar, A., J.A. Meier, A. Dasgupta, N. Diwanji, N. Deshpande, K. Saxena, N. Buwa, S. Inchanalkar, M.A. Schwartz, and N. Balasubramanian. 2016. Ral-Arf6 crosstalk regulates Ral dependent exocyst trafficking and anchorage independent growth signalling. *Cellular signalling*. 28:1225-1236.

Pellegatta, M., A. De Arcangelis, A. D'Urso, A. Nodari, D. Zambroni, M. Ghidinelli, V. Matafora, C. Williamson, E. Georges-Labouesse, J. Kreidberg, U. Mayer, K.K. McKee, P.D. Yurchenco, A. Quattrini, L. Wrabetz, and M.L. Feltri. 2013. alpha6beta1 and alpha7beta1 integrins are required in Schwann cells to sort axons. *The Journal of neuroscience : the official journal of the Society for Neuroscience*. 33:17995-18007.

Pereira, J.A., R. Baumann, C. Norrmen, C. Somandin, M. Miehe, C. Jacob, T. Luhmann, H. Hall-Bozic, N. Mantei, D. Meijer, and U. Suter. 2010. Dicer in Schwann cells is required for myelination and

axonal integrity. *The Journal of neuroscience : the official journal of the Society for Neuroscience*. 30:6763-6775.

Pereira, J.A., Y. Benninger, R. Baumann, A.F. Goncalves, M. Ozcelik, T. Thurnherr, N. Tricaud, D. Meijer, R. Fassler, U. Suter, and J.B. Relvas. 2009. Integrin-linked kinase is required for radial sorting of axons and Schwann cell remyelination in the peripheral nervous system. *The Journal of cell biology*. 185:147-161.

Pereira, J.A., F. Lebrun-Julien, and U. Suter. 2012. Molecular mechanisms regulating myelination in the peripheral nervous system. *Trends in neurosciences*. 35:123-134.

Personnic, N., G. Lakisic, E. Gouin, A. Rousseau, A. Gautreau, P. Cossart, and H. Bierne. 2014. A role for Ral GTPase-activating protein subunit beta in mitotic regulation. *The FEBS journal*. 281:2977-2989.

Peschard, P., A. McCarthy, V. Leblanc-Dominguez, M. Yeo, S. Guichard, G. Stamp, and C.J. Marshall. 2012. Genetic deletion of RALA and RALB small GTPases reveals redundant functions in development and tumorigenesis. *Current biology : CB*. 22:2063-2068.

Petersen, S.C., R. Luo, I. Liebscher, S. Giera, S.J. Jeong, A. Mogha, M. Ghidinelli, M.L. Feltri, T. Schoneberg, X. Piao, and K.R. Monk. 2015. The adhesion GPCR GPR126 has distinct, domain-dependent functions in Schwann cell development mediated by interaction with laminin-211. *Neuron*. 85:755-769.

Peterson, S.N., L. Trabalzini, T.R. Brtva, T. Fischer, D.L. Altschuler, P. Martelli, E.G. Lapetina, C.J. Der, and G.C. White, 2nd. 1996. Identification of a novel RalGDS-related protein as a candidate effector for Ras and Rap1. *The Journal of biological chemistry*. 271:29903-29908.

Poitelon, Y., S. Bogni, V. Matafora, G. Della-Flora Nunes, E. Hurley, M. Ghidinelli, B.S. Katzenellenbogen, C. Taveggia, N. Silvestri, A. Bachi, A. Sannino, L. Wrabetz, and M.L. Feltri. 2015. Spatial mapping of juxtacrine axo-glial interactions identifies novel molecules in peripheral myelination. *Nature communications*. 6:8303.

Poitelon, Y., C. Lopez-Anido, K. Catignas, C. Berti, M. Palmisano, C. Williamson, D. Ameroso, K. Abiko, Y. Hwang, A. Gregorieff, J.L. Wrana, M. Asmani, R. Zhao, F.J. Sim, L. Wrabetz, J. Svaren, and M.L. Feltri. 2016. YAP and TAZ control peripheral myelination and the expression of laminin receptors in Schwann cells. *Nature neuroscience*. 19:879-887.

Polzin, A., M. Shipitsin, T. Goi, L.A. Feig, and T.J. Turner. 2002. Ral-GTPase influences the regulation of the readily releasable pool of synaptic vesicles. *Molecular and cellular biology*. 22:1714-1722.

Pomeroy, E.J., L.A. Lee, R.D.W. Lee, D.K. Schirm, N.A. Temiz, J. Ma, T.A. Gruber, E. Diaz-Flores, B.S. Moriarity, J.R. Downing, K.M. Shannon, D.A. Largaespada, and C.E. Eckfeldt. 2017. Ras oncogene-independent activation of RALB signaling is a targetable mechanism of escape from NRAS(V12) oncogene addiction in acute myeloid leukemia. *Oncogene*. 36:3263-3273.

Pooya, S., X. Liu, V.B. Kumar, J. Anderson, F. Imai, W. Zhang, G. Ciraolo, N. Ratner, K.D. Setchell, Y. Yoshida, M.P. Jankowski, and B. Dasgupta. 2014. The tumour suppressor LKB1 regulates myelination through mitochondrial metabolism. *Nature communications*. 5:4993.

Porrello, E., C. Rivellini, G. Dina, D. Triolo, U. Del Carro, D. Ungaro, M. Panattoni, M.L. Feltri, L. Wrabetz, R. Pardi, A. Quattrini, and S.C. Previtali. 2014. Jab1 regulates Schwann cell proliferation and axonal sorting through p27. *The Journal of experimental medicine*. 211:29-43.

Raphael, A.R., D.A. Lyons, and W.S. Talbot. 2011. ErbB signaling has a role in radial sorting independent of Schwann cell number. *Glia*. 59:1047-1055.

Rebhun, J.F., H. Chen, and L.A. Quilliam. 2000. Identification and Characterization of a New Family of Guanine Nucleotide Exchange Factors for the Ras-related GTPase Ral. *Journal of Biological Chemistry*. 275:13406-13410.

Ridley, A.J., J.B. Davis, P. Stroobant, and H. Land. 1989. Transforming growth factors-beta 1 and beta 2 are mitogens for rat Schwann cells. *The Journal of cell biology*. 109:3419-3424.

Robinson, M.D., D.J. McCarthy, and G.K. Smyth. 2010. edgeR: a Bioconductor package for differential expression analysis of digital gene expression data. *Bioinformatics*. 26:139-140.

Rondaij, M.G., E. Sellink, K.A. Gijzen, J.P. ten Klooster, P.L. Hordijk, J.A. van Mourik, and J. Voorberg. 2004. Small GTP-binding protein Ral is involved in cAMP-mediated release of von Willebrand factor from endothelial cells. *Arterioscler Thromb Vasc Biol*. 24:1315-1320.

Rosse, C., S. L'Hoste, N. Offner, A. Picard, and J. Camonis. 2003. RLIP, an effector of the Ral GTPases, is a platform for Cdk1 to phosphorylate epsin during the switch off of endocytosis in mitosis. *The Journal of biological chemistry*. 278:30597-30604.

Rusanescu, G., T. Gotoh, X. Tian, and L.A. Feig. 2001. Regulation of Ras signaling specificity by protein kinase C. *Molecular and cellular biology*. 21:2650-2658.

Sablina, A.A., W. Chen, J.D. Arroyo, L. Corral, M. Hector, S.E. Bulmer, J.A. DeCaprio, and W.C. Hahn. 2007. The tumor suppressor PP2A Abeta regulates the RalA GTPase. *Cell*. 129:969-982.

Santos, O.A., M.C. Parrini, and J. Camonis. 2016. RalGPS2 Is Essential for Survival and Cell Cycle Progression of Lung Cancer Cells Independently of Its Established Substrates Ral GTPases. *PloS one*. 11:e0154840.

Schindelin, J., I. Arganda-Carreras, E. Frise, V. Kaynig, M. Longair, T. Pietzsch, S. Preibisch, C. Rueden, S. Saalfeld, B. Schmid, J.Y. Tinevez, D.J. White, V. Hartenstein, K. Eliceiri, P. Tomancak, and A. Cardona. 2012. Fiji: an open-source platform for biological-image analysis. *Nat Methods*. 9:676-682.

Schneider, C.A., W.S. Rasband, and K.W. Eliceiri. 2012. NIH Image to ImageJ: 25 years of image analysis. *Nat Methods*. 9:671-675.

Schwarzbraun, T., J.B. Vincent, A. Schumacher, D.H. Geschwind, J. Oliveira, C. Windpassinger, L. Ofner, M.K. Ledinegg, P.M. Kroisel, K. Wagner, and E. Petek. 2004. Cloning, genomic structure, and expression profiles of TULIP1 (GARNL1), a brain-expressed candidate gene for 14q13-linked neurological phenotypes, and its murine homologue. *Genomics*. 84:577-586.

Shah, N.M., M.A. Marchionni, I. Isaacs, P. Stroobant, and D.J. Anderson. 1994. Glial growth factor restricts mammalian neural crest stem cells to a glial fate. *Cell*. 77:349-360.

Shao, H., and D.A. Andres. 2000. A novel RalGEF-like protein, RGL3, as a candidate effector for rit and Ras. *The Journal of biological chemistry*. 275:26914-26924.

Shen, Y.A., Y. Chen, D.Q. Dao, S.R. Mayoral, L. Wu, D. Meijer, E.M. Ullian, J.R. Chan, and Q.R. Lu. 2014. Phosphorylation of LKB1/Par-4 establishes Schwann cell polarity to initiate and control myelin extent. *Nature communications*. 5:4991.

Sherman, D.L., M. Krols, L.M. Wu, M. Grove, K.A. Nave, Y.G. Gangloff, and P.J. Brophy. 2012. Arrest of myelination and reduced axon growth when Schwann cells lack mTOR. *The Journal of neuroscience : the official journal of the Society for Neuroscience*. 32:1817-1825.

Shipitsin, M., and L.A. Feig. 2004. RalA but not RalB enhances polarized delivery of membrane proteins to the basolateral surface of epithelial cells. *Molecular and cellular biology*. 24:5746-5756.

Shirakawa, R., S. Fukai, M. Kawato, T. Higashi, H. Kondo, T. Ikeda, E. Nakayama, K. Okawa, O. Nureki, T. Kimura, T. Kita, and H. Horiuchi. 2009. Tuberous sclerosis tumor suppressor complex-like complexes act as GTPase-activating proteins for Ral GTPases. *The Journal of biological chemistry*. 284:21580-21588.

Shirakawa, R., and H. Horiuchi. 2015. Ral GTPases: crucial mediators of exocytosis and tumourigenesis. *Journal of biochemistry*.

Sidiropoulos, P.N., M. Miehe, T. Bock, E. Tinelli, C.I. Oertli, R. Kuner, D. Meijer, B. Wollscheid, A. Niemann, and U. Suter. 2012. Dynamin 2 mutations in Charcot-Marie-Tooth neuropathy highlight the importance of clathrin-mediated endocytosis in myelination. *Brain : a journal of neurology*. 135:1395-1411.

Simicek, M., S. Lievens, M. Laga, D. Guzenko, V.N. Aushev, P. Kalev, M.F. Baietti, S.V. Strelkov, K. Gevaert, J. Tavernier, and A.A. Sablina. 2013. The deubiquitylase USP33 discriminates between RALB functions in autophagy and innate immune response. *Nature cell biology*. 15:1220-1230.

Singhal, S.S., L. Nagaprashantha, P. Singhal, S. Singhal, J. Singhal, S. Awasthi, and D. Horne. 2017. RLIP76 Inhibition: A Promising Developmental Therapy for Neuroblastoma. *Pharm Res*. 34:1673-1682.

Singhal, S.S., J. Singhal, J. Figarola, D. Horne, and S. Awasthi. 2015. RLIP76 Targeted Therapy for Kidney Cancer. *Pharm Res*. 32:3123-3136.

Spaargaren, M., and J.R. Bischoff. 1994. Identification of the guanine nucleotide dissociation stimulator for Ral as a putative effector molecule of R-ras, H-ras, K-ras, and Rap. *Proceedings of the National Academy of Sciences of the United States of America*. 91:12609-12613.

Stewart, H.J., A. Brennan, M. Rahman, G. Zoidl, P.J. Mitchell, K.R. Jessen, and R. Mirsky. 2001. Developmental regulation and overexpression of the transcription factor AP-2, a potential regulator of the timing of Schwann cell generation. *The European journal of neuroscience*. 14:363-372.

Sugihara, K., S. Asano, K. Tanaka, A. Iwamatsu, K. Okawa, and Y. Ohta. 2002. The exocyst complex binds the small GTPase RalA to mediate filopodia formation. *Nature cell biology*. 4:73-78.

Takaya, A., Y. Ohba, K. Kurokawa, and M. Matsuda. 2004. RalA activation at nascent lamellipodia of epidermal growth factor-stimulated Cos7 cells and migrating Madin-Darby canine kidney cells. *Molecular biology of the cell*. 15:2549-2557.

Taveggia, C., G. Zanazzi, A. Petrylak, H. Yano, J. Rosenbluth, S. Einheber, X. Xu, R.M. Esper, J.A. Loeb, P. Shrager, M.V. Chao, D.L. Falls, L. Role, and J.L. Salzer. 2005. Neuregulin-1 type III determines the ensheathment fate of axons. *Neuron*. 47:681-694.

Tazat, K., M. Harsat, A. Goldshmid-Shagal, M. Ehrlich, and Y.I. Henis. 2013. Dual effects of Ral-activated pathways on p27 localization and TGF-beta signaling. *Molecular biology of the cell*. 24:1812-1824.

Teodoro, R.O., G. Pekkurnaz, A. Nasser, M.E. Higashi-Kovtun, M. Balakireva, I.G. McLachlan, J. Camonis, and T.L. Schwarz. 2013. Ral mediates activity-dependent growth of postsynaptic membranes via recruitment of the exocyst. *The EMBO journal*. 32:2039-2055.

Tian, X., G. Rusanescu, W. Hou, B. Schaffhausen, and L.A. Feig. 2002. PDK1 mediates growth factor-induced Ral-GEF activation by a kinase-independent mechanism. *The EMBO journal*. 21:1327-1338.

Tracy, K., P.D. Velentzas, and E.H. Baehrecke. 2016. Ral GTPase and the exocyst regulate autophagy in a tissue-specific manner. *EMBO Rep*. 17:110-121.

van den Berg, M.C., I.J. van Gogh, A.M. Smits, M. van Triest, T.B. Dansen, M. Visscher, P.E. Polderman, M.J. Vliem, H. Rehmann, and B.M. Burgering. 2013. The small GTPase RALA controls c-Jun N-terminal kinase-mediated FOXO activation by regulation of a JIP1 scaffold complex. *The Journal of biological chemistry*. 288:21729-21741.

Vatsyayan, R., P.C. Lelsani, S. Awasthi, and S.S. Singhal. 2010. RLIP76: a versatile transporter and an emerging target for cancer therapy. *Biochem Pharmacol*. 79:1699-1705.

Velasquez, J.T., J.A. St John, L. Nazareth, and J.A.K. Ekberg. 2018. Schwann cell lamellipodia regulate cell-cell interactions and phagocytosis. *Molecular and cellular neurosciences*. 88:189-200.

Ventura, A., A. Meissner, C.P. Dillon, M. McManus, P.A. Sharp, L. Van Parijs, R. Jaenisch, and T. Jacks. 2004. Cre-lox-regulated conditional RNA interference from transgenes. *Proceedings of the National Academy of Sciences of the United States of America*. 101:10380-10385.

Vetter, I.R., and A. Wittinghofer. 2001. The guanine nucleotide-binding switch in three dimensions. *Science*. 294:1299-1304.

Viader, A., Y. Sasaki, S. Kim, A. Strickland, C.S. Workman, K. Yang, R.W. Gross, and J. Milbrandt. 2013. Aberrant Schwann cell lipid metabolism linked to mitochondrial deficits leads to axon degeneration and neuropathy. *Neuron*. 77:886-898.

Wallquist, W., S. Plantman, S. Thams, J. Thyboll, J. Kortesmaa, J. Lannergren, A. Domogatskaya, S.O. Ogren, M. Risling, H. Hammarberg, K. Tryggvason, and S. Cullheim. 2005. Impeded interaction between Schwann cells and axons in the absence of laminin alpha4. *The Journal of neuroscience : the official journal of the Society for Neuroscience*. 25:3692-3700.

Wang, H., C. Owens, N. Chandra, M.R. Conaway, D.L. Brautigan, and D. Theodorescu. 2010. Phosphorylation of RalB is important for bladder cancer cell growth and metastasis. *Cancer research*. 70:8760-8769.

Wang, L., G. Li, and S. Sugita. 2004. RalA-exocyst interaction mediates GTP-dependent exocytosis. *The Journal of biological chemistry*. 279:19875-19881.

Wang, M., and P.J. Casey. 2016. Protein prenylation: unique fats make their mark on biology. *Nature reviews. Molecular cell biology*. 17:110-122.

Wang, Q., J. Qian, J. Wang, C. Luo, J. Chen, G. Hu, and Y. Lu. 2013a. Knockdown of RLIP76 expression by RNA interference inhibits invasion, induces cell cycle arrest, and increases chemosensitivity to the anticancer drug temozolomide in glioma cells. *J Neurooncol*. 112:73-82.

Wang, Q., J.Y. Wang, X.P. Zhang, Z.W. Lv, D. Fu, Y.C. Lu, G.H. Hu, C. Luo, and J.X. Chen. 2013b. RLIP76 is overexpressed in human glioblastomas and is required for proliferation, tumorigenesis and suppression of apoptosis. *Carcinogenesis*. 34:916-926.

Wang, W., J. Liu, J. Qi, J. Zhang, Q. Zhu, and C. Qin. 2016. RLIP76 increases apoptosis through Akt/mTOR signaling pathway in gastric cancer. *Oncol Rep*. 36:2216-2224.

Webster, H.D., R. Martin, and M.F. O'Connell. 1973. The relationships between interphase Schwann cells and axons before myelination: a quantitative electron microscopic study. *Developmental biology*. 32:401-416.

Weis, K. 2003. Regulating access to the genome: nucleocytoplasmic transport throughout the cell cycle. *Cell*. 112:441-451.

Wennerberg, K., K.L. Rossman, and C.J. Der. 2005. The Ras superfamily at a glance. *Journal of cell science*. 118:843-846.

Woodhoo, A., M.B. Alonso, A. Droggiti, M. Turmaine, M. D'Antonio, D.B. Parkinson, D.K. Wilton, R. Al-Shawi, P. Simons, J. Shen, F. Guillemot, F. Radtke, D. Meijer, M.L. Feltri, L. Wrabetz, R. Mirsky, and K.R. Jessen. 2009. Notch controls embryonic Schwann cell differentiation, postnatal myelination and adult plasticity. *Nature neuroscience*. 12:839-847.

Wu, B., and W. Guo. 2015. The Exocyst at a Glance. *Journal of cell science*. 128:2957-2964.

Wu, J.C., T.Y. Chen, C.T. Yu, S.J. Tsai, J.M. Hsu, M.J. Tang, C.K. Chou, W.J. Lin, C.J. Yuan, and C.Y. Huang. 2005. Identification of V23RalA-Ser194 as a critical mediator for Aurora-A-induced cellular motility and transformation by small pool expression screening. *The Journal of biological chemistry*. 280:9013-9022.

Wu, L.M.N., Y. Deng, J. Wang, C. Zhao, J. Wang, R. Rao, L. Xu, W. Zhou, K. Choi, T.A. Rizvi, M. Remke, J.B. Rubin, R.L. Johnson, T.J. Carroll, A.O. Stemmer-Rachamimov, J. Wu, Y. Zheng, M. Xin, N. Ratner, and Q.R. Lu. 2018. Programming of Schwann Cells by Lats1/2-TAZ/YAP Signaling Drives Malignant Peripheral Nerve Sheath Tumorigenesis. *Cancer cell*. 33:292-308 e297.

Wu, Z., C. Owens, N. Chandra, K. Popovic, M. Conaway, and D. Theodorescu. 2010. RalBP1 is necessary for metastasis of human cancer cell lines. *Neoplasia*. 12:1003-1012.

Xu, L., P. Frankel, D. Jackson, T. Rotunda, R.L. Boshans, C. D'Souza-Schorey, and D.A. Foster. 2003. Elevated phospholipase D activity in H-Ras- but not K-Ras-transformed cells by the synergistic action of RalA and ARF6. *Molecular and cellular biology*. 23:645-654.

Xu, L., D. Salloum, P.S. Medlin, M. Saqcena, P. Yellen, B. Perrella, and D.A. Foster. 2011. Phospholipase D mediates nutrient input to mammalian target of rapamycin complex 1 (mTORC1). *The Journal of biological chemistry*. 286:25477-25486.

Yamaguchi, A., T. Urano, T. Goi, and L.A. Feig. 1997. An Eps homology (EH) domain protein that binds to the Ral-GTPase target, RalBP1. *The Journal of biological chemistry*. 272:31230-31234.

Yan, C., and D. Theodorescu. 2018. RAL GTPases: Biology and Potential as Therapeutic Targets in Cancer. *Pharmacol Rev*. 70:1-11.

Yang, D., J. Bierman, Y.S. Tarumi, Y.P. Zhong, R. Rangwala, T.M. Proctor, Y. Miyagoe-Suzuki, S. Takeda, J.H. Miner, L.S. Sherman, B.G. Gold, and B.L. Patton. 2005. Coordinate control of axon defasciculation and myelination by laminin-2 and -8. *The Journal of cell biology*. 168:655-666.

Yang, J., Q. Song, Y. Cai, P. Wang, M. Wang, and D. Zhang. 2015. RLIP76-dependent suppression of PI3K/AKT/Bcl-2 pathway by miR-101 induces apoptosis in prostate cancer. *Biochem Biophys Res Commun*. 463:900-906.

Yao, K., H. Xing, W. Yang, A. Liao, B. Wu, Y. Li, R. Zhang, and Z. Liu. 2014. Knockdown of RLIP76 expression by RNA interference inhibits proliferation, enhances apoptosis, and increases chemosensitivity to daunorubicin in U937 leukemia cells. *Tumour Biol*. 35:8023-8031.

Yu, W.M., M.L. Feltri, L. Wrabetz, S. Strickland, and Z.L. Chen. 2005. Schwann cell-specific ablation of laminin gamma1 causes apoptosis and prevents proliferation. *The Journal of neuroscience : the official journal of the Society for Neuroscience*. 25:4463-4472.

Yun, B., A. Anderegg, D. Menichella, L. Wrabetz, M.L. Feltri, and R. Awatramani. 2010. MicroRNA-deficient Schwann cells display congenital hypomyelination. *The Journal of neuroscience : the official journal of the Society for Neuroscience*. 30:7722-7728.

Zago, G., M. Biondini, J. Camonis, and M.C. Parrini. 2017. A family affair: A Ral-exocyst-centered network links Ras, Rac, Rho signaling to control cell migration. *Small GTPases*:1-8.

Zhang, D., Y. Han, and L. Xu. 2016. Upregulation of miR-124 by physcion 8-O-beta-glucopyranoside inhibits proliferation and invasion of malignant melanoma cells via repressing RLIP76. *Biomed Pharmacother*. 84:166-176.

Zhang, L.L., F.J. Xie, C.H. Tang, W.R. Xu, X.S. Ding, and J. Liang. 2017. miR-340 suppresses tumor growth and enhances chemosensitivity of colorectal cancer by targeting RLIP76. *European review for medical and pharmacological sciences*. 21:2875-2886.

Zhang, Y., X. Song, W. Gong, Z. Zhu, X. Liu, Q. Hou, Y. Sun, J. Chai, L. Zou, and J. Guan. 2015. RLIP76 blockade by siRNA inhibits proliferation, enhances apoptosis, and suppresses invasion in HT29 colon cancer cells. *Cell Biochem Biophys*. 71:579-585.

Zollinger, D.R., K.J. Chang, K. Baalman, S. Kim, and M.N. Rasband. 2015. The Polarity Protein Pals1 Regulates Radial Sorting of Axons. *The Journal of neuroscience : the official journal of the Society for Neuroscience*. 35:10474-10484.

9. Contributions

While not mentioned in the text to preserve the flow of reading it is very important to highlight that not all the work in this thesis has been conducted by me alone. The following is a list of people that contributed and the form of their contribution:

Joanne Jeker:	Technical support on immunoblots (Figure 5 D) and immunostainings (Figure 10 A, E), image acquisition (Figure 12), and quantifications (Figure 7, Figure 8, Figure 11, Figure 14, Figure 15).
Dr. Jorge Antunes Pereira:	Preparation of sections for SEM imaging, SEM image acquisition (Figure 7, Figure 8, Figure 14, Figure 15, Figure 16).
Dr. Daniel Gerber and Dr. Gianluca Figlia:	Preparation of primary rat Schwann cells (Figure 13)
PD Dr. Ned Mantei:	Cloning of lentiviral RalA-expression vectors (Figure 12).
Dr. Jonathan DeGeer:	Preparation and analysis of CNS images of inducible RalKO mice (Figure 16).
Martina Jungo:	Analysis of inducible RalKO mice at 6 MpT (Figure 15)
Catharine Aquino Fournier:	mRNA sequencing (Figure 9)
Lennart Opitz:	Analysis of mRNA sequencing data (Figure 9)

10. Acknowledgements

It goes without saying that a work such as this thesis cannot be done without the help and support of many people and I have been very fortunate to have met with wonderful people that have contributed to this work in one way or another.

First and foremost I want to thank Prof. Dr. Ueli Suter who not only gave me the opportunity to pursue this project in his lab but also provided an excellent working environment and support throughout my time as PhD student.

I want to thank my PhD committee members Prof. Dr. Martin E. Schwab and PD Dr. Hauke B. Werner whose insightful discussions and comments during our meetings, as well as general support have been very helpful.

I want to thank Dr. Pascal Peschard and the late Prof. Christopher J. Marshall for providing the Ral knockout mice.

I also want to thank Dr. Giovanna Lalli for providing the mutant Ral overexpression constructs, as well as the pGEX-RalBD construct for activity pull-downs of Rals.

I especially want to thank the people that have directly contributed to the work presented here: Dr. Jorge Antunes Pereira, Joanne Jeker (soon Gerber!), and Dr. Jonathan DeGeer for their support, as well as Dr. Daniel Gerber for his illustrations.

Furthermore I would like to thank PD Dr. Ned Mantei for his contribution and for excellent proof reading of the thesis along with Dr. Monica Ghidinelli. I also want to thank Dr. Gianluca Figlia for proof reading of the manuscript which directly translated into this thesis. I further want to thank Dr. Anne-Sophie Ernst for her corrections of the Zusammenfassung, and for being the best best-friend I could wish for.

During my time as PhD student I had the pleasure to supervise two talented semester students. I want to thank Martina Jungo and Maria Germann for their contributing work and wish both of them the best of luck for their future.

I also want to thank the whole Suter lab as well as former members for valuable discussions, contributions, and for creating a very enjoyable working environment.

I want to acknowledge the ETH core facilities that have helped me conduct my research, namely ScopeM for excellent support on everything microscope-related, the Functional Genomics Centre Zurich, especially Catherine Acquino Fournier and Lennart Opitz, for help with RNA sequencing, and all the caretakers of the ETH Phenomics Centre that do an excellent job in providing and caring for the experimental animals.

I especially want to thank my wonderful family and friends for all their support and love. You are all amazing and I wouldn't be where I am today if not for you.

And last but not least I want to thank my husband Johannes. I don't even know how to express my gratitude towards you for going with me through this time and always being there for me in all the good and bad moments. Either road you take, I shall go with you.

11. List of Abbreviations

11.1. General abbreviations

ATP	adenosine triphosphate
BOS	base of support
BSA	bovine serum albumin
CA	constitutively active
cDNA	complementary DNA
CNS	central nervous system
DAG	diacylglycerol
DIV	days *in vitro*
DMEM	Dulbecco's modified Eagle's medium
DN	dominant negative
DNA	deoxyribonucleic acid
E	embryonic
ECM	extracellular matrix
EDTA	ethylenediamintetraacetic acid
EdU	5-ethynyl-2'-deoxyuridine
ER	estrogen receptor
FCS	fetal calf serum
Flox	flanked by loxP sites
FRET	Förster resonance energy transfer
GAP	GTPase activating protein
GDI	guanine nucleotide-dissociation inhibitor
GDP	guanosine diphosphate
GEF	guanine nucleotide exchange factor
GST	glutathione-S-transferase
GTP	guanosine triphosphate
HBSS	Hanks' balanced salt solution
HEK	human embryonic kidney
HRP	horseradish peroxidase
IPTG	isopropyl β-D-1-thiogalactopyranoside
Lam	Laminin111
LB	lysogeny broth
MDCK	Madin-Darby canine kidney
MPNST	malignant peripheral nerve sheath tumors
MpT	months post tamoxifen injection
mRNA	messenger RNA
OD	optic density
P	postnatal
PA	phosphatidic acid

PAGE	polyacrylamide gel electrophoresis
PB	phosphate buffer
PBS	phosphate buffered saline
PCR	polymerase chain reaction
PFA	paraformaldehyde
PH	pleckstrin homology
PNS	peripheral nervous system
PVDF	polyfinylidene fluoride
qPCR	quantitative PCR
RA	Ras-association
RalBD	Ral-binding domain
REM	Ras exchanger motif
RNA	ribonucleic acid
RT	room temperature
RT-PCR	reverse transcription PCR
SC	Schwann cell
SCP	Schwann cell precursor
SDS	sodium dodecyl sulfate
SEM	standard error of mean
SZ	Schwann Zelle (*german*)
TBS-T	Tris-buffered saline with Tween-20

11.2. Names of genes and proteins

Arf	ADP-ribosylation factor
Arp2/3	actin-related protein 2/3
BACE1	beta-secretase 1
CC3	cleaved caspase 3
Cdc25	cell division control protein 25
Cdc42	cell division control protein 42
Cdk1	cyclin-dependent kinase 1
Dhh	desert hedgehog
Dlg1	discs large homolog 1
DNM2	dynamin 2
DRP1	density-regulated protein 1
EGF	epidermal growth factor
Egr2	early growth response 2
Exoc	exocyst complex component
FAK	focal adhesion kinase
FOXO4	forkhead box protein O4
Glut4	glucose transporter 4
Gnas	guanine nucleotide-binding protein G(s)
GPR126	g-protein coupled receptor 126
GPR56	g-protein coupled receptor 56
GSK3β	glycogen synthase kinase-3 beta
HDAC1/2	histone deacteylase 1/2
ICMT	isoprenylcystein carboxyl methyltransferase
IGF	insulin-like growth factor
IL-1	interleukin-1
ILK	integrin-linked kinase
Jab1	Jun activation domain-binding protein 1
JIP1	JNK-interacting protein 1
JNK	c-Jun N-terminal kinase
LCK	lymphoid cell kinase
LKB1	liver kinase B1, serine/threonine-protein kinase STK11
MAG	myelin-associated glycoprotein
MBP	myelin basic protein
MEK	mitogen-activated protein kinase kinase
Miz1	myc-interacting zinc finger protein

Mpz/P0	myelin protein zero
Mtmr2	myotubularin-related protein 2
mTOR	mammalian target of rapamycin
mTORC	mTOR complex
Myo1c	myosin 1c
NF1	neurofibromin 1
NRG1	neuregulin 1
N-WASP	Wiskott-Aldrich syndrome protein
Oct6	octamer-binding protein 6
Pals1	protein associated with Lin-7
Par3	proteinase-activated receptor 3
PAT	protein acetyltransferase
PI3K	phosphatidylinositol 3-kinase
PKA	protein kinase A
PKCα	protein kinase Cα
PLCγ	phospholipase Cγ
Plp	proteolipid protein
Pmp22	peripheral myelin protein 22
Rab	Ras-like protein in brain
Rac1	Ras-related C3 botulinum toxin substrate 1
Ral	Ras-like
RalBP1	Ral-binding protein 1
RalGDS	Ral guanine nucleotide dissociation stimulator
RalGPS	RalGEF with PH domain and SH3-binding motif
Ran	Ras-like nuclear GTPase
Ras	rat sarcoma
RBP-J	recombining binding protein suppressor of hairless
Rce1	Ras converting enzyme 1
Rgl	RalGDS-like
Rgr	RalGDS-related
Rheb	Ras homolog enriched in brain
Rho	Ras homolog
RLIP76	Ral-interacting protein of 76 kDa; RalBP1
ROCK	Rho-associated protein kinase
SH3BP1	SH3 comain-binding protein 1
Taz	Tafazzin
Tead1	TEA domain transcription factor 1
TGFβ	transforming growth factor β
TNF-α	tumor necrosis factor-α

TSC	tuberous sclerosis complex
VEGF	vascular endothelial growth factor
Vps34	phosphatidylinositol 3-kinase catalytic subunit type 3
WRC	wave regulatory complex
Yap	Yes-associated protein 1
ZONAB	ZO-1-associated nucleic acid-binding protein